Report No. CDOT-2014-1
Final Report

DESIGN OF MECHANICALLY STABILIZED EARTH WALL CONNECTIONS AND END OF WALLS SUBJECTED TO SEISMIC LOADS

Panos D. Kiousis
Judith Wang
Rebecca M. Walthall

January 2014

COLORADO DEPARTMENT OF TRANSPORTATION
DTD APPLIED RESEARCH AND INNOVATION BRANCH

The contents of this report reflect the views of the author(s), who is(are) responsible for the facts and accuracy of the data presented herein. The contents do not necessarily reflect the official views of the Colorado Department of Transportation or the Federal Highway Administration. This report does not constitute a standard, specification, or regulation.

Technical Report Documentation Page

1. Report No.	2. Government Accession No.	3. Recipient's Catalog No.
CDOT-2014-1		

4. Title and Subtitle	5. Report Date
DESIGN OF MECHANICALLY STABILIZED EARTH WALL CONNECTIONS AND END OF WALLS SUBJECTED TO SEISMIC LOADS	January 2014
	6. Performing Organization Code

7. Author(s)	8. Performing Organization Report No.
Panos D. Kiousis, Judith Wang, Rebecca M. Walthall	CDOT-2014-1

9. Performing Organization Name and Address	10. Work Unit No. (TRAIS)
Colorado School of Mines 1500 Illinois Street Golden, Colorado 80401	11. Contract or Grant No. 74.90

12. Sponsoring Agency Name and Address	13. Type of Report and Period Covered
Colorado Department of Transportation - Research 4201 E. Arkansas Ave. Denver, CO 80222	Final
	14. Sponsoring Agency Code

15. Supplementary Notes

Prepared in cooperation with the US Department of Transportation, Federal Highway Administration

16. Abstract

The 4th Edition of the AASHTO LRFD Bridge Design Specifications requires all states to design for a 1,000-year return period earthquake, as opposed to earlier editions' 500-year return period. In response to this requirement, the Colorado Department of Transportation (CDOT) sponsored this study to examine the impact that these more stringent design requirements have upon connection details in mechanically stabilized earth (MSE) walls. The objective of this study was to perform displacement-based dynamic finite element analyses of MSE walls to examine the response of selected internal components when subjected to seismic excitations such as those expected in Colorado. Details that were of particular interest were the upper block connections in modular block walls; the dynamic displacements of the ends of walls; and the relative displacements and motions between the wall facings, soil reinforcement, and soil. The results of this study show that segmental and modular block walls representative of typical current CDOT design practices performed well with respect to both serviceability and strength requirements, even under AASHTO's newly stringent requirement for the consideration of a 1,000-year return period earthquake.

Implementation:

The results of these linear elastic finite element studies indicate that seismic design for MSE walls in Colorado does not need to be routinely completed. The MSE walls, which were modeled based upon walls designed using current CDOT MSE wall design procedures, performed very well under all of the seismic loads examined. This means that CDOT's MSE walls do not need to be designed for seismic loads as per the AASHTO recommendation.

17. Keywords:	18. Distribution Statement
mechanically stabilized earth (MSE) walls, seismic design, connection details, finite element analysis (FEA), Peak Ground Accelerations (PGAs)	This document is available on CDOT's website http://www.coloradodot.info/programs/research/pdfs

19. Security Classif. (of this report)	20. Security Classif. (of this page)	21. No. of Pages	22. Price
Unclassified	Unclassified	145	

DESIGN OF MECHANICALLY STABILIZED EARTH WALL CONNECTIONS AND ENDS OF WALLS SUBJECTED TO SEISMIC LOADS

by

Panos D. Kiousis
Judith Wang
Rebecca M. Walthall

Report No. CDOT-2014-1

Sponsored by
Colorado Department of Transportation
In Cooperation with the
U.S. Department of Transportation
Federal Highway Administration

January 2014

Colorado Department of Transportation
Research Branch
4201 E. Arkansas Ave.
Denver, CO 80222

ACKNOWLEDGEMENTS

The authors wish to thank the CDOT-DTD Applied Research and Innovation Branch for funding this study and Aziz Khan for overseeing the project on behalf of CDOT. We wish to thank the project panel members, Lynn Croswell, Steve Yip, Daniel Alzamora (FHWA), Nurul Alam, Trever Wang, Hsing-Cheng Liu, C.K. Su, and Russel Cox, for their feedback throughout the project, and for their assistance in conducting site visits.

EXECUTIVE SUMMARY

This report presents the outcomes of a Colorado School of Mines (CSM) study on the research project, "Design of Mechanically Stabilized Earth Wall Connections and End of Walls Subjected to Seismic Loads." Mechanically Stabilized Earth (MSE) walls are often used for bridge abutments in highway design due to their low cost and high performance. These retaining walls are composite soil-structural systems, typically comprised of three major internal components: (1) a wall facing, such as stacked modular blocks or segmental paneling; (2) compacted reinforced soil materials; and (3) soil reinforcement, such as geogrid or galvanized metal strips, extending from the facing into the reinforced materials.

The objective of this study was to perform displacement-based dynamic finite element analyses of MSE walls to examine the response of selected internal components when subjected to seismic excitations such as those expected in Colorado. The motivation for this study was the elevated Peak Ground Accelerations (PGAs) mandated by the 2007 4th edition AASHTO LRFD Bridge Design Specifications. According to this revision, states are required to design highway-related projects for a more stringent, 1,000-year return period earthquake, as opposed to earlier editions' 500-year return period. As a result of this change, states that did not previously need to consider seismic loading may now need to re-evaluate their current detail design practices. For example, bridges built in certain locations in Western Colorado upon site class B soils now have to withstand PGAs up to 0.14g as opposed to the previous maximum PGA of 0.025g.

The new PGA magnitudes in Colorado are still considered relatively low with respect to more seismically active regions; however, they are no longer negligible and merit further examination. It is therefore necessary to understand the impact that the new design requirements have upon MSE wall details. The behavior of specific details that have been identified in this study to be of particular interest include: (1) potential vertical chatter and horizontal sliding separation of the upper blocks of modular block walls; (2) the relative dynamic transverse displacements of the tapered wing walls as compared to the main body of the walls; (3) the relative displacements between the wall facings and the reinforced soil block; and (4) the seismically induced tensile stresses in the geogrid reinforcement. The approach to achieve these objectives involved three major tasks: (1) literature review of the-state-of-the-art in displacement-based MSE wall design; (2) a national state Department of Transportation survey

to determine how other DOTs have approached these issues; and (3) displacement-based analysis of dynamic behavior of MSE walls based on the Finite Element Method.

From the literature review (Task 1), it was found that many studies have been performed with many others currently underway in order to find alternative methods to the conventional pseudo-static equilibrium methods used in the AASHTO code. However, to the CSM research team's best knowledge, no previous studies have specifically addressed the design of the connections or ends of wall treatments under the 2007 AASHTO specifications with the more stringent 1,000-year return period seismic design requirements. Additionally, based upon the responses to the national state DOT survey prepared, distributed, and collected by the CSM research team (Task 2), none of the responding state DOTs have as of yet observed MSE wall damage directly attributable to seismic or dynamic loading effects. The only state DOT that reported performing similar research to examine the effects of more stringent seismic design loads was Washington DOT, which is currently performing this study; to the authors' current best knowledge, the Washington DOT report has not yet been published.

The third task involving displacement-based, finite element analysis was carried out using the commercially available Finite Element software, LS-Dyna. Two segmental panel MSE wall models (15 ft and 30 ft in height) as well as two modular-block MSE wall models (15 ft and 30 ft in height), all with geogrid reinforcing, were analyzed. The wall dimensions, reinforcing length and spacing were taken from Colorado MSE wall shop drawings provided by CDOT. It was concluded that the maximum recorded ground motion in Colorado available from the United States Geological Survey (USGS)'s database of historic recorded motions is too small to be useful for our study purposes. Therefore, potential earthquake motions that are representative of the elevated AASHTO requirements that could potentially occur in Colorado have been generated using the USGS's 2002 Interactive Deaggregation tool combined with the Peak Ground Acceleration (PGA) values determined from the AASHTO Calculator for three sites spread across Colorado. These motions were applied to the MSE wall models. Additional real, more extreme seismic earthquake motions, as recorded in the 1940, El Centro, California earthquake and the 2008 Illinois earthquake, were also used as loading input to investigate MSE wall behavior under more significant seismic loads. Both types of 15 ft MSE walls were simulated, subjected to all five selected seismic motions. The 30 ft high walls were subjected to

the same five motions plus an additional synthetic motion based upon the natural frequency of the walls to demonstrate the effects of resonance.

The results of this study show that MSE walls performed well when subjected to seismic loadings that reflect the updated 1,000-year return period earthquakes in Colorado. The natural periods of the 15 ft wall models were found to be 0.13 s, while the natural periods of the 30 ft walls were found to be 0.28 s. The mode shapes were dominated by shear behavior, which causes swaying in and out at different locations along the wall. The maximum overall displacements were all less than 0.5 in under seismic loading. No yield stresses were exceeded for the concrete facing units, the geogrid reinforcement, or the geogrid to facing unit connectors. None of the specific examined connection details such as corner joints and reinforcement connections were found to suffer from any detrimental issues.

TABLE OF CONTENTS

LIST OF FIGURES

LIST OF TABLES

1.0 INTRODUCTION

The objective of this research was to model the dynamic behavior of Mechanically Stabilized Earth (MSE) wall connections and details when subjected to Colorado-specific, 1000-year seismic loads. To achieve this objective, the following three tasks were performed:

- Literature review of the-state-of-the-art in displacement-based MSE wall design;
- The preparation and distribution of a national survey to determine if and how other state DOTs have examined these issues; and
- Displacement-based, finite element analyses of the dynamic behavior of MSE walls subjected to representative seismic loadings.

The AASHTO LRFD Bridge Design Specifications [1] address the seismic design of MSE walls by the use of pseudostatic, overall limit equilibrium analysis. This approach has worked wall in examining global equilibrium. However, it does not address with equal success the detailed stresses and deformations of the individual, internal MSE wall components and connections. Therefore, finite element analyses were performed to determine relative dynamic displacements between individual MSE wall components. Two different types of MSE walls (modular block and segmental panel walls) were modeled at two different heights, 15 and 30 feet. The seismic loading applied to these models was based upon three synthetic earthquake motions generated by the United States Geological Survey's (USGS) 2002 deaggregation tool for three sites spread across the geographical extents of Colorado. Additional simulations were performed to examine the performance of the MSE walls under more extreme seismic loading conditions: both types of walls at both heights were loaded using actual recorded earthquake motions in California and Illinois, while the 30 ft wall models were loaded with motions centered about their natural frequency to examine the effects of resonance. These finite element analyses were used to evaluate the dynamic behavior of MSE walls, especially with regard to their internal connection details. Conclusions were drawn that can be used by the Colorado Department of Transportation (CDOT) to upgrade and validate their design methodologies for MSE wall connections and components based upon the more stringent 2007 4th edition LRFD seismic requirements.

1.1 Background

Mechanically Stabilized Earth (MSE) walls are often used for bridge abutments in highway design due to their low cost and high performance. MSE walls are retaining soil structures with manmade reinforcement materials that extend into the retained soils. The main components of an MSE wall are shown in Figure 1.1 and include the original ground foundation, the reinforced soil block, and the retained fill. The reinforced soil block consists of a wall facing, reinforcement materials, and selected backfill material. The wall facing is typically relatively thin (~6 to 8 in) and can consist of segmental or full height panels, or stacked modular blocks. The reinforcement can consist of extensible materials such as geogrids or inextensible materials such as galvanized metallic meshes or strips. In this study, only geogrid reinforcement is examined because it is the most commonly used type of reinforcement in Colorado DOT applications. Geogrid reinforcement is commonly made of high density polypropylene which is formed into a grid pattern. Geogrids can carry large tensile loads in the perpendicular direction to the wall facing. The open aperture structure interlocks with natural fill materials [2].

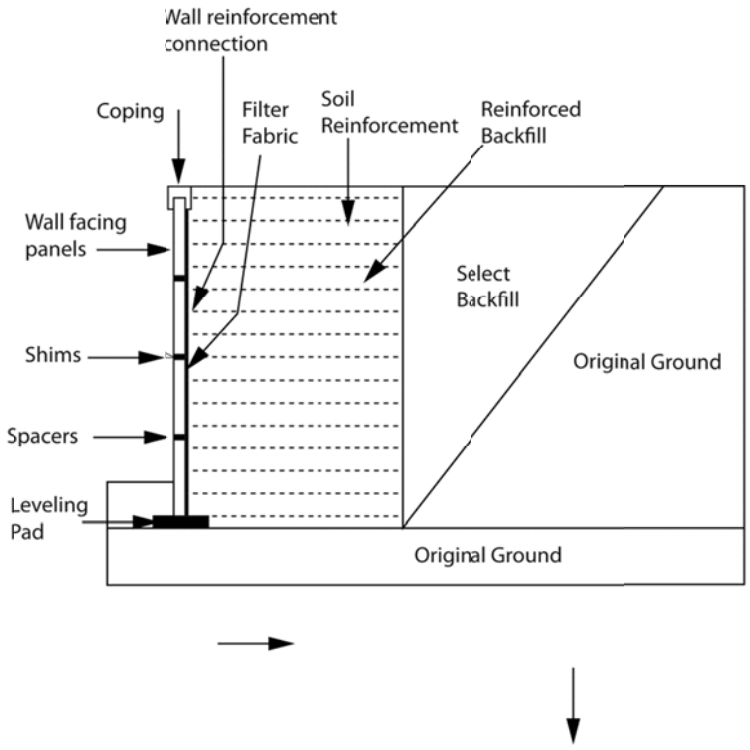

Figure 1-1: MSE wall schematic

There are three main types of MSE wall facings commonly used in Colorado: modular block, segmental panel, and full panel [4]. Modular block walls use concrete blocks as facing units that are designed specifically to fit on top of one another in a wall formation (Figure 1.2). Grooves are cut into the block to increase the coefficient of friction. There is also a lip at the end of the block to help block alignment. These wall facing units are typically held together by gravity and friction, while grouting may be used at the top layers. Soil reinforcement extending into the reinforced block is usually placed every 2 or 3 layers of blocks. These walls can reach up to 40 ft in height or more in Colorado and can be built very quickly [2].

Figure 1-2: Modular block facing unit [2]

The construction procedures for segmental panel walls are slightly more complicated, as the panel facing must be temporarily propped up with supports before the soil behind it can be compacted [3]. This is in contrast to modular block walls, where the soil may be compacted as the blocks are stacked. Depending on the panel type and panel manufacturer, the soil reinforcement can be attached at joints already built into the panel to be extended into the reinforced soil block (see Appendix C, Figure C - 1 for example segmental panel specifications). The third type of MSE wall, which uses full height panels for facing, is often considered the most complex, as the full height panels require temporary bracing during the placement and compaction of the reinforced soil [4]. Due to the difficulty in constructing these full-height panel walls, there were no full height panel wall specifications provided by CDOT. Therefore, this study focuses on aspects of the detailing of modular block walls and segmental panel walls.

MSE segmental panel walls are generally constructed according to the following procedure (e.g. [3]). First, the site is prepared by cutting or filling to grade, removing unwanted material, and then rolled to required compaction. Next, a leveling pad excavation is dug, and the leveling pad is placed. The leveling pad is a concrete foundation for the facing of the MSE wall. After at least 12 hours of curing, the first row of panels is placed on the leveling pad and

temporarily braced. Then the second row is placed. Next, the selected soil backfill is placed and compacted to the level of the first row of connections. The reinforcement may then be placed perpendicular to the wall panels. Another row of wall panels is added, and this procedure is repeated until the wall is finished [3]. The modular block walls follow the same basic procedure except bracing is not needed in the supporting of the facing units. Grouting is sometimes added to the top layer of bricks to restrict movement. MSE walls are sometimes built with wing walls that are bent back into the soil. The height and orientation of the side walls are often different from that of the uniform main facing wall and therefore may alter the wall dynamic behavior. Wing walls often taper down to a lower overall height than of the main wall, particularly in modular block walls. This study therefore additionally examines the effects of potential relative displacements between the main and wing walls due to seismic loading.

In summary, the components of the MSE wall that are specifically examined in this study during seismic events are: (1) the relative displacements between the modular block and segmental wall facings and the soil reinforcement, (2) the relative motions of the upper blocks in modular block MSE walls, and (3) the relative motions between the side wing walls and the main facing wall. Internal stresses in the facings and the soil reinforcement are also examined. These dynamic responses are quantified when the walls are subjected to synthetic seismic loads generated by the USGS 2002 deaggregation tool for three sites across Colorado, scaled up for the more stringent peak ground accelerations (PGA) specified by the 2007 4th edition AASHTO revision. They are further examined under higher levels of seismic loading to investigate MSE wall detail behaviors under more significant seismic duress.

1.2 Motivation for Work

Currently, the AASHTO LRFD Bridge Design specification [1] is used for the design of MSE walls. Although this document discusses overall seismic loading considerations using pseudostatic limit equilibrium analysis procedures, it does not address the detailing of specific internal connections or ends of wall treatments for composite MSE wall systems. Since the 2007 version of the AASHTO LRFD Bridge Design Specification, state DOTs are now required to design for a 1,000-year return period earthquake as opposed to the previous 500-year return period earthquake requirement. This more stringent requirement means that bridges built in

Colorado on site class B (shear wave velocities of 2,500 to 5,000 ft/s) soils may have to use PGAs as high as 0.14g in their designs as opposed to the previous maximum PGA of 0.025g. The new PGA magnitudes in Colorado are still considered relatively low with respect to more seismically active regions; however, they are no longer negligible and merit further examination. The current PGA values to be designed for usage in the conterminous United States are shown in Appendix A, Figure A - 1.

CDOT has therefore sponsored this study in order to examine the effects of the increased AASHTO design acceleration requirements on MSE wall detailing. One of the primary potential concerns is the possibility of vertical vibration in the top blocks of a modular block MSE wall, causing the upper blocks to lose contact and vertically "chatter" during a seismic event. The vertical displacements of these top blocks are monitored in finite element situations in order to observe whether or not this behavior is of significance. Another potential concern is the relative displacement response of a tapered down end-of-wall. If the main body of an MSE wall is subjected to seismic motions, it creates a wave that could propagate along the length of the wall until it arrives at the tapered ends. This wave in the main body of the wall results a slower displacement response due to the large mass; however, in order to conserve energy, the wave is forced to speed up in the shorter tapered ends because there is significantly less mass. This smaller end-of- wall may therefore experience a "whipping" effect driven by the momentum of the larger portion of the wall responding to the ground motion. The horizontal displacement of the tapered down wall is monitored to evaluate the intensity and effects of this behavior. If the angled wing walls are subjected to seismic loading, this part of the wall can be moving out of phase of the main wall. The connections between these two intersecting walls are also studied to determine if excessive shear stresses are developed. A third potential concern is in the relative displacements between the wall facings and soil reinforcement and the resulting stresses. The wall facings and geogrid connections are examined to determine if they are able to withstand the tensile forces due to seismic loading.

1.3 Objectives

The objective of this study was to examine the performance of specific detailing components of MSE walls when subjected to seismic excitations such as those expected for a

1,000-year return period for Colorado. The approach to achieve this objective involved the creation and interpretation of displacement-based, finite element models of typical Colorado MSE walls subjected to seismic motions representative of the elevated PGAs mandated by the 2007 4th Edition of the AASHTO LRFD Bridge Design Specifications. These analyses were requested by CDOT such that the detailing of specific MSE wall components (the connections of the upper blocks in modular block walls to the rest of the wall system; the dimensions and connections of the side ends of walls to the main walls; and the relative motions between the wall facings, soil, and soil reinforcement) could be evaluated based upon quantitative deformation-based analyses.

1.4 Approach

To fulfill the objectives of this study, the following tasks (as quoted from the original CSM proposal) were performed:

Task 1: Perform a literature review to determine if there has been similar research that will aid CDOT in improving the practice. Review practices in other state DOTs regarding Seismic Detail and EOW treatment.

Task 2: Conduct a national survey of state DOTs to determine if other states have had similar problems and if so, their solutions and recommendations.

Task 3: Displacement based analysis involving:

1. *Determining appropriate seismic ground motions for Colorado*
2. *Performing a review of existing MSE walls to determine the mechanical and geometric properties of current representative detail specifications*
3. *Performing a limited number of dynamic finite element analyses to observe the deformation behavior of the individual components as well as the ends-of-walls*

2.0 LITERATURE REVIEW

2.1 Real-World Observations of MSE Wall Performance Under Seismic Loading

MSE walls have been noted to generally perform well during seismic events (e.g. [5]). However, there are a few cases of documented damage in MSE walls as well as in gravity earth walls during earthquakes. Although gravity earth walls' engineering behaviors are much less complex than MSE walls in terms of potential interactions between internal components, studying their behavior under seismic loading conditions can indicate potential hazards in MSE walls due to reinforcement breakage or connection failures. During the Taiwan Chi-Chi earthquake on September 21, 1999, multiple soil retaining gravity walls within 30 km of the Chlungpu fault suffered severe damage (e.g., [6]). One particular failed wall in this area was comprised of stacked concrete blocks and built in order to retain a steep excavation along a highway. This wall failed due to sliding of the stacked component concrete blocks along the construction joints. The concrete had been placed in five pours with no special treatment provided for the connection joints. The top two blocks fell off during the earthquake due to low frictional resistance at the flat construction joint. The frictional resistance was not sufficient to withstand the dynamic earth pressure [6]. This behavior in a gravity earth wall could potentially be seen in a modular block MSE walls if the seismic loads are high enough to overcome the weights and frictional interfaces of the top blocks. The top blocks have the potential to "chatter" off of the wall system, particularly if grouting is not used to keep the upper blocks in place.

Additionally, global serviceability in the aftermath of earthquake events of retaining walls is also a concern. Several retaining earth walls and embankments experienced serious damage during the 1995 Kobe earthquake in Japan after being exposed to heavy rainfall [5]. Masonry soil walls, unreinforced concrete panel walls, and unreinforced concrete gravity walls experienced the most severe damage due to the high acceleration of 0.7g caused by the Kobe earthquake. Typical types of damage induced in these types of walls can be seen in Figure 2.1. However, one MSE wall with panel facings was noted to experience minimal damages compared to theses other types of retaining walls. The MSE wall's only noticeable response to the Kobe earthquake was a relatively minor displacement at the top of the wall, ranging from 100 mm to 260 mm. The Kobe earthquake proved the seismic resilience of MSE walls as compared to other

forms of retaining walls, resulting in most of the failed retaining structures being rebuilt as MSE walls [5]. However, it is yet unclear how the internal connections in the MSE walls will perform under seismic loadings, as the observed damages were with respect to global, external serviceability and not internal relative deformations of individual components.

Figure 2-1: Typical forms of damage to (a) gravity (b) gravity leaning and (c) masonry unreinforced walls in the 1995 Kobe earthquake [5]

Another documented case study of a MSE wall subjected to seismic loading was recorded from a 1999 seismic event in Turkey [7]. This earthquake was a significant event with a 7.4 magnitude and occurred north of the Anatolian Fault. The MSE wall was a 100 meter long retaining wall system built as a double faced or back-to-back type wall (see Figure 2.2). The wall facing was comprised of segmental concrete panels, and the reinforcement consisted of

metallic strips extending into the backfill soil. The wall failed at a location adjacent to a collapsed bridge abutment due to breakage of the metallic soil reinforcement.

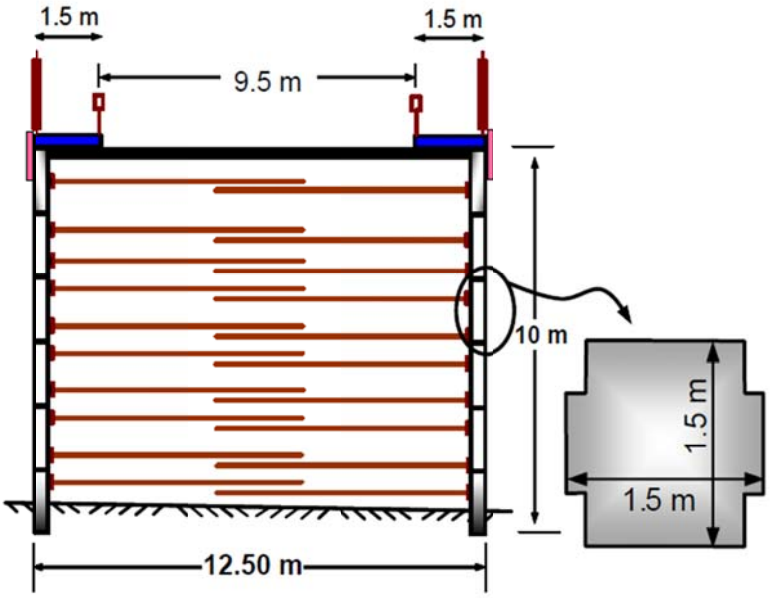

Figure 2-2: Schematics of double-faced MSE system with reinforced concrete facing panels [7]

The system was subjected to a PGA which was approximately 0.4g in the horizontal direction and 0.26g in the vertical direction. The vertical ground deformations appeared to be the main source of damage for the MSE wall in the approach ramp section. The facing panel connections with the metallic reinforcements did not fail, however, and the flexible joints between panels allowed large displacements and differential settlements. Large panel separations and cracks were observed at higher levels but not at lower elevations [7]. However, although the vertical earthquake component appeared to be the main cause of damage in this earthquake, the vertical component of the Turkey earthquake was much higher than the horizontal 0.14g PGA expected in the 1,000-year Colorado earthquake. As the vertical component of seismic activity is generally significantly lower than the horizontal component, the vertical component of a potential Colorado earthquake is expected to be smaller than the PGA of 0.14g and is neglected for this study.

2.2 Experimental Investigations of MSE Wall Behavior Under Seismic Loading

There have been several experimental studies on models of MSE and cantilever walls in order to understand the behavior of the wall during a seismic event. These experimental data have been used in conjunction with numerical modeling methodologies in an attempt to calibrate and validate the results of the numerical models. Some of the most common tests performed use instrumented small scale models vibrated using shake tables. Shake table experiments performed on gravity earth walls give experimental indications of how MSE walls might behave if the connections to the soil reinforcement are lost. Bathurst et al. [8] and Zarnani and Bathurst [9] performed and analyzed data from shake table tests on gravity wall models, focusing primarily upon evaluating the global behavior of the walls. Ling et al. [10] performed large-scale shake table tests to validate analytical design methods of modular block MSE walls backfilled with dry sands. These tests focused upon the behaviors of the individual components of the MSE walls. The Kobe earthquake motion was scaled to a peak acceleration of 0.4g and applied in one direction horizontally. This same motion was then scaled to a maximum acceleration of 0.86g and applied again preceding the 0.4g scaled motion as secondary shaking. Transducers were used to measure lateral and vertical earth pressures, wall facing displacements, crest settlement, reinforcement strains, and accelerations within the soil and facing blocks. Under earthquake loading, the displacement was largest at the top of the wall: for the first shaking cycle with a maximum acceleration of 0.4g, the wall peak displacements were 3 to 7 mm. The reinforcement tensile loads throughout the height of the wall for the first loading cycle range from 0.5 to 1.0 $\frac{kN}{m}$. [10]. The maximum acceleration and resulting tensile loads from Ling et al.'s [10] study are comparable to those found in the finite element models subjected to the 1940 El Centro, California earthquake motions used for the present study; these are discussed in detail in Chapter 7.

Further experimental shake test table studies were performed to examine the relative motions in the reinforced soil component of MSE walls in particular. A series of 1-g shaking table tests were conducted on several 1 m high reinforced-soil models by Sabermahani et.al. [11]. The effects of parameters such as soil density, reinforcement length, spacing and stiffness on the seismic response of the model walls were studied. Several potential deformation modes

and shapes were examined. The distribution of the shear stiffness modulus, G, and damping ratio, ξ, of the reinforced soil along the wall height was assessed. It was found that walls built with more extensible reinforcements have larger transverse deformation which often leads to a bulging mode of failure, which corresponds to an internal single failure surface detected in the reinforced zone and no external failure surface. Additionally, walls that are shorter in length, have closer reinforcement spacing, or have stiffer reinforcement usually have failure mechanisms that form behind the reinforced zone in the form of the overturning mode rather than the bulging mode. Therefore, this study found that reinforcement stiffness governs the mode of deformation and failure mechanism of a wall under seismic conditions [11].

Shake table tests have also been performed to examine the effects of facing properties on seismic response. Results from the reactions developed at the toe of reduced scale MSE wall models on shake tables indicate that facing stiffness and toe restraint provide additional resistance to wall lateral movement. El-Emam and Bathurst [12] used models with 1 meter high rigid panel facings. The variables they examined include facing stiffness, facing inclination angle, input base motion characteristics, and boundary conditions at the toe. Their results show that the thin inclined wall facing had the least displacement and that hinged wall toe configurations performed better than sliding wall toe [12]. In a similar study [13] it was shown that the magnitude of the lateral wall displacement is dependent on reinforcement length, stiffness, and number of reinforcement layers. Fourteen 1-m high wall models at 1/6 scale were produced and placed on shake tables. The variables were reinforcement stiffness, length, and vertical spacing. Increasing the ratio of reinforcement-length to wall-height reduced the reinforcement connection loads significantly. The empirical AASHTO/FHWA design method underestimates the magnitude of the reinforcement connection loads at higher base accelerations. The current design methods either neglect or underestimate the vertical toe loads [13].

MSE walls have also been tested on the small-scale using geotechnical centrifuge modeling procedures. Three different tests were performed by Siddharthan et al. [14] by placing two wall models at a time back to back on a centrifuge. Bar mat reinforcement and a backfill consisting of a fine dry granular soil was used for all prototypes. The input motions started with peak ground accelerations of 0.48g and steadily increased in magnitude. It was seen that the wall deformations were not uniform over the height of the wall: the first wall model had a base deformation of approximately 8 mm, while the middle and top both displaced 6 mm relative to

the bottom with a peak acceleration of 0.48g. With this wall exposed to a peak acceleration of 0.83g, the bottom displaced 28 mm, the middle 20 mm, and the top 4 mm relative to the bottom. The other wall models had similar displacements. However, no catastrophic failures were observed. This study shows that the soil, reinforcement, and wall facings typically behave as one unit and indicates that the relative displacements during a seismic event may be relatively small. This conclusion supports the observations made of the analyses presented in Chapter 7 of the present study, in which it is observed that the finite element MSE walls generally behave monolithically as one unit.

Dewoolkar et al. [15] studied the effects of cantilever retaining walls with liquefiable backfills. They compared a finite element analysis using the program DIANA-SWANDYNE II to experimental centrifuge tests. In this experiment two tests were performed on a model 6 inches tall and .25 inches thick on a 400g-ton centrifuge. In the first test, the soil was saturated with distilled water, while in the second test the soil was saturated with methylcellulose. The centrifuge test models experience an acceleration that can be scaled by a factor of N to earth's gravity. Therefore, a fluid, such as methylcellulose, that is N times more viscous than water can be used to reduce the soil permeability by a factor of N. Instrumentation installed in the model included miniature accelerometers, LVDTs, strain gages, and miniature total stress gages. From the experiment, it is clear that there were higher excess pore pressures in the methylcellulose-saturated soil because of the slower dissipation of excess pore pressures. This soil also settled more than the water saturated soil. The pore pressure transducer for the methylcellulose - saturated soil and water-saturated soil reach a state of cyclic mobility, liquefaction, after the first five to six loading cycles. The finite element results matched up to the experimental results fairly well. It is recommended that pore pressures be taken into account for retaining wall design [15]. However, the three-phase nature of the soil examined in Dewoolkar et al's [15] work is beyond the scope of the present study; the soil materials in this study were modeled as linear continuum materials using a total stress approach.

Other types of experimental testing procedures have also been performed on MSE walls to understand the displacement behavior of the connections between the facing and the reinforcement and the soil. Abdel-Rahman and Ibrahim [16] performed tests to observe loading and unloading cycles of both soil and geogrid. A testing apparatus was designed and built to perform uniaxial tension tests on geogrids, direct shear tests on soils, and pullout tests for

geogrids from soils. For each geogrid a series of static and cyclic loading conditions were carried out. From their studies, Abdel-Rahman and Ibrahim concluded that: (1) geogrid horizontal displacement increases with increasing load cycles until there is full slippage; (2) geogrids with higher stiffness can endure more loading cycles; (3) higher static factors of safety against geogrid slippage show more resilience in dynamic loading situations; (4) horizontal displacements of geogrid per load cycle increase at lower interface normal stresses; and (5) during cyclic loading tests, geogrids can fail by tension in the longitudinal direction, shear in the transverse direction, or a combination of these two. These factors should be taken into account when designing geogrid placed at lower levels in seismically active zones.

Reinforcement layers are placed between the masonry units of MSE walls. These connections can be frictional or clipped. In order to fully understand the maximum loads and displacements these connections can take, a full scale pull out test was designed by Bathurst [17]. The tensile load deformation properties are determined by geometry and type of geosynthetic-facing unit interface; quality of the facing material; type of facing unit (hollow or solid); tolerances on facing or block dimensions; quality of construction; and thickness, structure and polymer type of the geosynthetic. Approximately a dozen different types of modular blocks in combination with several different geogrids have been tested over a period of two years using the testing apparatus developed at the Canadian Royal Military College. The strength of the geogrid and modular blocks can differ depending on depth and site conditions. It was shown that strong uniaxial polyethylene geogrid in combination with solid masonry concrete units are able to carry up to 134 kPa normal stress more than a weak uniaxial woven polyester geogrid in combination with a hollow masonry concrete unit filled with crushed stone [17]. The uniaxial polyethylene geogrid in combination with solid masonry blocks is what is observed in the present study. These two materials work well together in that they reduce stresses and have small deformations.

2.3 Current Design Codes and Guidelines

When analyzing MSE walls, the goal is to create a reinforced earth block that acts as a vertical gravity retaining wall. Typically, design procedures treat the entire MSE wall (the facing, the selected compacted backfill, and the soil reinforcement) as a gravity wall for stability

analysis with added internal checks on failure modes through the reinforced soil block. The reinforcement causes a reactive effect in that the lateral deformations caused by the weight of the soil and surface loading is resisted by the frictional interface between the soil and the reinforcing layers. This induces confinement in the soil, which increases its strength and provides it with an apparent cohesion which allows for vertical planes without additional support. Figure 2.3 shows the possible failure modes of an MSE wall due to: (a) external instability; (b) combined external and internal instabilities, also known as compound instabilities; and (c) internal instability.

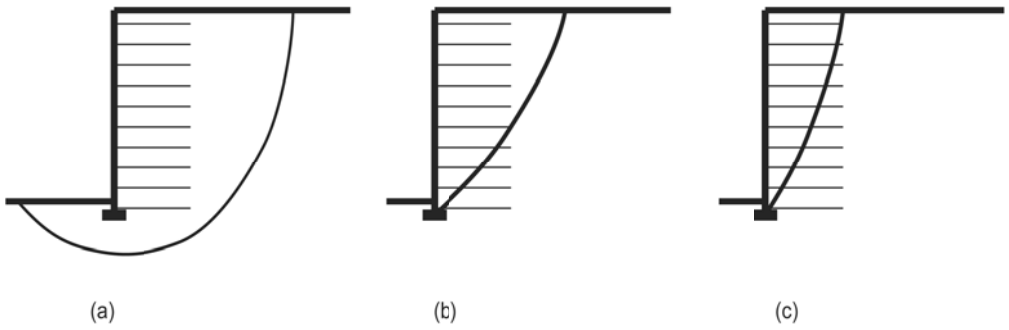

Figure 2-3: External, compound, and internal failure modes

The static design of MSE walls is well-defined in the AASHTO LRFD Bridge Design specifications [1]. Static external stability of an MSE wall is determined by the same procedures as used for gravity retaining walls with a vertical face and is typically based upon Coloumb or Rankine theory. These checks include overturning, sliding, and bearing capacity. The static internal stability is determined from the strength characteristics of the fill material, the tensile strength of the reinforcement, the spacing of the reinforcement, and the frictional characteristics of the soil-reinforcement interface. From these parameters, the maximum tie force is calculated as well as tie thickness and length depending on the assumed factor of safety and life span of the wall. If tensile failure of the reinforcement at any level were to occur, this would lead to progressive collapse of the wall. Slip at the soil-reinforcement interface can lead to redistribution of stresses and progressive deformation of the wall. The soil and reinforcement reaction can be treated in two different ways. The first way treats the MSE wall as an anchored flexible retaining wall in situations where geotextiles and geogrids are used. The second method is the coherent gravity method which is commonly used when metal strips are used for reinforcement.

Seismic analysis of MSE walls is defined in the AASHTO LRFD document under section 11.10.7. [1]. External stability is examined by the Mononobe-Okabe (M-O) Method [18]. This method is a pseudostatic limit equilibrium method and is a direct extension of the static Coulomb theory. Pseudostatic limit equilibrium methods, while computationally straight-forward, do not provide any information on the deformation behavior of the system. This method therefore does not provide the necessary relative displacement motions between individual MSE wall components such as the facing blocks or panels, reinforcement, and soil necessary to do detail and connection design. The M-O method describes earthquake loading as a simple harmonic motion for engineering applications. The displacement due to the seismic event can be described as:

$$y = A\sin\left(\frac{2\pi}{T}t\right) \tag{2-1}$$

where A is the amplitude of the harmonic motion, T is the period, and y is the displacement from the original position at any time t. Taking the second derivative yields the acceleration with a maximum amplitude, a, given by:

$$a = \frac{4\pi^2}{T^2}A \tag{2-2}$$

This maximum amplitude of acceleration can be resolved into horizontal and vertical components and is used to determine the effects of seismic loading on massive structures. Earthquake pressures are most dangerous when the horizontal acceleration is directed perpendicular to the wall and the vertical acceleration is directed upwards. If these accelerations and soil weight due to gravity are combined and applied to static conditions, then using M-O theory the active seismic earth pressure,P_{ae}, is expressed by:

$$P_{ae} = \frac{1}{2}\gamma H^2(1 - k_v)K_{ae} \tag{2-3}$$

where γ is the unit weight of the soil and H is the total height of the wall. k_v is the pseudostatic seismic vertical inertia factor, found by dividing the vertical component of the maximum acceleration by gravity, and K_{ae} is the active earth pressure coefficient defined as:

$$K_{ae} = \frac{\cos(\varphi - \theta - \psi)^2}{\cos(\psi)\cos(\theta)^2\cos(\delta + \theta + \psi)\left(1 + \sqrt{\frac{\sin(\delta + \varphi)\sin(\varphi - \beta - \psi)}{\cos(\delta + \theta + \psi)\cos(\beta - \theta)}}\right)^2} \tag{2-4}$$

where ψ is the resultant angle between the pseudostatic horizontal and vertical components of acceleration, φ is the angle of friction of the earth, δ is the angle of friction between the earth and the back of the wall, β is the angle of the earth surface with the horizontal, and θ is the angle of the back of the wall with the vertical. These variables are displayed in Figure 2.4 [18].

When determining the external stability in the AASHTO document, it is assumed that there is a potential phase difference between the M-O active earth pressure, P_{AE} , acting behind the wall, and the reinforced zone wall inertial force, P_{IR}. Therefore, a reduced base width of 0.5H is used to determine the wall inertial load which only accounts for sixty percent of the total wall inertia, see Figure 2.5 [1]. The dynamic soil thrust and reduced wall inertial force acting on the reinforced zone are then added to the static forces and overturning and sliding is checked.

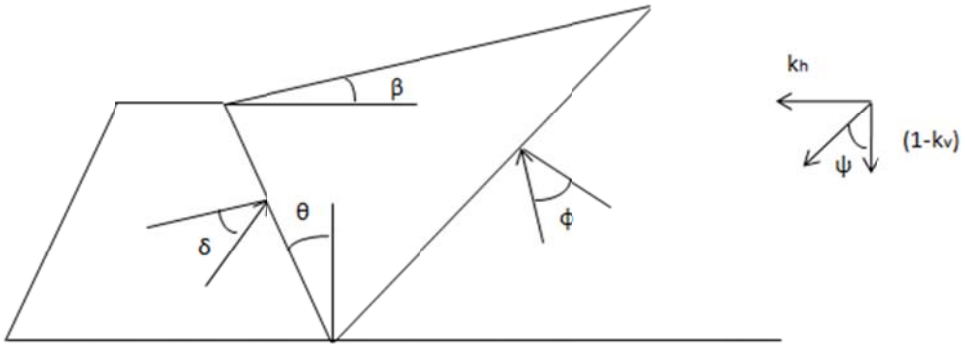

Figure 2-4: Mononobe-Okabe and Coulomb Theory variables

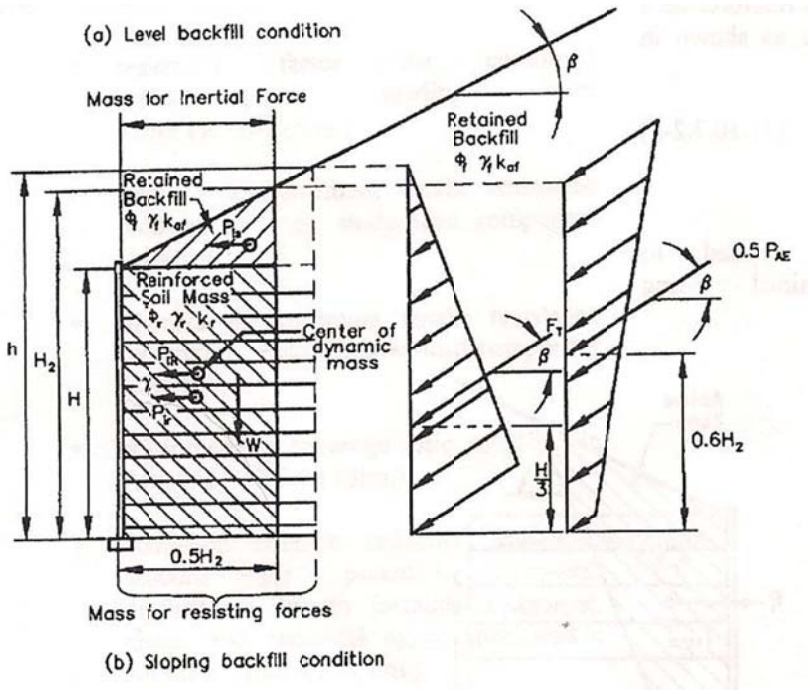

Figure 2-5: Seismic external stability of an MSE wall [1]

The internal stability under dynamic loading is checked by first dividing the reinforced zone into an active and a resistive zone (Figure 2.6). The horizontal inertia forces caused by the seismic acceleration on the mass of the active zone must be resisted by the reinforcements of the resistive zone. The resistive zone reinforcement must be strong enough and developed sufficiently within the resistive zone to withstand horizontal inertia and the static forces. The pseudostatic inertial force acting on the active zone is calculated and distributed to each reinforcement layer in proportion to the resistance that extends beyond the active/resistive boundary. The dynamic tensile force is then added to the static tensile force and checked against the allowable tensile force for each layer.

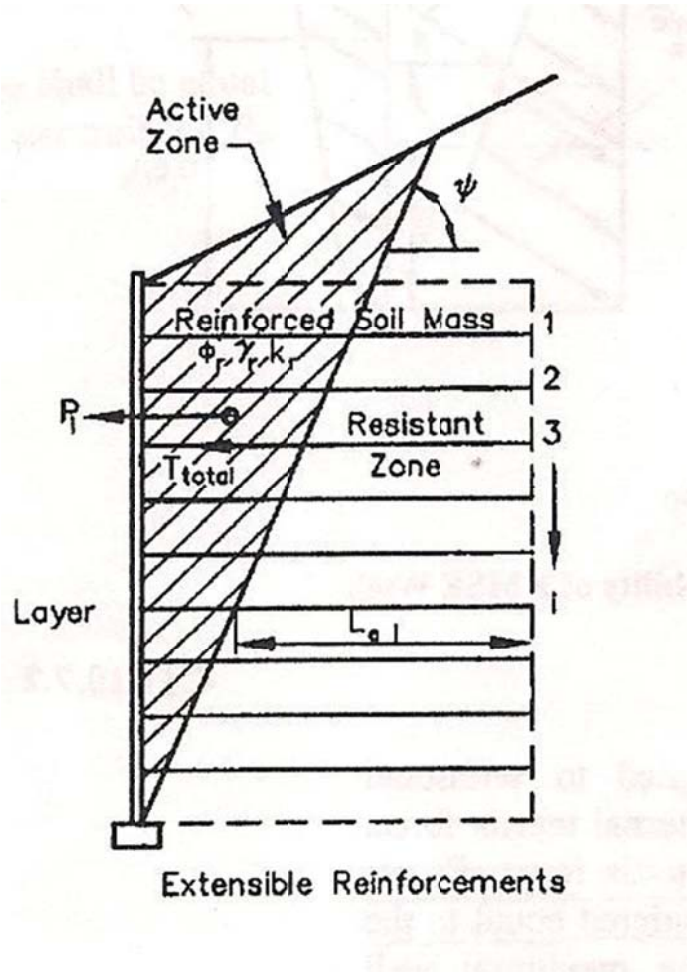

Figure 2-6: Active and resistance zones for internal stability [1]

There have been many concerns raised about the AASHTO LRFD code procedure, specifically examining whether or not this method is truly conservative and what seismic design values should be used. One of the most significant studies in addressing these concerns is described in the National Cooperative Highway Research Program (NCHRP) Report 611 [19]. This report addresses the seismic analysis and design of retaining walls, buried structures, slopes, and embankments. The results of this report are summarized as follows.

In current MSE wall design procedures, behavior as described by the M-O method deals with homogeneous, cohesionless materials. Observations from limit equilibrium slope stability analysis shows that the stability of a given slope is very sensitive to soil cohesion. Because the current M-O method can only be used for simple cohesionless soil cases, the NCHRP has extended the M-O equation to account for cohesive soils. Charts are presented that show active

earth pressure coefficients as a function of the horizontal seismic coefficients for different soil cohesions normalized by unit weight of the soil and height of the wall. It is seen that a soil with a friction angle of 40 degrees and horizontal seismic coefficient of 0.3 will have $k_{AE} = 0.4$ for a cohesionless soil and $k_{AE} = 0.25$ for a wall height of 20 feet with 200 psf cohesion. Another issue with the M-O pseudostatic method is that the M-O solution for the seismic active earth pressure increases significantly for walls with slopes and higher seismic coefficients. Therefore, when performing an external stability check, instead of the peak acceleration used in the AASHTO code, it is recommended that the height-dependent average seismic coefficient be used. It is also recommended that the total wall mass should be used to compute the inertial load instead of 50% according to AASHTO. For external stability it is recommended that the sliding block method be used with the total active earthquake force with a revised displacement functions given in section 7-6 of the NCHRP 611 Report [19].

The current internal stability design approach for MSE walls is given by AASHTO and assumes that the internal inertial forces that cause tensile forces in the reinforcement act on the same active pressure zone as the static loading case. This active earth zone is assumed to be bilinear for inextensible reinforcement and linear for extensible reinforcement. It is recommended in NCHRP 611 that the wall height dependent average seismic coefficient be used. The current method distributes the total inertial force to each of the reinforcement layers in proportion to the effective resistance lengths. This gives higher tensile forces in lower reinforcement layers, which is opposite to what the M-O equation describes. Due to this contradiction, the report recommends that a deformation design approach be used, using a finite element computer analysis [19]. This CDOT supported study follows through with that recommendation and complements the pseudostatic codified methods with the ability to model the dynamic displacements of the multiple components involved in a MSE wall, allowing for a quantitative basis for detail and connection design.

2.4 Current Research in Proposed Modifications to Current Design Codes and Guidelines

Much research has been and is still being performed to improve the pseudostatic limit equilibrium methods used by the AASHTO LRFD bridge design specifications [1]. Many

alternative numerical methods have been proposed. The NCHRP 611 report [19] addresses the noted limitations of the AASHTO code. This report includes cohesion with the M-O equation based on Prakash and Saran [20], Richards and Shi [21], and Chen and Liu [22]. Prakash and Saran [20] considered only the horizontal earthquake acceleration. The pressure due to self-weight of the soil and cohesion therefore resulted in different failure planes and thus could not be considered a practical situation. An expression for active thrust applied by cohesive backfills considering both horizontal and vertical earthquake coefficients was then introduced by Richards and Shi [21]. The approach by Prakash and Saran [20] has been extended to include retaining walls with an inclined backfill by Shukla and Gupta [23]. They developed an expression to include the total active force from the cohesive backfills on the retaining wall based on the Coulomb sliding wedge concept, considering both horizontal and vertical earthquake accelerations and maximizing the pressure to define a single failure plane [23]. When these methods are compared, Shukla and Gupta's method computes lower values of passive earth pressure than previous methods. This is because this method maximizes the total active force in order to produce one single failure plane. This is a more realistic model for calculating earth pressures [23].

Other research has been completed that can improve AASHTO's equilibrium method. Cai and Bathurst [24] consider the failure modes of external sliding along the base of the MSE wall, inertial sliding along a reinforcement layer and through the facing, and the block interface shear between facing column units. They demonstrate that a consistent application of the M-O theory may be conservative in that it requires more reinforcement closer to the wall crest. Displacements must also be taken into account when designing MSE walls. An example of displacement-based methodology is given for the stability analysis of the three potential failure modes of the modular block MSE wall. Excessive deformations can occur happen every time the ground acceleration is larger than the critical acceleration for each failure mode. The deepest interface layer is the most critical layer for internal sliding. Available facing shear capacity is not critical in the design of MSE walls. For seismic conditions, the most critical condition exists at the top-most layer for block-block/block-geosynthetic interfaces [24].

Choudhury et al. [25] compare the different methods to compute the active and passive earth pressures under seismic conditions for retaining walls, as well as for design of earth dam and shallow foundations. For retaining walls, mostly pseudostatic force-based and displacement-

based analyses are used to compute seismic earth pressures. In pseudostatic force-based analyses, the effects of the earthquake are applied as constant horizontal and vertical accelerations. These pseudostatic accelerations are then converted to horizontal and vertical inertia forces. The M-O method is commonly used, but it overestimates passive earth pressures when the wall friction angle is more than one third of the soil friction angle. In order to correct this, a curved rupture surface analysis is considered. The point of application of the seismic load is determined using the method of slices. The displacement-based analysis was also modified to analyze retaining walls using either a coupled rotational and translational approach, a decoupled translational approach, or a decoupled rotational approach. It is concluded that displacement-based analysis should be used rather than pseudostatic limit equilibrium analyses for the safe and economical seismic design of retaining walls. The point of application of seismic earth pressures should be computed based on logical analysis instead of an arbitrary selection as suggested by design codes.

Displacement-based methods are seen to be a good complement or alternative to the simplified M-O method. There have been many research projects that compare and evaluate the different displacement-based methods. The external stability of MSE walls is analyzed by using the same procedure as a cantilever retaining wall. When comparing finite difference methods to Newmark's sliding block method [26], it is shown that Newmark's method is not always conservative. In a study performed by Callisto and Soccadato [27], of twenty four different cases of cantilever walls with different properties and dimensions, it is shown that the largest accelerations always occur at the top of the wall. Walls with less stiffness accumulate more permanent deformations. Callisto and Saccadato recommend that for severe earthquakes, the critical acceleration be determined through an iterative process using limit equilibrium. This critical acceleration can be compared to the max acceleration in the vicinity to determine the magnitude of likely permanent displacements. Instantaneous distribution of contact stresses in the wall can produce larger bending moments than calculated using the critical acceleration. Therefore it is recommended that a representative bending yield strength of the wall be provided for each wall section [28].

Siddharthan et al. [28] present a computational model that predicts the permanent deformations including the distribution of these displacements for multiblock models. Four different small-scale experimental models were examined in dynamic geotechnical centrifuge

tests in order to obtain results. The applied accelerations ranged from 0.48g to 0.9g. The model is split into three different layers of movable blocks to find relative displacements. The permanent deformations of the wall were then calculated when a determined threshold acceleration was exceeded [29], resulting in the presented model for permanent deformations.

Cai and Bathurst [29] discuss the results for different displacement-based analyses for seismic loading on MSE walls. The amount of movement of the soil structure cannot be determined from pseudostatic methods, which are most commonly used. Newmark's sliding block method [26], Franklin and Chang's upper bound method [30], Richards and Elm's upper bound method [31], Whitman and Liao's mean fit method [32], and Cai and Bathurst's mean upper bound method [29] use peak acceleration and peak velocity as reference parameters. The results of all these methods are compared, with Richard and Elm's [31] being the most conservative. Methods using maximum acceleration and predominant period as reference parameters include Sarma's method [33], Makdisi and Seed's method [34], Yegian et al.'s method [35], and Amdraseys and Menu's [36]. A comparison of these methods is performed. It is shown by a case study that these methods fall within a reasonably narrow band. According to statistical data, Ambrseys and Menu [36] and Yegian et al [35] give better estimates of permanent displacements because these methods use a probability of exceedance [29].

Using LRFD methodology in the design of MSE walls has been problematic due to a lack of statistical data for probabilistic analysis of load and resistance parameters. Bathurst et al. [37] discuss how to calibrate load factors in the LRFD method. The probability of failure for a bridge is approximately 1 in 5000, and for geotechnical foundations it is proposed to be 1 in 1000. The probability of an MSE wall failure is much lower than this because of the redundancy of the soil reinforcement. LRFD is based on comparing reduced strength properties to increased load values, scaled by specified design factors. The multiple factors are based on statistical data from past experience. In order to calibrate these factors, a bias value is used of measured to predicted load and resistance values. The cumulative distribution function (CDF) is then used to calculate the probability associated with each bias value. Caution must be taken when rejecting outliers at the tails of the distribution curves because these control the estimate of the probability of failure. The older Allowable Stress Design (ASD) method can be used as a useful check until more statistical data is collected relevant to the materials of MSE walls [37].

It is obvious that from these studies there is a need for a more accurate simplified method that can be implemented in the AASHTO LRFD code. This method should be able to predict the relative deformations and displacements of the multiple components involved in a MSE wall. There have been no studies performed in determining how the connections of the geogrid to the facing units or the facing unit to facing unit connections within the walls perform under seismic loads. Since the components' interaction with each other is not clearly understood, there is currently no quantitatively based method for detail and connection design. This study aims to give insight into this issue by determining what stresses and displacements are developed at these MSE wall connections.

2.5 Finite Element Analysis of Retaining Wall Structures

Finite element methods are informative tools for MSE and other retaining wall designs as they may be used to approximate the deformation and stress responses of realistic structures with potentially complex geometries and loading conditions (e.g. [38] - [41]). The literature documenting research utilizing finite element methods for the examination of multiple aspects of MSE and retaining wall behavior is both vast and broad in scope. The following section summarizes some of the most closely related studies to the present work, providing the context for this study.

A recent study [38] evaluating the validity of finite element models for MSE wall behavior was conducted on an MSE wall, located along the I-15 reconstruction project through Salt Lake City, Utah. Instrumentation was placed in the soil to monitor foundation response. The recorded data were used to calibrate a finite element model of the MSE wall using the software Plaxis [38]. Another study comparing the real-world behavior of MSE walls to finite element predications involved the investigation of a of a two tiered five meter MSE wall [39]. The MSE wall was built, and a static surcharge load was applied by placing a precast concrete box on top and filling it with ready mix concrete as seen in Figure 2.7. Wall facing displacements and reinforcement strains were measured using LVDTs placed in the middle of the wall. ABAQUS 2006 was used to perform a finite element analysis. The results from both analyses match up fairly well, and the physical model test was used to calibrate the FEA results. It was seen that a loading pressure that exceeded the design pressure caused wall displacements and reinforcing

strains that were within the serviceability limits. The top reinforcement was most affected by the loading. The load carrying capacity of the wall was governed by the failure of the backfill soil and reinforcement pull out strength rather than the rupture reinforcement strength. It is also seen from the finite element analysis that it is importat to consider the tensile resistance of the reinforcement for walls with an isolated footing load due to evidence of a principle strain rotation [39].

Figure 2-7: Two tiered MSE wall and surcharge load using concrete box [39]

Further researchers have used finite element modeling to examine specific detailing aspects of MSE walls. Rowe and Ho [42] studied the interaction between reinforcement stiffness and friction angle. A plane strain finite element model was created, using the program AFENA. It was observed that the magnitude of the vertical force transferred to the facing depends only on the friction angle and the facing/soil interface friction angle. It was found that the absolute maximum reinforcement force increases with increasing reinforcement stiffness density,

decreasing facing/soil friction angle, decreasing backfill friction angle, and decreasing facing rigidity [42].

Cantilever walls have similar global equilibrium behavior to MSE walls. More insight on soil-wall interaction is gained through dynamic finite element analyses of these walls. Green et al. [43] performed a series of non-linear dynamic response analyses of cantilever retaining walls to determine the appropriateness of the M-O method. The finite differences program FLAC was used to analyze an incremental retaining wall with backfill exposed to a dynamic loading. Interface elements were used in the model between the wall and the soil to allow relative movements and permanent displacements to occur. Lateral pressures imposed on the stem of the wall were in good agreement with the active earth pressures determined using traditional pseudostatic Coulomb expressions as well as the stresses predicted by the M-O method where accelerations are low. At larger levels of acceleration, however, the M-O method did not predict the stem stresses as well. This is due to the relative flexibility of the structural wedge, consisting of the cantilever wall and the backfill contained within, and the different motions of the driving soil wedge. Both of these violate the assumptions of the M-O method [43].

Since damage can occur from the clapping of the wall against the soil during seismic events, a geofoam buffer has been considered as a solution to global equilibrium of cantilever walls by Trandafir and Ertugral [44]. Expanded polystyrene (EPS) geofoam is proposed as an efficient way to reduce the seismic earth pressures between a rigid non-yielding retaining wall and the soil backfill. It is hypothesized that this geofoam can act as a seismic buffer in case of an earthquake, and the viability of this hypothesis is examined within the finite element environment. The boundary conditions used in the finite element model involve restrained horizontal and vertical relative displacements along the bottom of the cantilever wall model. There is also an absorbing boundary along the vertical edge in the far field. The time history of the horizontal earthquake acceleration from the October 23, 2004 Chuetsu, Japan was used on the model. It was found that smaller permanent seismic deformations occur with the geofoam [44]. Absorbing boundaries are also used in the present study. The absorbing boundaries are referred to as “non-reflecting” boundaries and are applied at boundaries representing infinite extension of soil.

Counterforts are much like cantilever walls in that they are large precast concrete free-standing retaining wall structures. The design of such walls under earthquake loads using

Newmark's sliding block method and finite element analysis was presented by Davies et al. [45]. In order for Newmark's method to show consistent and rational results for both forced-based and displacement-based design requirements, there needs to be a 50% reduction in the peak ground acceleration value used, Davies et al. [45].

MSE walls are more difficult to model than cantilever walls using finite elements. However, finite element methods are one of the most accurate tools for determining stresses, strains, and displacements of these walls, due to their complex geometries. Karpurapu and Bathurst [40] perform a study on finite element modeling of MSE walls. They discuss the details of the finite element method and models used to simulate the response of two constructed full-scale MSE walls. The program GEOFEM is used because this program provides nonlinear constitutive models for soil-polymeric reinforcement interfaces, as well as soil-facing block interaction. A modified form of a hyperbolic function is used to model soil in order to capture dilation behavior. The FE models of two types of MSE walls were loaded with surcharge until failure. The first wall simulated a full height panel wall and the second simulated a segmental panel wall. Both structures demonstrated a well-developed internal failure through the reinforcement zone. The uppermost reinforcement layer of the full height panel wall ruptured at the panel wall connection. Strains within the reinforcement were highest at panel connections and at the location of the internal soil failure plane. The segmental panel wall failed in two distinct steps: initial shear failure of the soil in the reinforced zone and load transfer to the reinforcement [40].

Cai and Bathurst [46] present results for a two dimensional finite element analysis of a MSE wall model consisting of modular block facing units using the program TARA-3. With these types of walls it is very important to consider the block-block, block-geogrid, and geogrid-soil interfaces. Interface shear between the wall components is modeled using slip elements. The soil is modeled as a non-linear hysteretic stress-strain material. The reinforcement is modeled using a hysteretic model as well. Slip elements obey the behavior of the Mohr-Coulomb criterion. Relative displacements and shear forces are seen to be greatest at interfaces where a geosynthetic is present. Limit equilibrium method reinforcement forces were consistently greater than those observed in the FE model. The horizontal accelerations predicted at different locations in the unreinforced soil mass and facia column showed that peak accelerations occurred at the same time across the wall system [46].

Yogendrakumar et al. [41] examined two different finite element analysis approaches to model MSE walls under seismic loading. These are called the equivalent linear elastic method and the incremental elastic approach. These are computed using QUAD4B and TARA-3 respectively and compared with field results. The QUAD4B program uses the equation of motion and assumes the wall is a damped elastic model. It is described by Poisson's ratio, shear-strain dependent shear modulus, and equivalent viscous damping ratio. An iterative process is required to determine the shear modulus and damping ratio. In order to determine permanent deformations, Newmark's method must be used [26]. TARA-3 uses the tangent shear and tangent bulk modulus. It also uses a Rayleigh type viscous damping. The program allows both static and dynamic analysis which gives more realistic results and allows for permanent deformations to be calculated. The field test was done at UCLA by setting blasts off in front of an MSE wall and recording the accelerations in the wall. The experimental and predicted results are in good agreement for both programs except for QUAD between 0.25 and 0.69 seconds where excessive accelerations were predicted. It is concluded that the incremental elastic approach is the more accurate method to use [41].

The previous studies provide a precedent that the finite element method is an appropriate means for modeling the behaviors of MSE walls. The literature also proposes several alternative methods to the M-O method as well as several different ways to perform a finite element analysis on retaining structures give more accurate results. To the knowledge of the authors, there has not been specific research in the area of design of better connections or the prevention of top block chatter on modular block walls or the end of wall treatment. In general, MSE walls have performed fairly well in seismic events due to the wall flexibility. However, there have been incidences of MSE wall failures with seismic events with large vertical components. The study of MSE wall detailed connections under seismic loading is the next step to contribute to this vast field of research.

3.0 NATIONAL DOT SURVEY

To determine if other state Departments of Transportation have examined the effects of the revised AASHTO code on their MSE wall designs, a national survey of state DOTs was performed. Beginning May 2010, a survey prepared by the CSM research team was mailed electronically to all state DOTs. A list of DOT employees contacted is listed in Appendix B. The survey questions were presented as follows:

- Approximately how many MSE walls does your state DOT maintain?
- Approximately what percentage of your total retaining walls are MSE walls?
- Are there any common problems you have observed on the MSE walls especially regarding paneling, coping or connections?
- Do you have procedures or standards in your state for detailing MSE walls? If yes, can you provide a web link or direction to acquire your standard and specification data?
- Has your state DOT conducted and observed performance issues in your retaining wall systems that are attributed to dynamic or seismic load effects? If yes, have they been documented, and can you provide us a link to or the actual documentation?
- Has your state DOT studied dynamic or seismic effects on MSE walls? If yes, have they been documented, and can you provide us a link to or the actual documentation?

Forty departments (80%) completed the survey. Of the responding DOTs, thirty-nine (98% or the responding) maintain MSE walls in their states. This is another indication of the ease of constructability and cost effectiveness of MSE walls as seen by Tatsuoka et al [6]. Twenty-nine (73% of the responding) use the AASHTO LRFD Bridge Design Specifications currently. Of those that do not use the AASHTO code, most are moving to implement this code within approximately one year. Eighteen (45% of the responding) of the state DOTs design their walls for seismic loads. Two (5% of the responding) have performed seismic research to improve retaining wall designs. This section summarizes the received responses. It is important to note that the issues of MSE wall detailing associated with the facing connections, corner joints, and ends of walls under the more stringent seismic loadings mandated by the 2007 AASHTO LRFD specifications have not yet been studied by other state departments of transportation. The

AASHTO LRFD specifications present design guidelines for soil reinforcement to facing connections but do not account for seismic loading.

3.1 MSE Wall Numbers and Observed Problems

The number of MSE walls maintained in each state ranges from 0 to over 1,500. The percentage of MSE retaining walls compared to the total number of retaining walls range from 0% to 100%. Most states are moving towards using more MSE walls due to their low cost and high effectiveness.

The most commonly reported problems regarding MSE wall connections and coping involve differential settlement along the wall and drainage issues. Differential settlement causes the connections to rotate, be smashed together, or be pulled apart. Drainage issues have resulted in vegetation growing in the gaps between components. The second most commonly reported issue involves inefficient construction work. Contractors sometimes over-compact the fill close to the panels, resulting in a bulging of the walls. The fill close to the panels must be compacted lightly using hand-held compactors in no more than three passes. Contractors also sometimes place fill in higher than specified lifts, resulting in incomplete compaction. Poorly glued filter fabric over joints as well as panel misalignment has caused leaking. In addition, corrosion of metallic strips and joints was reported as an issue. There have also been concerns of the effect of truck impact on the walls.

3.2 Current State DOT Codes and Design Guidelines

The eleven states that do not currently use the AASHTO LRFD Bridge Design Specification also do not design their walls for seismic loads. Nine of the states that do use the AASHTO LRFD specification do not design for seismic loads because of their low seismicity zone. Only a few states that take into account seismic loads have elaborated on or have changed the AASHTO LRFD bridge design specifications to be more conservative. These changes however, do not address connections specifically.

The state of Arizona requires 75 percent of the factor of safety value (1.5 for sliding, 2.0 for overturning, 1.5 for compound stability, and 1.5 for pullout) to be used when performing

seismic analysis [47]. California includes a conventional pseudostatic analysis in MSE wall design but does not utilize internal seismic loading considerations [48]. The state of Idaho has wall height restrictions that apply in higher seismic zones [49]. South Carolina DOT uses the AASHTO LRFD Bridge Design specification for internal stability except all accelerations coefficients used are determined using wave scattering effects. The external stability is determined using their own procedure with increased load factors and different acceleration values [50]. The Washington DOT uses the K-stiffness method [51] to perform the static portion of the internal stability analysis. The K-stiffness method is used in conjunction with AASHTO LRFD Specification sections 11.10.7.2 and 11.10.7.3. The seismic load resulting from the inertial force of the wall active zone within the reinforced soil mass, T_{md}, from AASHTO is added to $T_{\max}$ found from the K-Stiffness method. The load resistance factors can then be found in table 15-6 [52].

The Oregon DOT designs MSE walls in accordance with the AASHTO LRFD specifications except for a few minor changes noted in the ODOT Geotechnical Design Manual. If the Mononobe-Okabe method is applicable to the MSE wall to be designed, then K_h will be determined by Eq. C11.6.5-1 of the AASHTO LRFD specification if applicable:

$$K_h = 0.74A_s\left(\frac{A_s}{d}\right)^{0.25} \quad \textbf{(3-1)}$$

where A_s is the earthquake acceleration coefficient and d is the lateral wall displacement. The lateral wall displacement is equal to 2 inches, or K_h will be equal to the peak seismic ground acceleration coefficient modified by short-period site factor in accordance with AASHTO LRFD Article 3.10.3.2. Next, the maximum earthquake acceleration coefficient, A_m, is determined using K_h. If K_h is greater than 0.45g, then A_m is set equal to K_h. This value is then used to determine the total seismic active lateral thrust E_{ae} using the Mononobe-Okabe method (Equations 2-4 and 2-5). From this, the dynamic horizontal thrust P_{ae} can be calculated by taking the difference of E_{ae} and P_a. If it is determined that the Mononobe-Okabe method is not applicable, external stability seismic analyses using the General Limit Equilibrium (GLE) method in accordance with FHWA (2009) are performed. The seismic internal stability analysis

is in accordance with AASHTO LRFD specification Article 11.10.7.2 except the maximum earthquake acceleration A_m will not be reduced for wall movement [53].

3.3 Seismic Effects Studied and Research Performed

None of the responding states have reported performance issues with their MSE wall systems that are attributed to dynamic or seismic load effects. This may be attributed to the fact that significant earthquakes in the United States are not very common, and MSE walls are not specifically checked before and after seismic events. Only two states (California and Washington) have performed seismic research on structures similar to MSE walls.

Caltrans sponsored an experimental study on a full sized soundwall mounted on top of a concrete stem wall, called type 1SW using the University of California, San Diego shake table to perform this research. Caltrans has also sponsored funded studies on the behavior of soil nail wall facings and nails under increased loading. These studies have shown that nail load and facing capacity are primarily influenced by facing panel thickness, bearing plate size, and soil stiffness, while nail spacing and reinforcement ratios contribute to deformations [55]. Research is also being carried out that includes field investigations using new technologies to assess corrosion of modern metal-reinforcement systems. With these data, it is expected to improve the predictive capabilities of existing computational models for corrosion potential, metal loss, and service life of metal-reinforced systems and to incorporate this into the LRFD method for design. This report has been published as NCHRP 675 “LRFD Metal Loss and Service-Life Strength Reduction Factors for Metal-Reinforced Systems.”

The Washington DOT has a current national pooled fund study on MSE walls which includes investigation of seismic design. This report should be completed in 2012. This research involves the investigation of MSE wall strength and deformation using the K stiffness method. They are investigating if they can extend this method to apply to marginal quality backfill material and full-scale field walls. The walls will be monitored for validation. This method may eventually be incorporated into the AASHTO specifications. They are also looking into LRFD procedures for geotechnical seismic design. This project has been proposed to develop a framework for computing load and resistance factors for the seismic design of geotechnical

elements for transportation infrastructure. The current loads do not use LRFD and therefore are overly conservative [56].

In addition to these initiatives undertaken by individual state DOTs, the Federal Highway Administration (FHWA), Chile's Ministry of Public Works (MOP), University Transportation Center, Washington State Department of Transportation, University of Nevada, and Missouri University of Science and Technology all worked together to organize the transportation infrastructure reconnaissance team (TIRT) in order to observe the damages to transportation infrastructure caused by the February 27, 2010 earthquake located offshore of Maule, Chile. Two different types of MSE walls were observed at eight different sites. The MSE wall types consisted of either precast segmental panels with metallic reinforcement or modular blocks with geosynthetic reinforcement. All of the MSE walls performed very well except for at three of the sites.

At the first site, one particular modular block wall was built such that the top three blocks of the wall were not supported by backfill. These blocks were put in place to hide a surface water drainage ditch. Because these blocks were supported by only their own self-weight and the frictional connection system, they toppled off of the wall due to the horizontal earthquake acceleration. This failure mode is one of particular concern to CDOT and is examined in the finite element studies described in later chapters.

At the second site, three different full-height segmental panel walls were damaged at joint and corner details. Two of the walls experienced separation of a full height joint due to a rotation that caused the backfill to push and spill outwards. The cause of this may have been either inadequate soil reinforcement embedment length or poor placement and compaction of fill due to the tight geometries at the joint. The third wall at this site was the most severely damaged of the three and showed signs of sliding and rotation. It was speculated that this may have occurred due to liquefaction of the sand beneath the wall.

The third site with seismically induced damage involved modular block MSE walls. These walls experienced severe cracking of the facing blocks and an outward lateral deformation of approximately 4 inches. The height of these walls, 33 ft, combined with a tight corner radius has difficulty in resisting seismic loading. This cracking was caused by a shear band as seen in Figure 3.1 [54].

1 mm = 0.039 inches

Figure 3-1: Wall cracked blocked pattern in 45 degree shear bands

4.0 COLORADO SEISMIC MOTIONS

In the original solicitation, CDOT requested that real ground motions recorded in the state of Colorado be used in this study. After an extensive search of the Incorporated Research Institutions for Seismology (IRIS) database using the program JWEED and discussions with multiple officials in the Golden branch of the USGS, it was determined that all there exist no seismic motion recordings in Colorado with sufficient intensity to meet the objectives of this project. Although earthquakes up to an estimated magnitude of 6.6 on the Richter scale have occurred in Colorado, these larger earthquakes occurred before the time of recording stations in Colorado. The largest acceleration found in the IRIS database for Colorado has a PGA of $0.0003\frac{m}{s^2}$ from an earthquake of magnitude 3.7 recorded by a station 50 miles away from its epicenter; this PGA is so small as to be indistinguishable from signal noise. Therefore, due to the lack of recorded information in Colorado, it was decided that stochastic seismograms, as well as recorded earthquakes from other states (California and Illinois), and motions created using the natural frequencies of the walls would be used instead.

4.1 Stochastic Seismograms

Stochastic seismograms are often used to approximate ground motions in areas where no records are available. The simulation of stochastic seismograms is referred to as the "stochastic method" [57]. This method uses random phase spectrum modifiers such that the motion is distributed over a duration related to the most hazardous earthquake magnitude and to distance from the source. This method uses source, path, and site parameters in functional forms to predict these ground motions and is commonly used by engineers because it is particularly useful for simulating higher-frequency ground motions [57].

For this study, the USGS 2002 Interactive Deaggregation tool was used to create three different mean stochastic seismograms from Colorado sites using a target 1,000-year return period Peak Ground Acceleration (PGA). These stochastic seismograms are the best estimate of horizontal Colorado ground motions available that incorporate the frequencies of Colorado site conditions. The sites selected include: (1) the maximum PGA site (see Figure A-1 of Appendix A), with coordinates 38.2 N 107.5 W; (2) a transition from the mountains to the plains of

Colorado toward the south, with coordinates 37.6 N 104.9 W where PGA tends to be higher; and (3) a site selected in the eastern plains of Colorado, with coordinates 39.0 N 102.9 W. These three sites were selected to be geographically spread out across the geographic extents of Colorado. If a different specific location is of concern, the same methodology may be used for the selected site. Because of certain fault locations, the duration of the Eastern Colorado earthquake was 10 seconds longer than the other two earthquakes. This earthquake was trimmed to a 10 second duration to match the durations of the other earthquakes. This was done in order to reduce model run times while retaining the strongest portions of the signals. All three site locations, shown in Figure 4.1, give a broad representation of Colorado site conditions.

Figure 4-1: Stochastic seismogram site locations

Site classes are assigned to sites based on the shear wave velocity of the upper 30 meters of soil. As the shear wave velocity decreases, so does the stiffness of the rock/soil as seen in Table 4-1 [58]. The maximum PGA value for a site class B in Colorado is 0.14g. For site classes A, C, D, E, and F this PGA value must be multiplied by a site class factor. The approximate velocity of the upper 30 meters of soil in Colorado is shown in Figure 4.2.

Table 4-1: Site classifications [58]

Site Class	$\bar{v}_s$	$\bar{N}$ or $\bar{N}_{ch}$	$\bar{s}_u$
A. Hard rock	>5,000 ft/s	NA	NA
B. Rock	2,500 to 5,000 ft/s	NA	NA
C. Very dense soil and soft rock	1,200 to 2,500 ft/s	>50	>2,000 psf
D. Stiff soil	600 to 1,200 ft/s	15 to 50	1,000 to 2,000 psf
E. Soft clay soil	<600 ft/s	<15	<1,000 psf
	Any profile with more than 10 ft of soil having the following characteristics: - Plasticity index PI > 20, - Moisture content $w \geq 40\%$, and - Undrained shear strength $\bar{s}_u < 500$ psf		
F. Soils requiring site response analysis in accordance with Section 21.1	See Section 20.3.1		

For SI: 1 ft/s = 0.3048 m/s 1 lb/ft^2 = 0.0479 kN/m^2

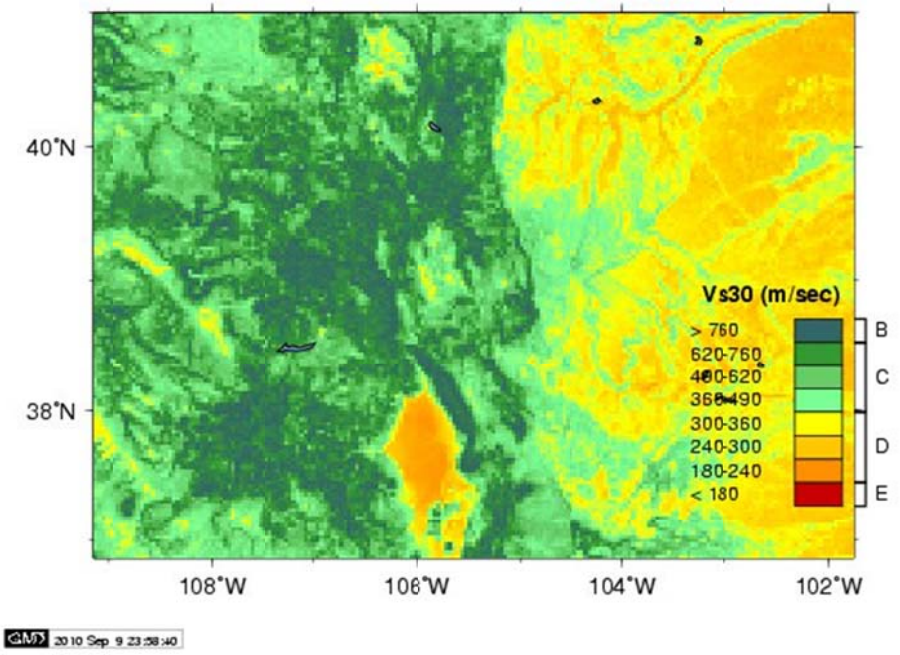

Figure 4-2: USGS Colorado soil site class map [59]

According to Figure 4.2, there is no broad site class E or F designation in Colorado. Therefore, the synthetically generated seismograms were scaled to account for Class D soil conditions as well as the maximum PGA value for a 1,000-year return period earthquake found in Colorado. The maximum combination of PGA and soil site class would be the maximum

PGA value of 0.14g combined with a site class of D which has a site factor of 1.6. This gives a maximum design acceleration value of 0.22g. Each of the stochastic seismograms was scaled to reflect this maximum design acceleration for Colorado. This is a conservative approach because the PGA value of 0.14 g is an over-prediction for most of the Colorado sites.

The acceleration versus time motions for the stochastic seismograms are shown in Figures 4.3-4.5 for the maximum PGA site, the mountain to plain transition site, and the East Colorado site, respectively. The frequency spectra for each of these seismograms are shown in Figures 4.6-4.8. The acceleration vs. time graphs are numerically integrated to obtain displacement vs. time graphs as shown in Figures 4.9-4.11. Ultimately these displacements are applied as prescribed, time-varying forcing conditions to the MSE wall models used in this study.

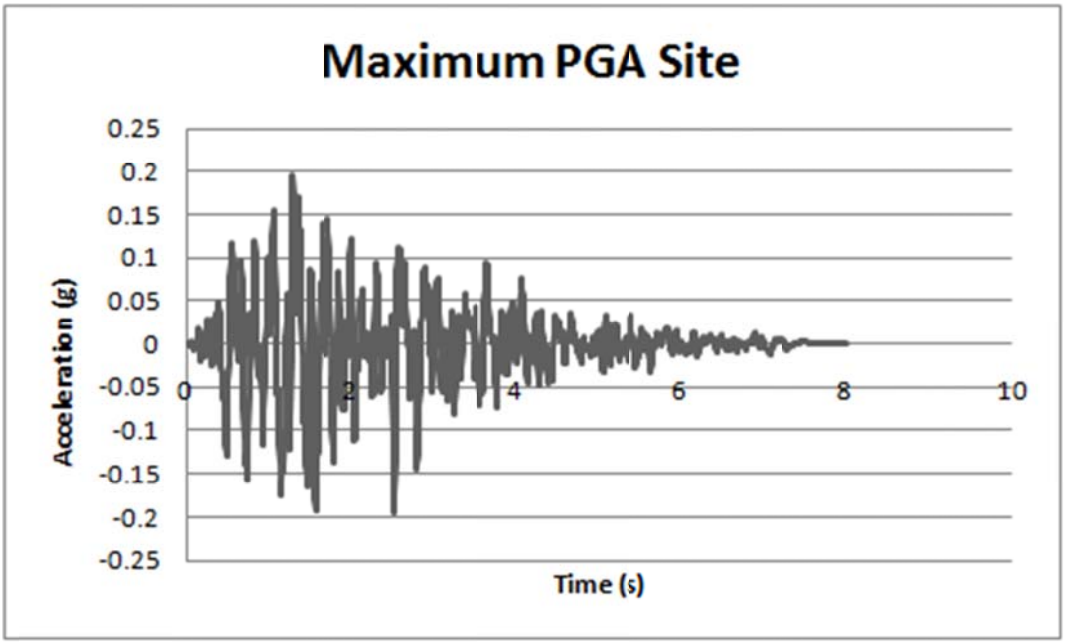

Figure 4-3: Stochastic seismogram accelerations from maximum PGA site

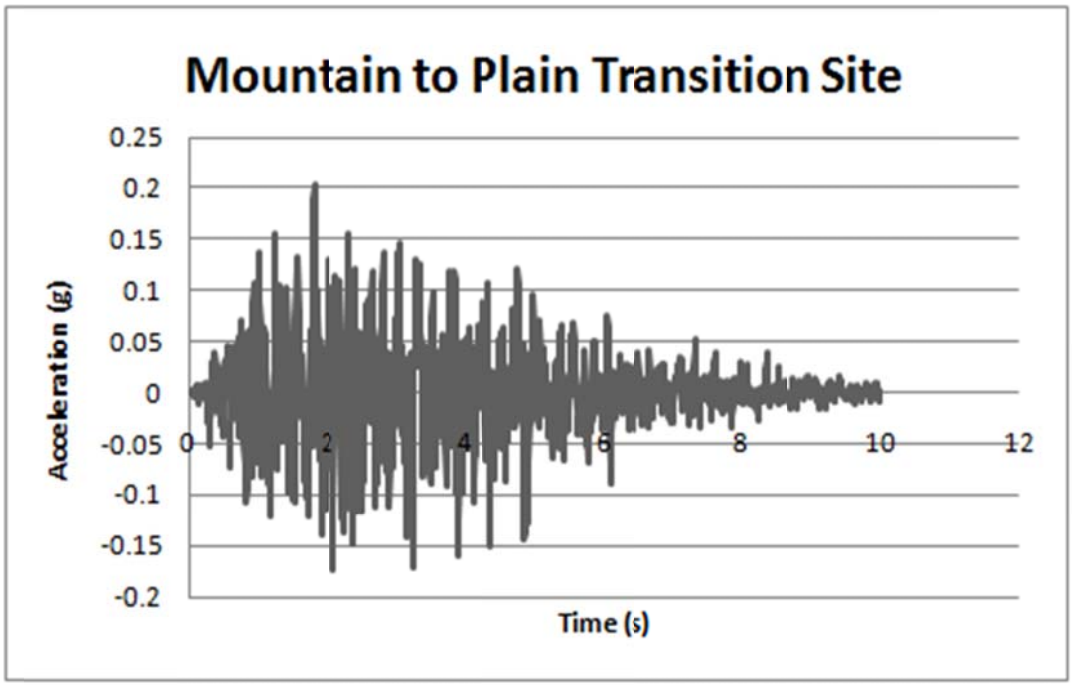

Figure 4-4: Stochastic seismogram accelerations from mountain to plain transition site

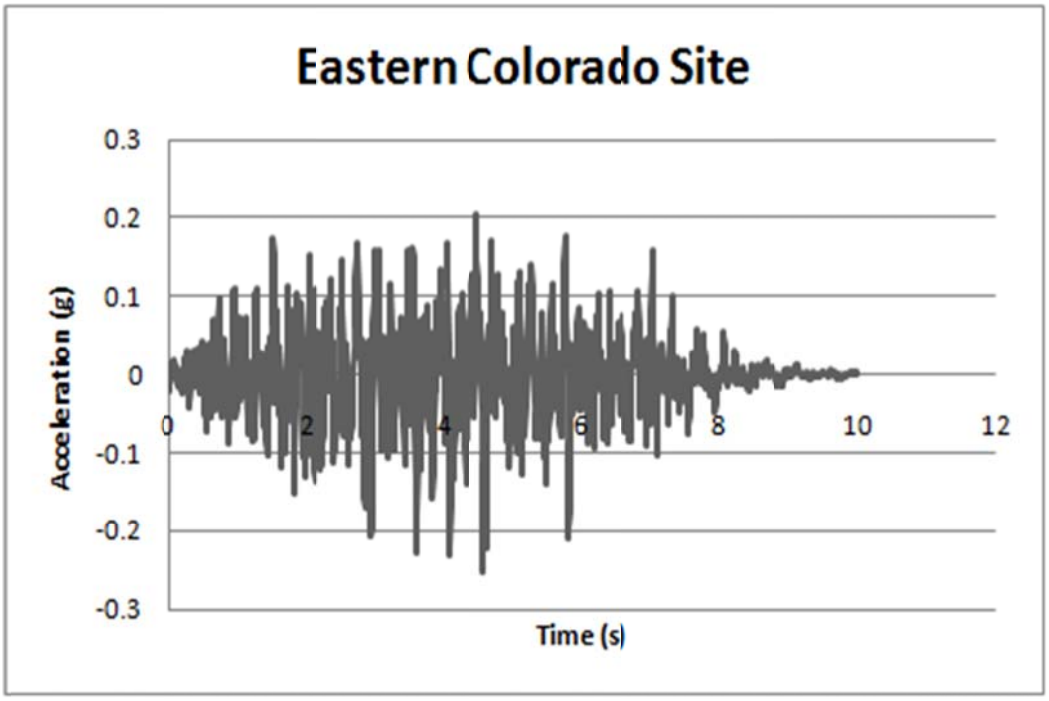

Figure 4-5: Stochastic seismogram accelerations from Eastern Colorado site

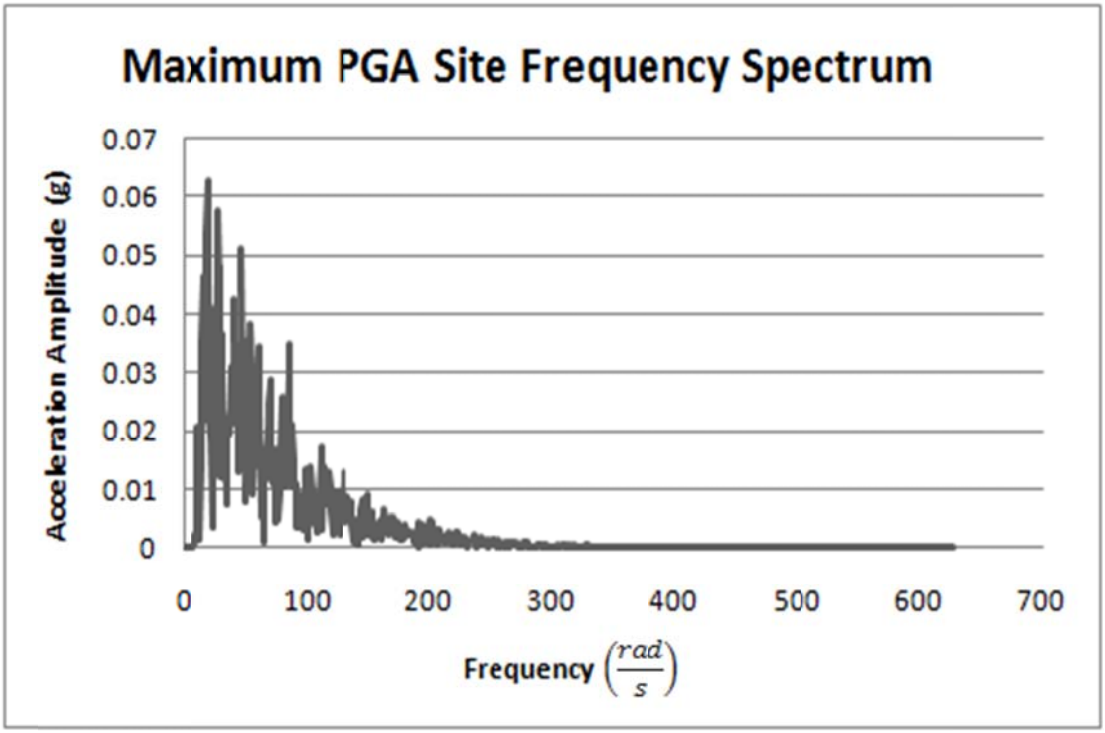

Figure 4-6: Frequency spectrum for max PGA site stochastic seismogram

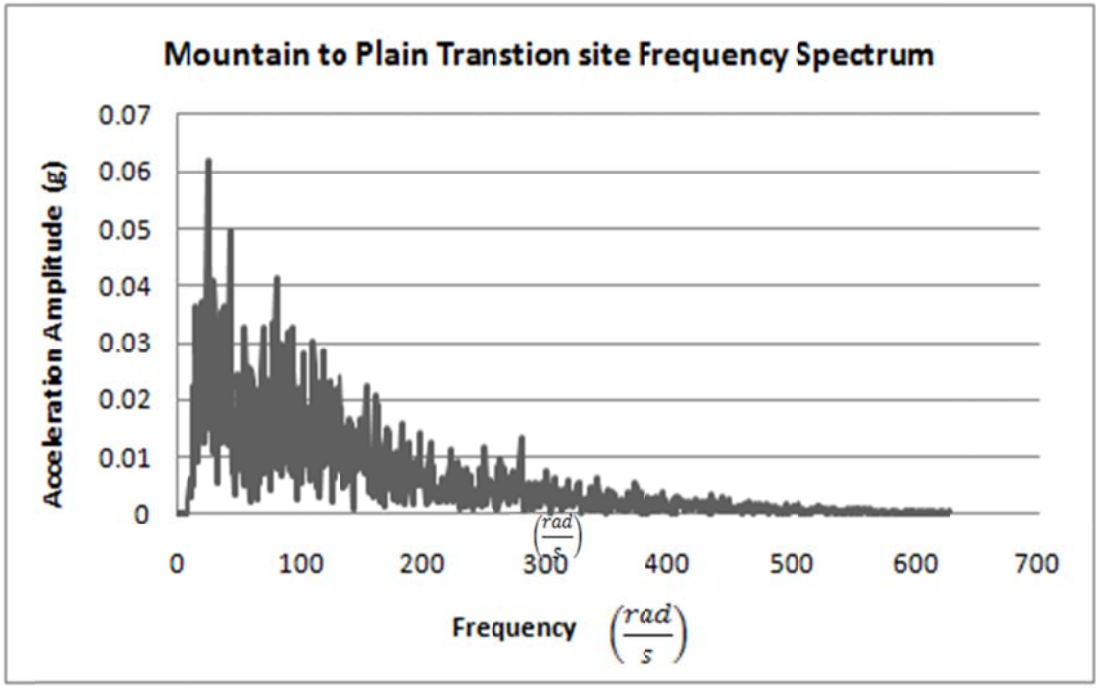

Figure 4-7: Frequency spectrum for mountain to plain transition site stochastic seismogram

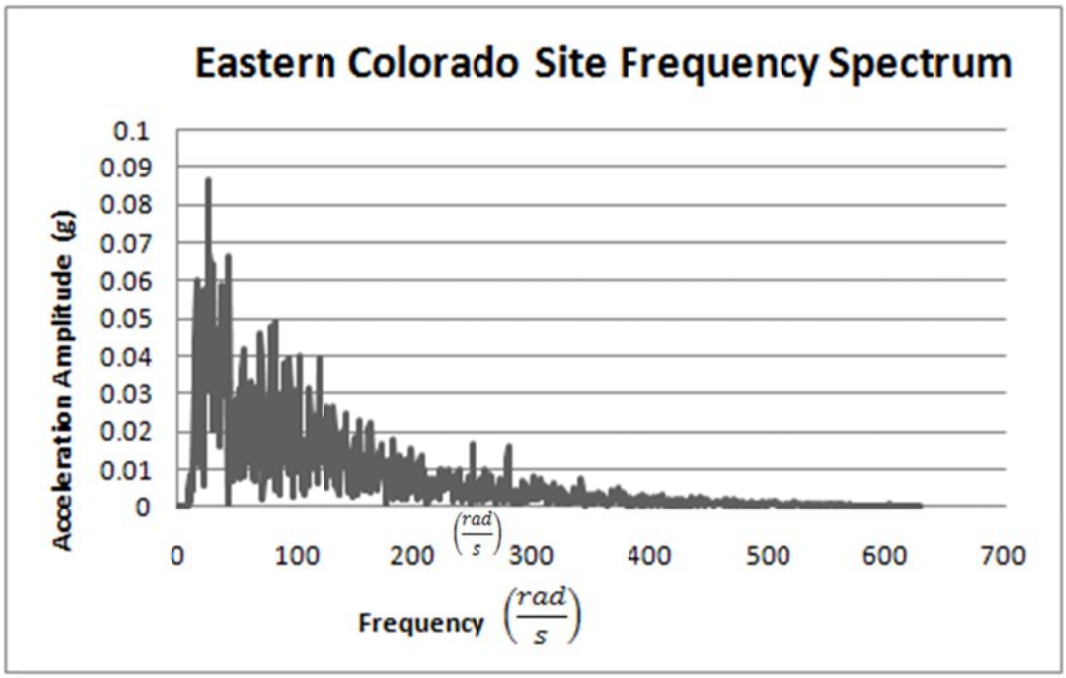

Figure 4-8: Frequency spectrum for Eastern Colorado site stochastic seismogram

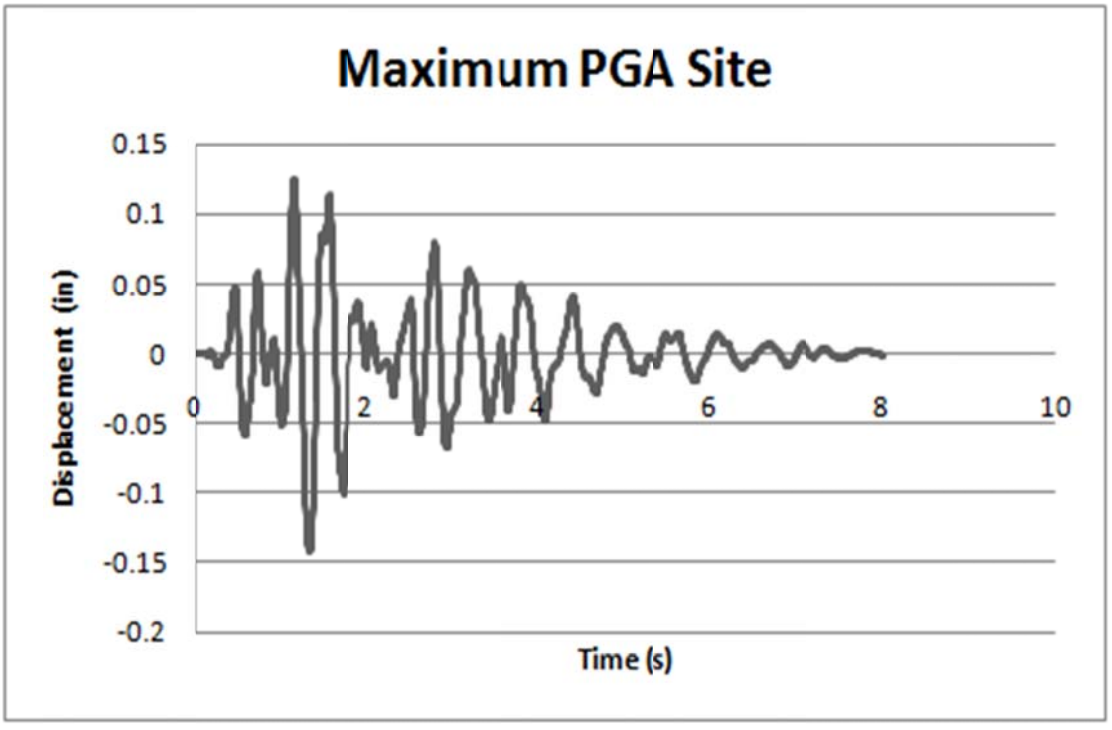

Figure 4-9: Maximum PGA site displacements vs. time

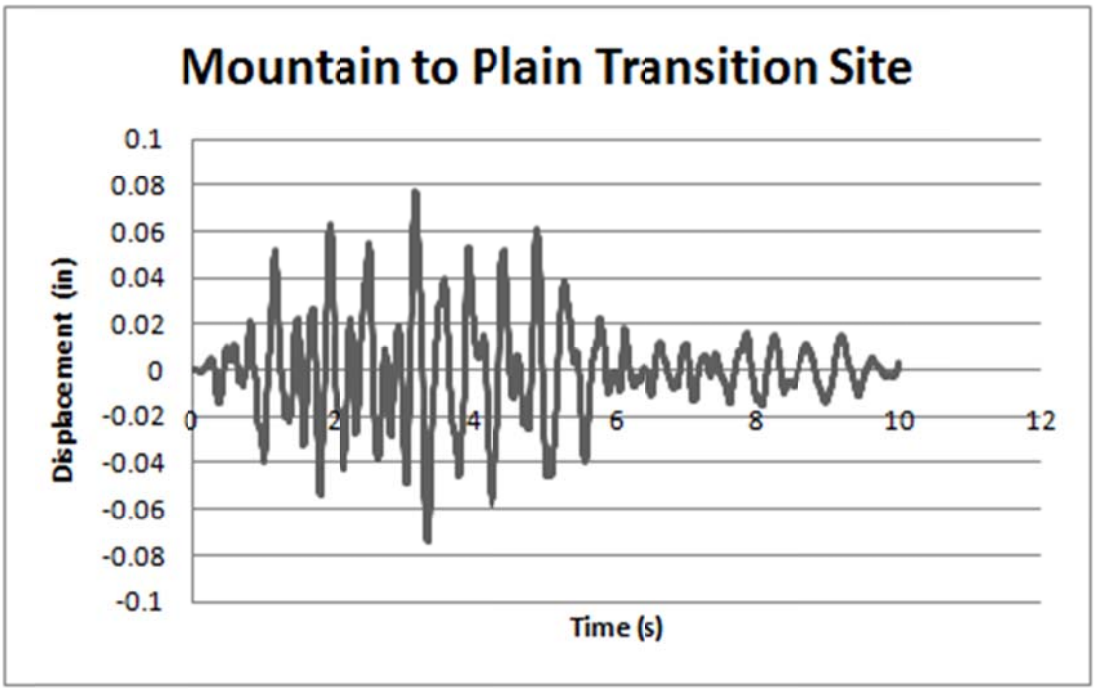

Figure 4-10: Mountain to plain transition site displacements vs. time

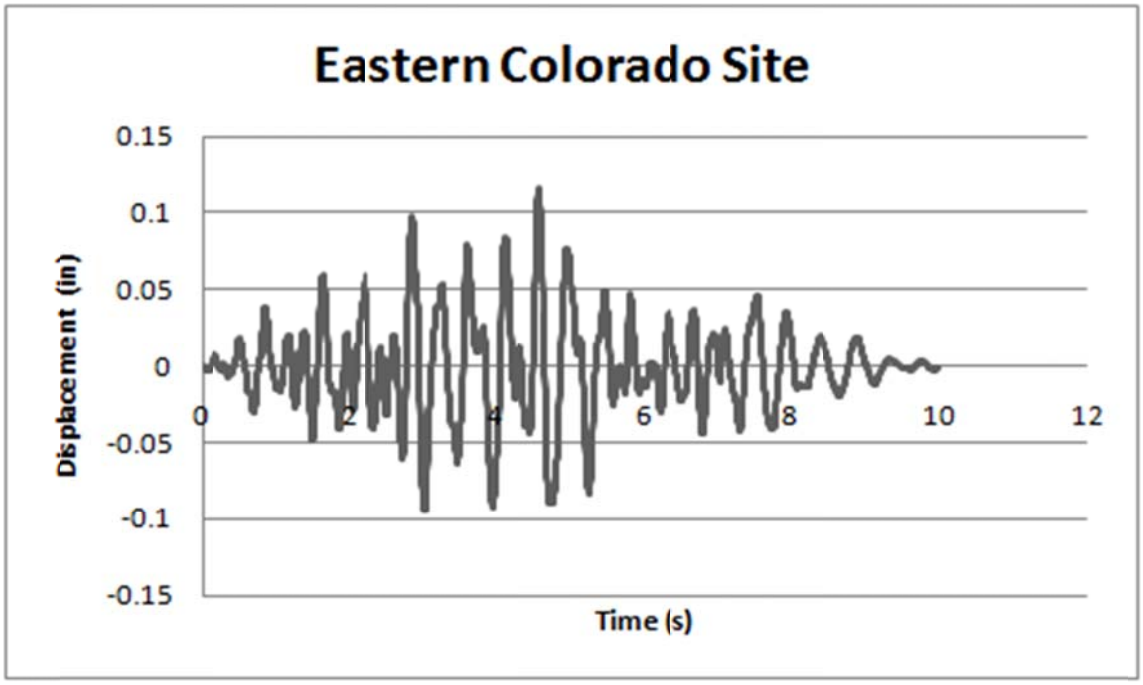

Figure 4-11: Eastern Colorado site displacements vs. time

4.2 Real Earthquake Motions Applied

Since stochastic seismograms are an estimate of ground motions, real recorded horizontal earthquake motions from Illinois and California were additionally applied to represent actual earthquake loading conditions, albeit more extreme than those to be expected in Colorado. On April 18, 2008 a 5.2 magnitude earthquake occurred in southeastern Illinois and was picked up by several recording stations, one of which was only 9.7 km away. It was recommended by USGS officials that this motion be used because the motion is representative of what could happen in Colorado, and the frequency content of this earthquake is similar to the natural frequencies of the model MSE walls being used in this study. The acceleration vs. time seismogram of this motion is shown in Figure 4.12. The benchmark El Centro, California earthquake is also used for this study. On May 18, 1940 a magnitude 7.1 earthquake struck Imperial Valley in El Centro, California. This earthquake is known as the El Centro earthquake and is commonly used because of the amount of recorded data for this seismic event. The acceleration vs. time seismogram is shown in Figure 4.13. Only the first 10 seconds of this record was used in order to decrease model run times. The first 10 seconds of the El Centro earthquake acceleration vs. time plot is shown in Figure 4.14.

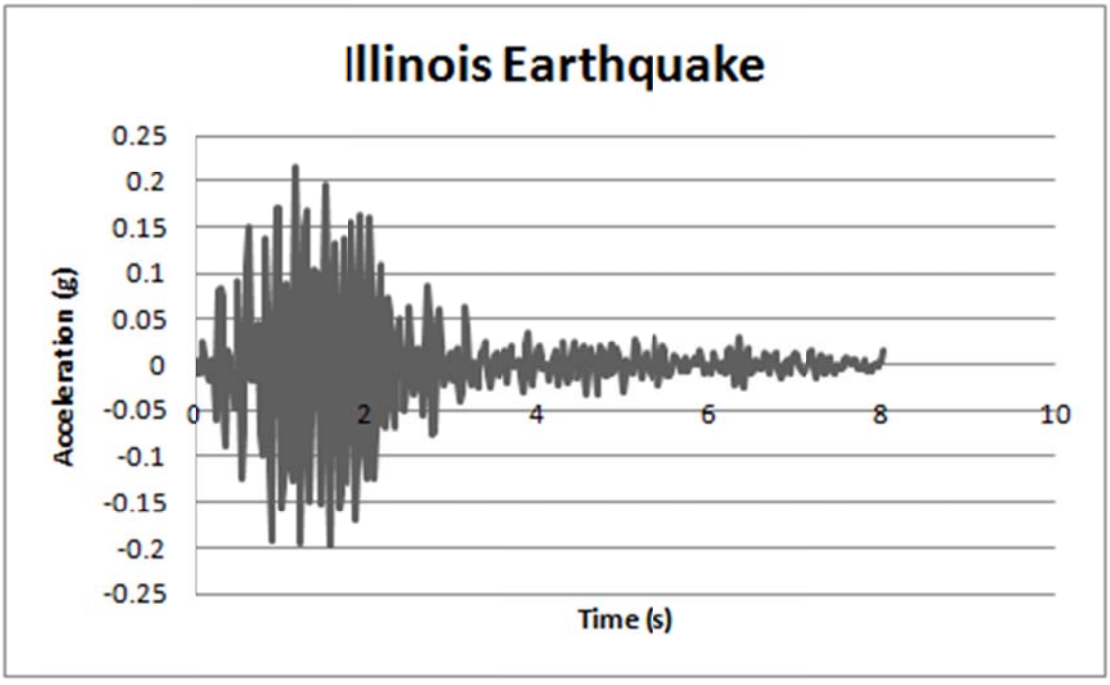

Figure 4-12: Illinois earthquake recorded accelerations vs. time

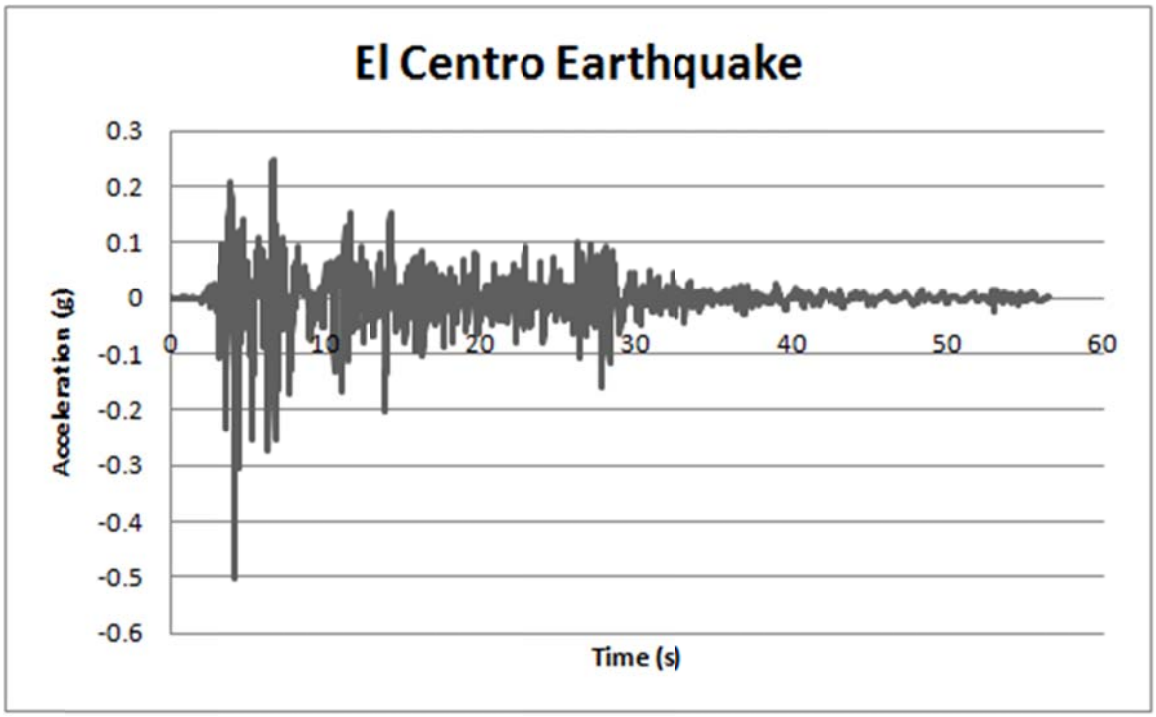

Figure 4-13: Full El Centro earthquake acceleration vs. time recording

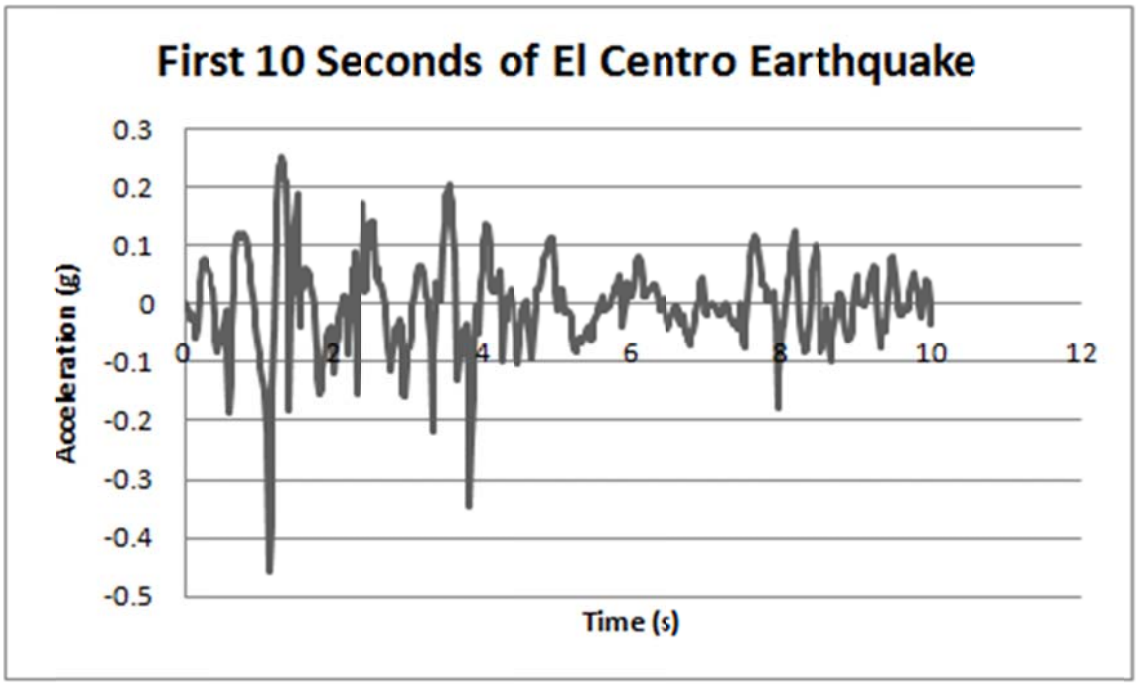

Figure 4-14: First 10 seconds of the El Centro earthquake recorded accelerations vs. time history

The frequency spectra for both the Illinois earthquake and the first 10 seconds of the El Centro earthquake are shown in Figures 4.15 and 4.16.

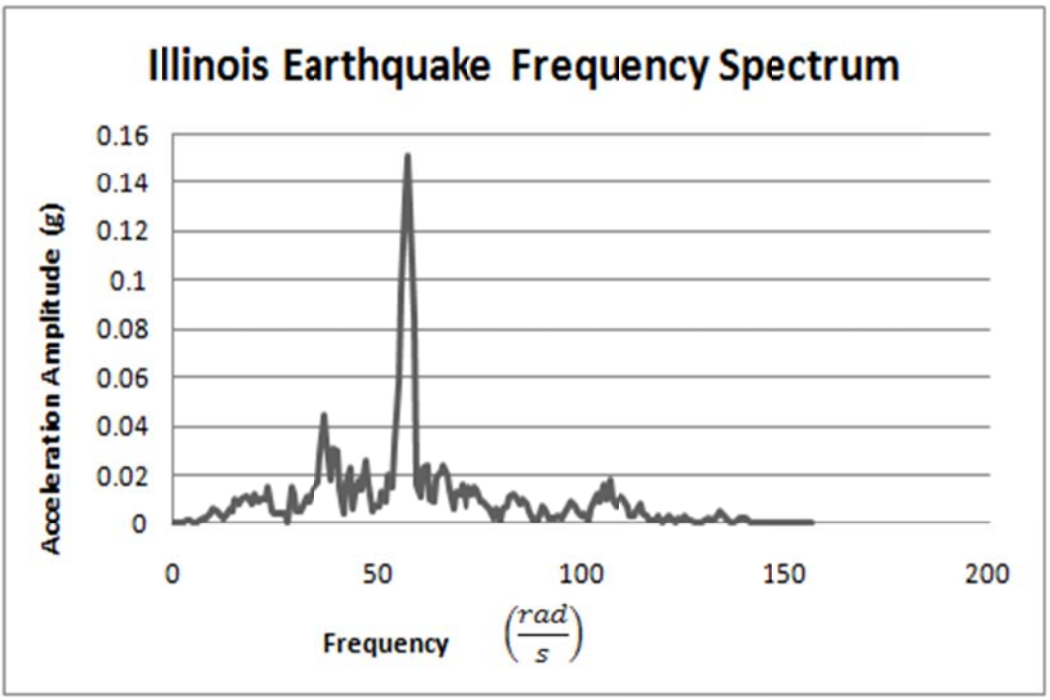

Figure 4-15: Illinois recorded earthquake frequency spectrum

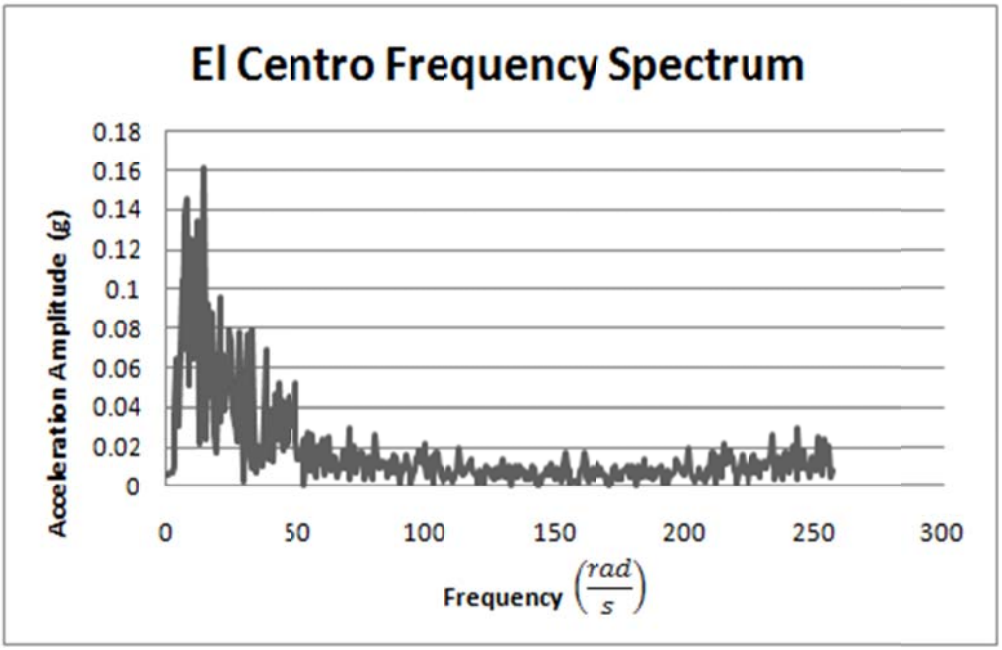

Figure 4-16: First 10 seconds of El Centro earthquake frequency spectrum

The displacements calculated from numerical integration of the recorded accelerations are shown in Figures 4.17 and 4.18. These were ultimately applied to the MSE wall models in this study.

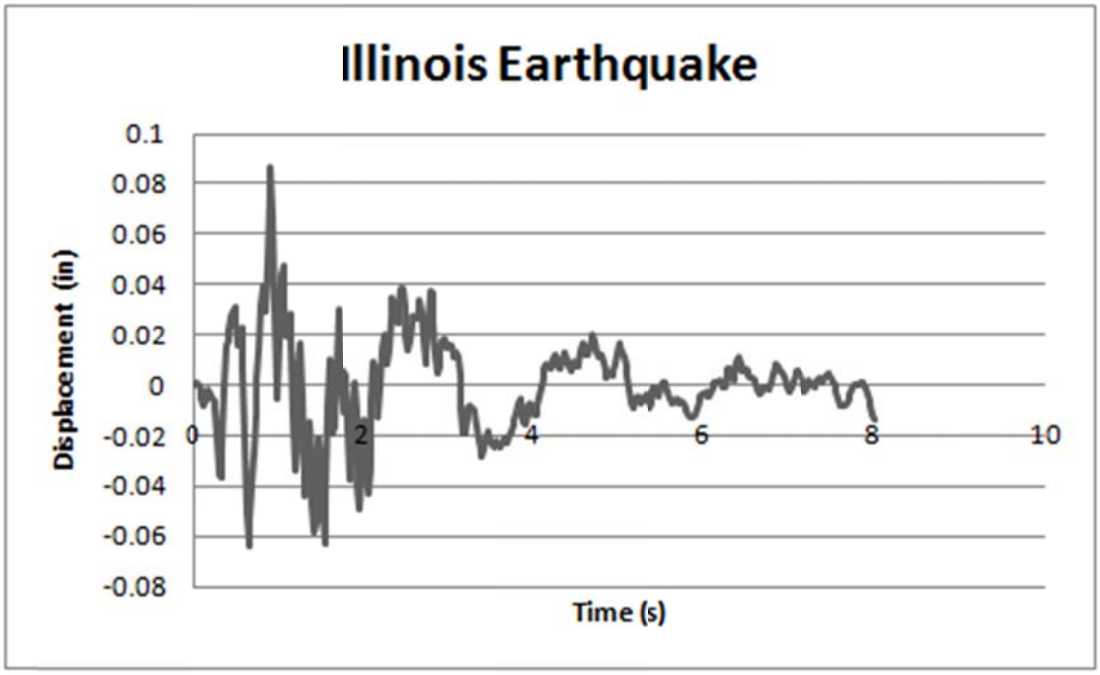

Figure 4-17: Illinois recorded earthquake displacements

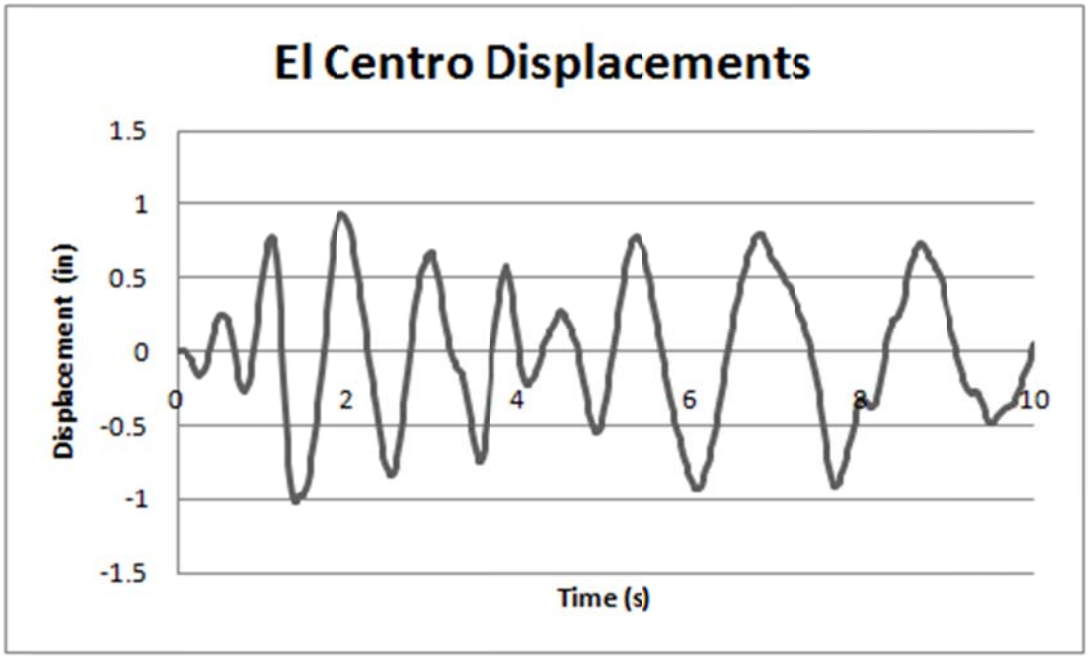

Figure 4-18: First 10 seconds of El Centro earthquake displacements

4.3 Motions Created with Natural Frequency of the 30 Foot MSE Walls

In addition to these seismic motions applied to the bases of the MSE wall models, synthetic motions were generated for the 30' walls to examine the effects of resonance on the structures. The motivation for these additional input motions is that excitation comprised of frequencies around and at the first natural frequency of the systems will result in the most extreme dynamic displacement response. The excitation of the MSE walls at their resonant frequency thus allows us to observe potentially the "worst case scenario." These additional studies were performed for the 30 foot tall walls only for illustrative purposes; the same procedures may be used for the 15 foot tall walls if desired; the resulting trends should be the same.

With a maximum design acceleration, an earthquake motion can be synthetically generated using the computational algorithm previously created by Andrés G. Lastra Núñez [60]. In this algorithm, the natural frequency of the MSE wall (0.28 seconds, as will be discussed further in Chapter 7) as well as a maximum amplitude of earthquake motion (0.22g as previously described) can be used to generate a resonant earthquake specific to the structure. Random numbers are generated and then multiplied by ten different percentages of the natural frequency. These are then used as the amplitude in the equation $A\sin(\Omega t)$, where A is the amplitude, Ω is the natural frequency and t is the time. In order to reduce run times, only the first 10 seconds of the motion were used. These shorter motions are sufficient to apply to the models in order to observe deformations due to the fact that they create the worst case scenario of resonance. These motions were applied to the 30 ft high wall models used in this study. Figure 4.19 shows the displacement applied to the 30 ft wall models using the motion created from the natural frequencies of the wall.

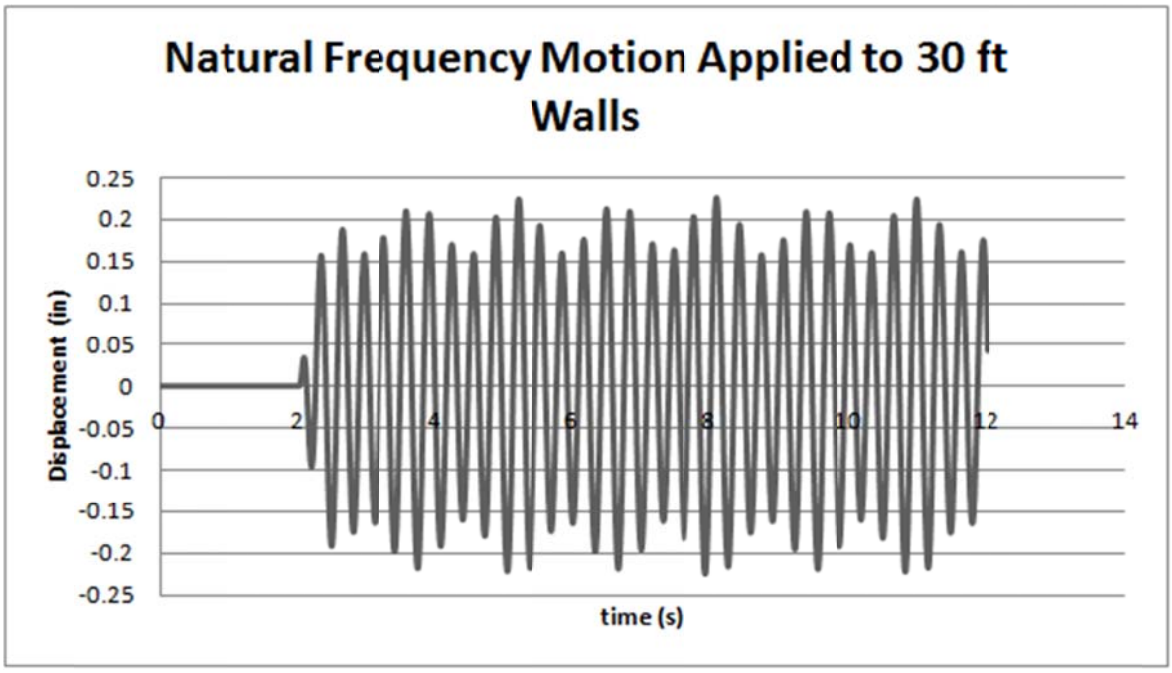

Figure 4-19: Natural frequency motion applied to 30 ft walls

5.0 LS-DYNA VALIDATION AND EXPERIMENTATION

The dynamic finite element program LS-Dyna is used in this study to observe displacements and interface stresses in connections and ends of walls of MSE wall models with the earthquake loadings selected in the previous chapter. In order to validate the understanding of the usage of this program, simple systems that can be verified with alternative analysis techniques were modeled.

In order to make a rough validation of the program's calculated displacements, a simple block model was created in LS-Dyna and subjected to the El Centro earthquake acceleration. The first mode of this model is easily approximated theoretically. A single degree of freedom model with natural frequency equal to that of the first mode of the block model was also created and was solved computationally using Newmark's method of constant acceleration. The simple block model created in LS-Dyna consisted of 125 solid elements that made up a 1m x 1m x 1m block made of an elastic material with a Young's modulus of 70,000 Pa, Poisson's ratio of 0.3, and mass density of 2,700 $\frac{kg}{m^3}$. This block has all nodes fixed at the bottom and is subjected to the El Centro earthquake motion globally in the horizontal direction. The horizontal displacements, as seen in Figure 5.1, were measured from a corner node located at the top of the block.

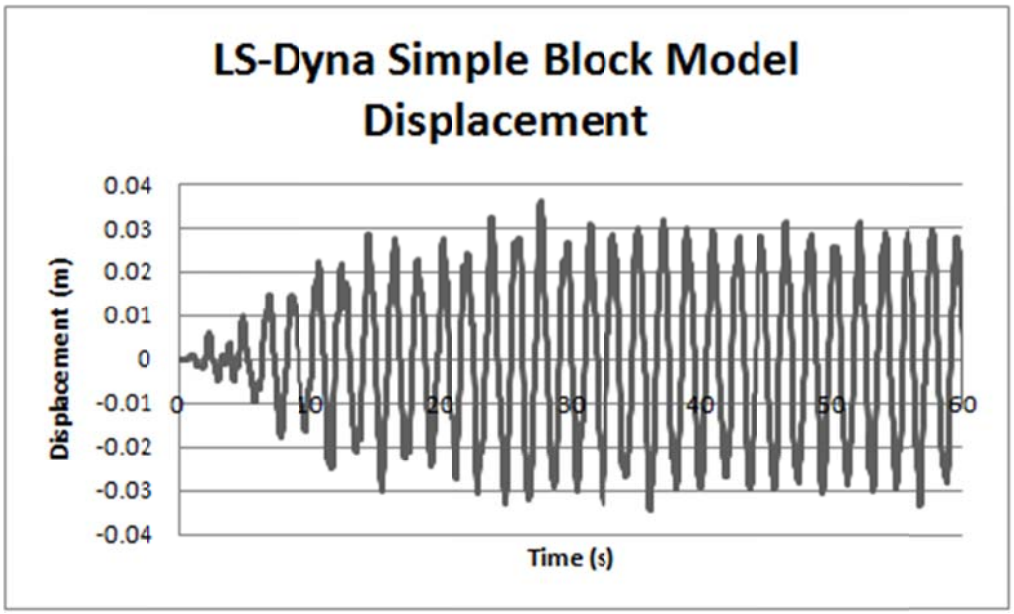

Figure 5-1: Displacement response of the top of a 1m x 1m x1m block subjected to the El Centro seismic motion using LS-Dyna

Using Hooke's Law for shearing stress and strain, the stiffness of this block to shear deformation is calculated as presented in Equations 5-1 to 5-3. Hooke's Law for shearing stress and strain is

$$\tau_{xy} = G\gamma_{xy} \tag{5-1}$$

Where τ_{xy} is the shear stress across the top of an element shown in Figure 5.2, G is the shear modulus of the element, and γ_{xy} is the angle of deformation shown in Figure 5.2.

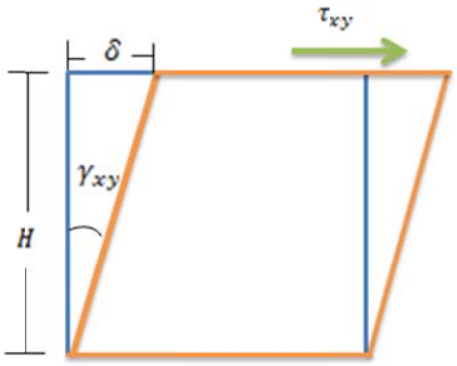

Figure 5-2: Shearing stress and strain deformations

The shear modulus is calculated as

$$G = \frac{E}{2(1+\nu)} \tag{5-2}$$

Where E is Young's modulus and ν is Poisson's ratio of the block material used in the LS-Dyna model. This results in a shear modulus of 26,923 Pa. The angle γ_{xy}, for small strains, can be expressed as $\frac{\delta}{H}$. Shear stress can also be written as force over a cross sectional area or $\frac{F}{A}$. Substituting these expressions into Equation 5-1 and solving for the force yields the following:

$$F = \left(\frac{GA}{H}\right)\delta \; or \; F = \left(\frac{2GA}{H}\right)\delta_m \tag{5-3}$$

Where δ_m is the deformation at mid-height, which is the center of mass of the block. When this equation is compared to Hooke's law of elasticity, shown in Equation 5-4, it is seen that the stiffness of this system can be calculated as per Equation 5-5.

$$F = K\delta_m \tag{5-4}$$

$$K = \left(\frac{2GA}{H}\right) \tag{5-5}$$

Using a shear modulus of 26,923 Pa, a cross sectional area of 1 m^2, and a height of 1 m, the stiffness is calculated to be $53846 N/m$. The mass of this simple block system was also calculated as per Equation 5-6.

$$m = \rho V \tag{5-6}$$

where ρ is the mass density of the system, 2,700 kg/m^3, and V is the volume of the system, 1 m^3. This gives a total mass of 2,700 kg.

Using this calculated mass and stiffness, a single degree of freedom system displacement response analysis was performed. Even though the LS-Dyna simple block model is a multi-degree of freedom system and the shear block analysis is a single degree of freedom system, the LS-Dyna block system can be effectively approximated as a single degree of freedom system vibrating in its first shear mode. This analysis was done using Newmark's method [e.g., 60] to calculate the displacement response at every time step. The output for both the LS-Dyna simple bock system and the shear block analysis using Newmark are shown in Figure 5.3. The agreement of these two separate analysis procedures on a similar system indicates that the assignment of a prescribed time-varying displacement motion is being performed correctly in LS-Dyna.

The small differences between the two models are attributed to the facts that (a) the first mode stiffness of the block was calculated on the assumption that the block is subjected to simple shear, which is a reasonable but not exact approximation, and (b) the other modes of the block have a small, but not entirely negligent, effect in its response.

Next, a modal analysis validation was performed on a simple steel cantilever column fixed at its base (Figure 5.4) to verify that modal analysis techniques were being correctly implemented. The first two modes were computed by LS-Dyna and matched up reasonably well with the exact closed-form analytical solutions as given by Chopra [61]. Figure 5.4 shows the steel cantilever beam in the second mode.

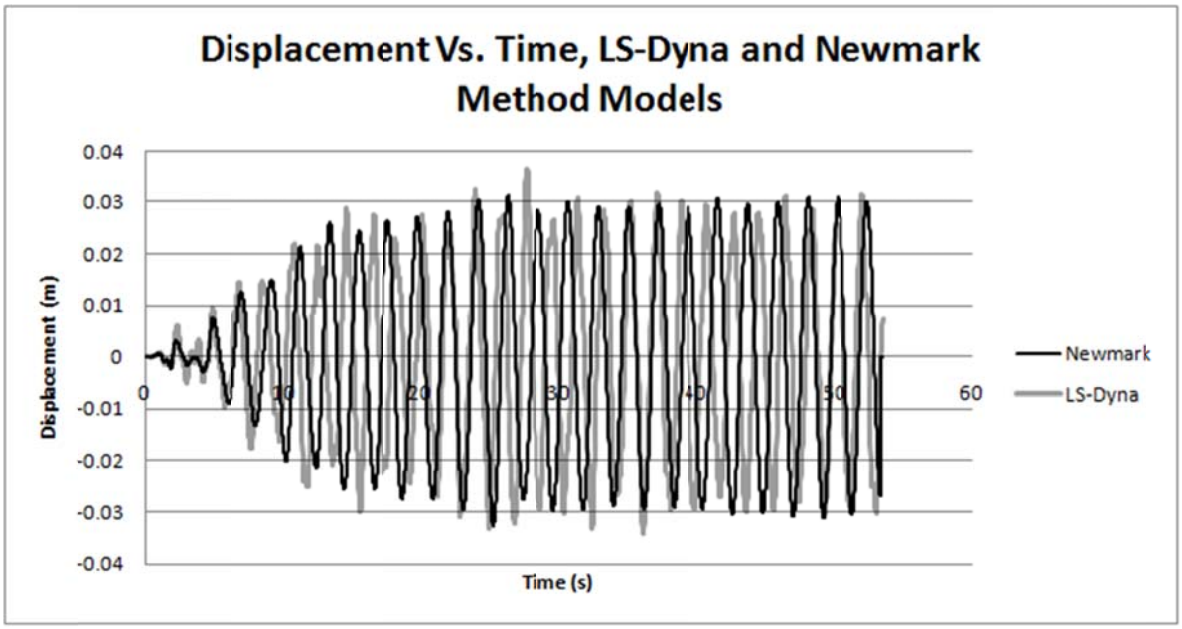

Figure 5-3: Response of a single degree of freedom system using same stiffness and mass of the LS-Dyna simple block analysis from El Centro seismic motion using Newmark's Method compared to LS-Dyna simple block model.

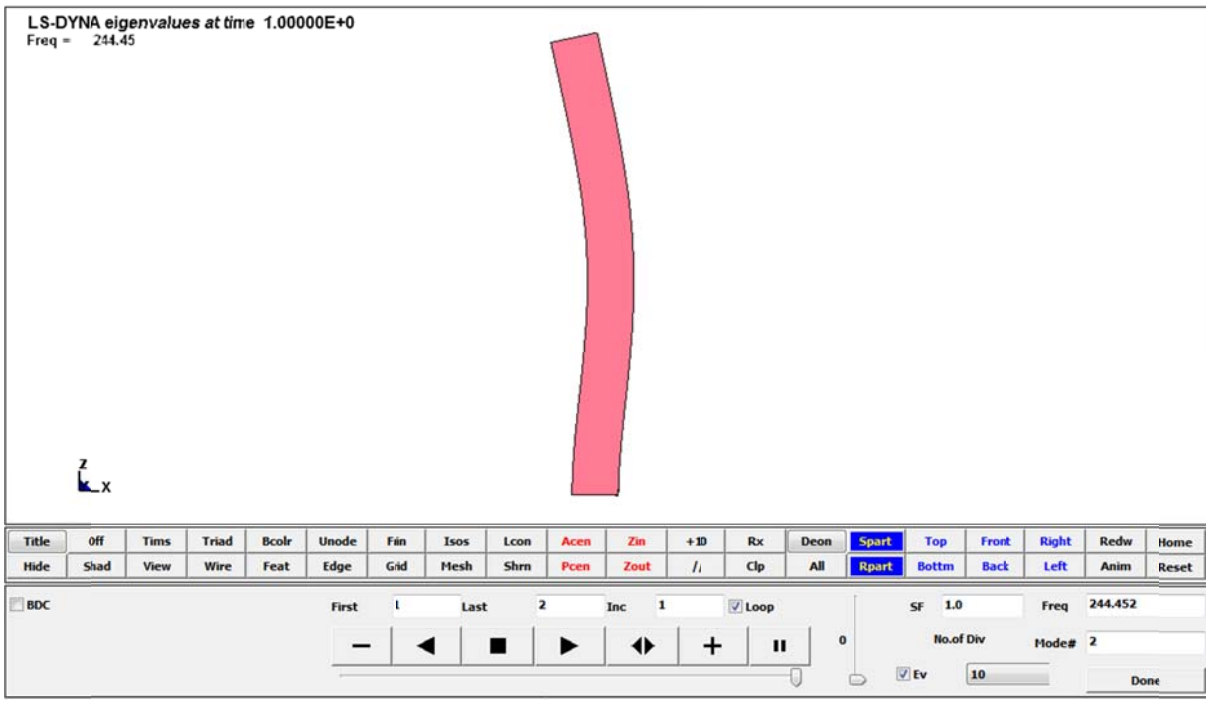

Figure 5-4: Cantilever modal analysis in LS-Dyna

The beam was designed with a cross-sectional area of .04 m^2, length of 2 m, density of 7850 kg/m^3, Young's modulus of 2 x 10^{11}Pa, and moment of inertia of 1.3 x 10^{-4} m^4. Given these parameters, the mass per unit length of the system can be calculated as:

$$m_b = \rho A = 314 \frac{kg}{m} \tag{5-7}$$

Using this mass, the first and second frequencies of the system can be calculated as:

$$\omega_1 = \frac{3.516}{L^2}\sqrt{\frac{EI}{m_b}} = 252.9 \frac{rad}{s} \tag{5-8}$$

$$\omega_2 = \frac{22.03}{L^2}\sqrt{\frac{EI}{m_b}} = 1585 \frac{rad}{s} \tag{5-9}$$

To convert these circular frequencies back to frequencies:

$$\frac{\omega_1}{2\pi} = 40.3\text{Hz} \tag{5-10}$$

$$\frac{\omega_2}{2\pi} = 252.2\text{Hz} \tag{5-11}$$

The first two frequencies of this problem, simulated with 3-D blocks, were calculated by LS-Dyna as 40.8 Hz and 244.4 Hz which are reasonably close to the exact frequencies calculated above.

6.0 MSE WALL MODELS

Based on the shop drawings provided by CDOT, it was determined that the most common characteristics of the multiple types of MSE walls built in Colorado would be incorporated in the MSE wall finite element models for testing. Full height panel walls are rarely used because of the difficulty in building them. The two most common types of MSE walls are panel walls and modular block walls. Two basic models of each of these types of walls were built for this study, a 15 foot high wall and a 30 foot high wall. These walls are modeled with geogrid reinforcement. The selection of geogrid reinforcement was made based upon an on-site discussion on May 5, 2010 with CDOT personnel during the construction of the Shaffer's Crossing MSE wall, where it was noted to be one of the most commonly used types of MSE reinforcement in Colorado.

6.1 Segmental Panel Wall Geometry and Materials

The 15 foot high segmental panel wall model was based on the shop drawing provided by CDOT listed in Appendix C, Figures C - 2 and C - 3. This wall was built mostly of CDOT type A panels. These panels are 0.5 feet thick, 5 feet high and 9 feet long (Appendix C, Figure C - 1). The reinforcement is attached to the back of these panels at two places: 12 in and 48 in above the bottom edge. The 15 foot constructed model consists of 3 panels in the vertical direction for the main wall and 12 panels in the horizontal direction. This makes the main wall a total of 108 ft long and 15 ft high. The main wall is flanked on either side by two wing walls. The wing walls form a 30 degree angle with respect to the main wall (Figure 6.1). The wing walls consist of 2 full type-A panels vertically and 3 panels horizontally making either wing wall 27 ft long. Three panels with sloping top edges are connected at the top starting at a height of 15 ft and tapering to an end height of 12 ft (Figure 6.1). The panel elements are comprised of shell elements that are free to rotate at the segmental panel connections. The different colors of the models do not indicate different material properties but are used to differentiate between each wing wall and main wall.

The reinforcement for the panel model extends 19 feet into the soil and is connected as one solid sheet extending from the wing walls to the main wall. The top reinforcement layer is

only connected to the main wall due to the sloping nature of the wing walls (Figure 6.2). The reinforcement is modeled using shell elements as well. The different colors here again do not indicate differences in material properties but show the top reinforcement layer in contrast with the other layers that are attached to the wing walls.

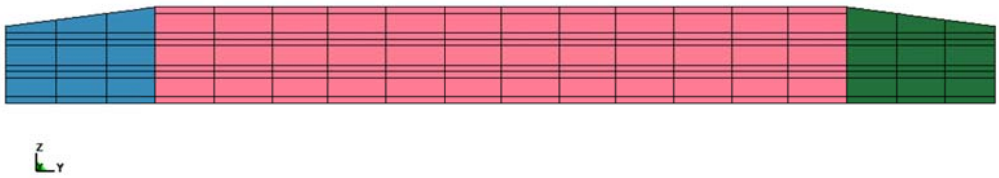

Figure 6-1: Front view of segmental panel wall model

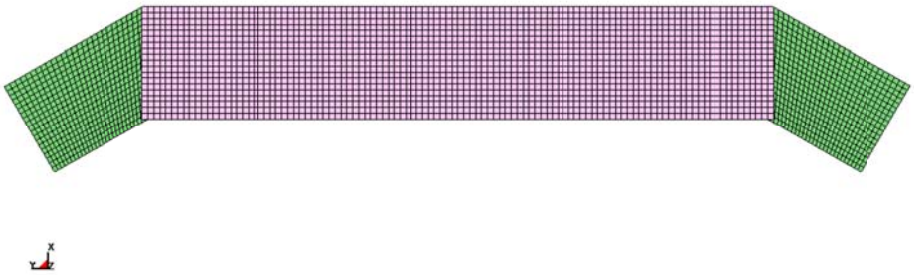

Figure 6-2: Top view of reinforcement for segmental panel wall model

The model fill is built of solid elements and matches the height of the wall. It extends for approximately 30 feet in depth. The soil mesh for the panel wall can be seen in Figure 6.3.

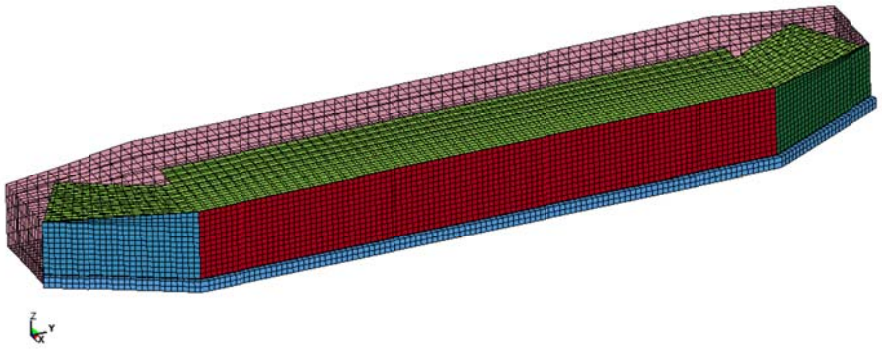

Figure 6-3: Segmental panel wall model, isometric view

The same geometry is applied to the 30 foot wall model except that the height of the wall is doubled. The soil, geogrid and length of the wall are the same as the 15 foot high wall as seen in Figure 6.4. See Appendix D for connection and construction details.

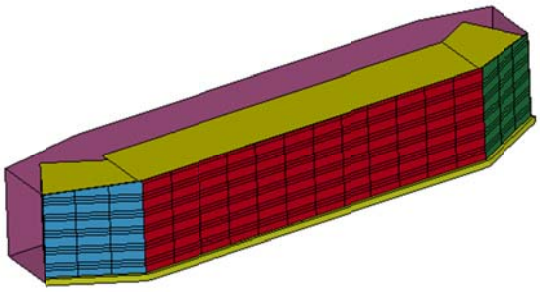

Figure 6-4: 30 foot wall model isotropic view

A layer of solid elements is added to the back side of the soil that is made of an orthotropic elastic material. This material is stiffer in the z (vertical) direction than in the x and y (horizontal) directions. These soil elements are only added for the modal analysis to prevent unrealistic vertical deformation modal shapes. These elements are 12 inches thick. These elements are not included in the time analyses. A row of solid elements is added to the front of the wall at the toe for the earthquake analysis. These solid elements represent the fill that is required in front of the base of the wall facing panels. These elements are two feet in height and one foot deep.

Table 6-1 shows the material properties used for each material for all wall models. The material properties of concrete were taken to have a unit weight of 150 lb/ft^3 [62] or a mass density of $2.27x10^{-4}\ lbs \cdot s^2/in^4$. Young's modulus and Poisson's ratio where also taken from Engineeringtoolbox.com [62]. The reinforcement is made from High Density Polypropylene (HDPE) these material properties where obtained from Wikipedia [64], Engineering toolbox [62], and the Marlex engineering properties for HDPE [65]. The soil properties were found from geotechnicalinfo.com [66] using a dense sand. The densities for the HDPE and soil materials were calculated the same way as the concrete density.

Table 6-1: Elastic material properties

	Density $(lbs \cdot s^2/in^4)$	Young's Modulus (psi)	Poisson's Ratio
Concrete	$2.27x10^{-4}$	$3.99x10^{6}$	0.2
Reinforcement (HDPE)	$8.85x10^{-5}$	$1.16x10^{5}$	0.4
Soil	$1.95x10^{-4}$	$1.39x10^{4}$	0.3

The orthotropic elastic material properties are based on the elastic soil properties except that the modulus of elasticity is made to be 6 times stiffer in the Z direction giving a modulus of elasticity of 83,400 psi. For orthotropic elastic elements the material properties must satisfy the relation:

$$\frac{\nu_{yz}}{E_y} = \frac{\nu_{zy}}{E_z} \quad \textbf{(6-1)}$$

where $\boldsymbol{\nu_{yz}}$ is the Poisson's ratio for the Y, $\boldsymbol{\nu_{zy}}$ is the Poisson's ratio for the Z direction, $\boldsymbol{E_z}$ is Young's modulus for the Z direction and $\boldsymbol{E_y}$ is Poisson's ratio for the Z direction. This results a Poisson's ratio of about 0.05 in the Z direction. The shear modulus of elasticity can also be calculated for each direction's elasticity by Equation 5-2, which results in a shear modulus of 5,346 psi in the X and Y directions and 39,714 psi in the Z direction.

6.2 Modular Block Wall Geometry

The main difference between the modular block wall and the panel wall is that the finite element model of the modular block wall is comprised of solid elements instead of shell elements such that no-penetration, compression only contacts are enforced at the between the top rows of the modular block layers. The modular block wall is built of blocks that are 8 in high, 18 in wide, and 11 in deep. The main wall is 23 blocks high, and 72 blocks in length giving it a total height of 15.3 ft and total length of 108 ft. The wing walls still angle into the soil at 30 degrees. These walls taper down to 2 ft on each end with a total length of 30 ft. The reinforcement is

placed every 2 blocks or 16 in. The soil and orthotropic elements have also been rebuilt to fit the geometry of the wall (Figure 6-4).

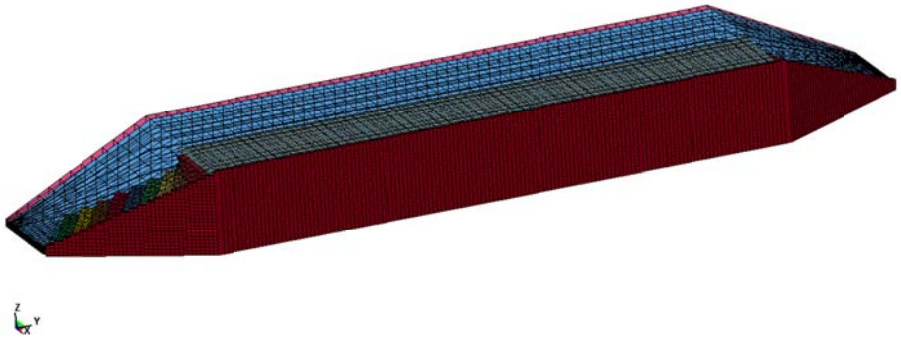

Figure 6-5: Modular block wall isometric view

The reinforcement is layered so that it shortens with the geometry of the wall shown in Figure 6.6. The reinforcement extends 17 feet into the fill as seen from the shop drawings listed in Appendix C, Figure C - 4. The modular block wall is constructed similarly to the panel wall except that between the top layer of detached blocks and the next layer of blocks and between the third row of blocks and the rest of the wall the blocks are detached to observe a “chattering” effect. Figure 6.7 shows the places in which blocks were detached.

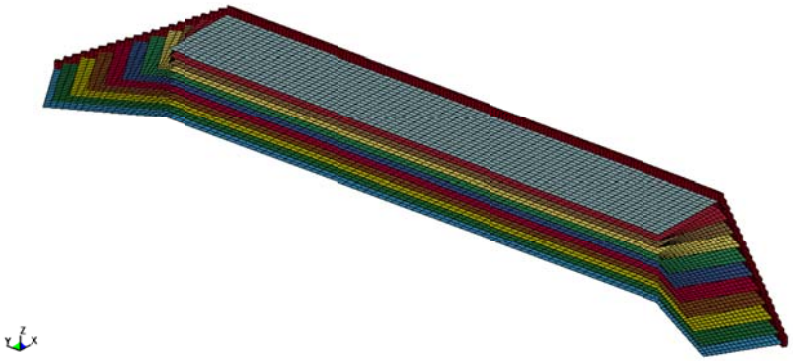

Figure 6-6: Modular block wall view of reinforcement

Figure 6-7: Showing free edges of modular block wall

The 15 foot modular block wall was doubled in height to create the 30 foot modular block wall seen in Figure 6.8. Again, the reinforcement, soil and wall lengths are the same. See Appendix D for connection and construction details.

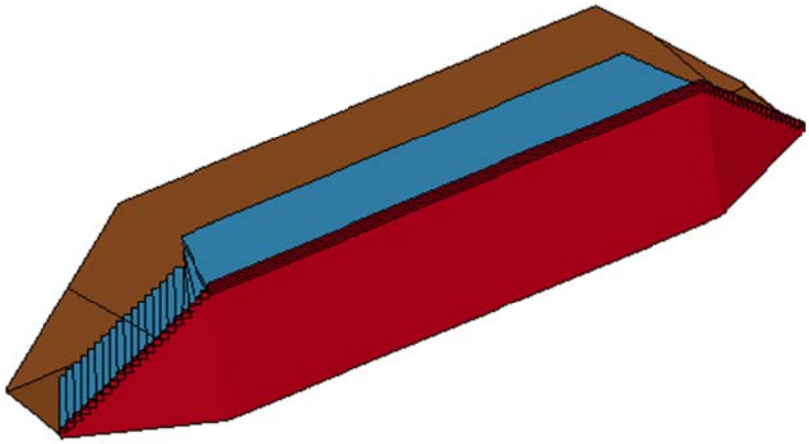

Figure 6-8: 30 foot modular block wall isotropic view

6.3 Loading and Boundary Conditions

The boundary conditions for these models are applied to all nodes that are in contact with the ground. These nodes have all rotations constrained as well as translation in the Y and Z directions. The next boundary condition applied is the non-reflecting boundary condition. This is applied to all nodes that represent a fictitious boundary of a soil that extends infinitely in the horizontal direction. This option prevents artificial reflection of waves back into the soil everywhere that there is an infinite boundary.

For all models, gravity is applied linearly over a period of two seconds before the earthquake displacements are applied. This allows for the model to come to rest from gravity loading before the earthquake displacements are applied. The earthquake displacements are applied to the back and bottom of the earthquake model.

7.0 RESULTS AND ANALYSIS

7.1 Results for 15 Foot High Walls

7.1.1 Modal Analysis Results

Modal analyses were performed on the 15 foot high panel and modular block walls in order to determine the natural period of the wall structures and the first three mode shapes. These analyses were also performed in order to determine what mode shape is most dominant for MSE wall structures. For the panel wall, the frequency for the first mode is calculated to be 7.58 Hz which gives a natural period of 0.13 s and a circular natural frequency of 47.6 rad/s. The natural period and circular natural frequency of the 15 foot panel wall for all three mode shapes are listed in Table 7-1.

Table 7-1: Modal analysis results for segmental panel wall

	Natural Period (s)	Natural Frequency (rad/s)
mode 1	0.132	47.6
mode 2	0.127	49.6
mode 3	0.121	52.0

The first mode causes the structure to bow in and out as seen in the top view of Figure 7.1. Figures 7.1-7.3 are all top views of the MSE wall models where the facing units are located in the most positive X direction.

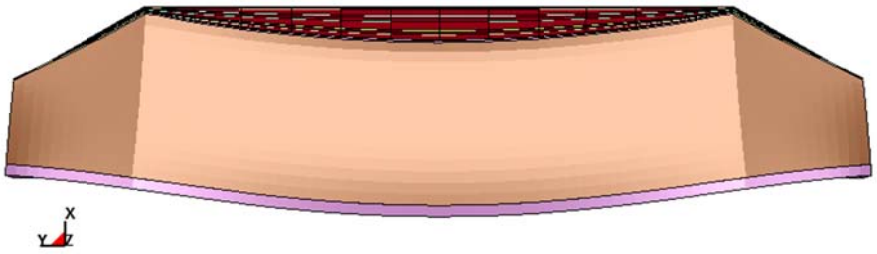

Figure 7-1: Mode shape 1 of the 15 foot segmental panel wall

The second mode shape creates a wave in which the two wall joints swing back and forth as see in Figure 7.2.

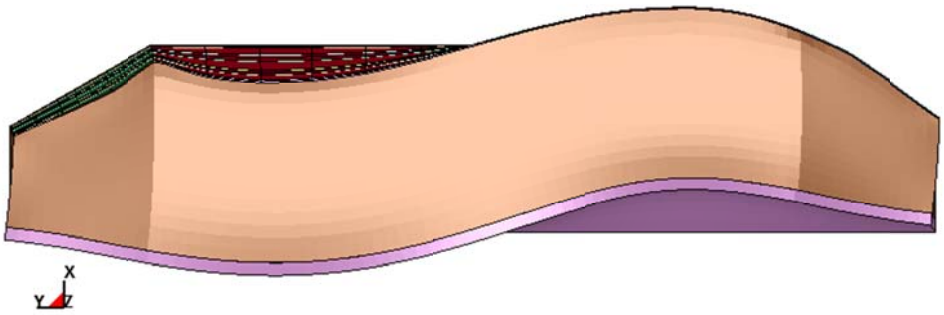

Figure 7-2: Mode shape 2 of the segmental panel wall

In the third mode shape, the wall sways back and forth with respect to the y axis instead of the x axis as seen in Figure 7.3 and Figure 7.4.

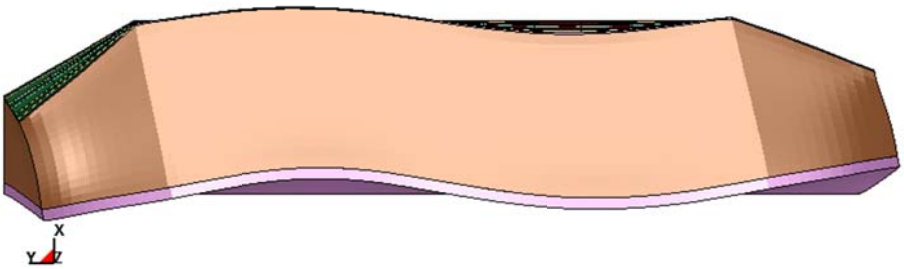

Figure 7-3: Mode shape 3 of the 15 foot panel wall

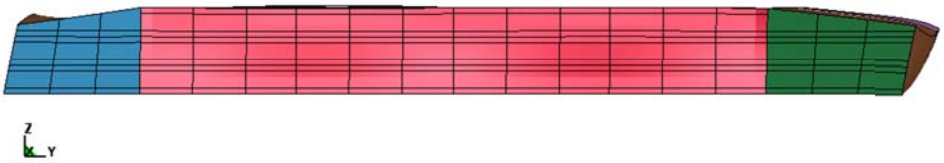

Figure 7-4: Front view of mode 3 of 15 foot segmental panel wall

The mode shapes and modal frequencies of the 15 foot modular block wall are very similar to those of the 15 foot panel wall. These natural periods and circular natural frequencies are listed in Table 7-2. The mode shapes are the same as the15 foot panel wall and are shown in Figures 7.5-7.7.

Table 7-2: Modal analysis results for 15 foot modular block wall

	Natural Period (s)	Natural Frequency ($\frac{rad}{s}$)
mode 1	0.133	47.4
mode 2	0.126	49.8
mode 3	0.118	53.2

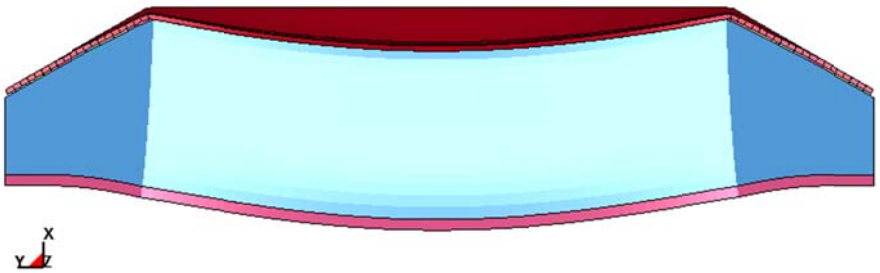

Figure 7-5: Mode shape 1 of 15 foot modular block wall

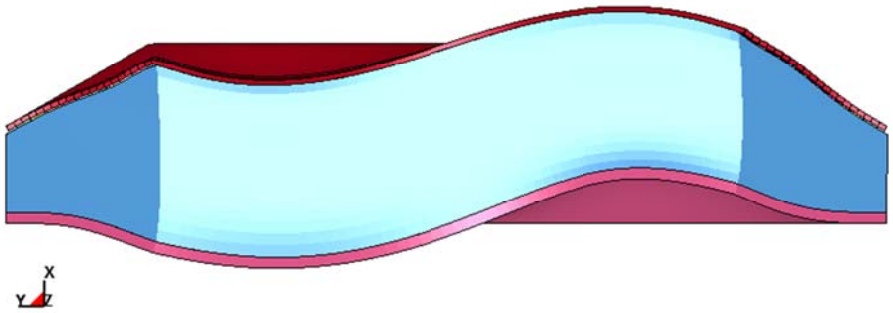

Figure 7-6: Mode shape 2 of 15 foot modular block wall

The proximity of magnitudes between the first, second, and third natural frequencies was independently verified using thick plate element model of this wall using the structural engineering software RISA-3D. The plate elements in Risa-3D were made with the same dimensions as the concrete panel wall and were given a thickness of 30 ft to simulate the soil geometry from LS-Dyna. The Risa-3D analysis was calculated to have a slightly lesser volume than LS-Dyna. Since the volumes from LS-Dyna and Risa-3D are not exactly the same, Risa-3D showed slightly higher frequencies as seen in Table 7-3.

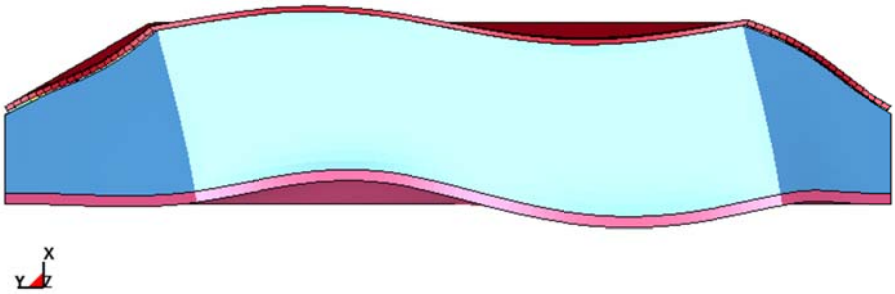

Figure 7-7: Mode shape 3 of 15 foot modular block wall

Table 7-3: Modal analysis of just soil elements

Mode Shape	LS-Dyna Circular Frequencies$\left(\frac{rad}{s}\right)$	Risa 3-D Circular Frequencies$\left(\frac{rad}{s}\right)$
1	38.9	39.1
2	39.7	41.1
3	41.6	44.5
4	44.3	47.2
5	45.7	49.7

Both analyses show that the first five mode shape frequencies are very close together. This is due to the fact that both of these programs model three dimensional analyses. The first mode shapes of the system are all derived from the swaying motion of the wall soil structure. This motion is carried to different locations of the wall and occurs in different directions to make the next five frequencies. This is why the frequencies are so close together. Most importantly however, it is verified with the RISA 3D analysis that the first few modes exhibit unusually close proximity to their magnitude. This is attributed to the fact that the higher modes of deformation do not occur along the length of the cantilever structure, but, instead they occur along its cross-sectional width.

Bathurst and Hatami [67] showed that the natural frequency in Hz of an MSE wall can be modeled as a two-dimensional, linear elastic medium of width B and height H contained by two rigid vertical boundaries and a rigid base and subjected to horizontal base excitation given by Equation 7-1 [68].

$$f = \left(\frac{1}{4H}\right)\sqrt{\frac{G}{\rho}}\sqrt{1+\left(\frac{2}{1-\nu}\right)\left(\frac{H}{B}\right)^2} \quad \textbf{(7-1)}$$

Using a height of 176 in and a width of 360 in and the same material properties listed previously, this gives a natural frequency of 9.78 Hz or 61.5 $\frac{rad}{s}$. Although this only models a two-dimensional wall, it is still close to the frequencies calculated from LS-Dyna. Richardson and Lee proposed that the fundamental period, T, of MSE walls constructed with steel strip reinforcement can be estimated empirically using Equation 7-2 [69].

$$T = 0.020H \; to \; 0.033H \quad \textbf{(7-2)}$$

where H is the height of the wall in meters and T gives you the natural period of the wall in seconds. Converting the height of the current study's MSE wall model to meters and multiplying by 0.03 gives the result of $T = 0.13\,s$ which matches what was found by LS-Dyna. The fundamental frequency of the MSE walls studied by Hatami and Bathurst were found to have frequencies of 32.0 to 52.2 rad/s^2 using this relationship. The possible explanation for the difference in predicted fundamental frequencies using Equation 7-1 and 7-2 is that the empirical relationship by Richardson and Lee is applicable to walls retaining a relatively narrow soil volume beyond the reinforced zone [69]. The Richardson and Lee assumption is similar to the way the 15 foot wall models are built in this study but does not apply to the 30 foot wall models.

7.1.2 Earthquake Analysis Results of the 15 Foot Segmental Panel Wall

To demonstrate that the no-penetration contacts are being appropriately implemented between the 15 foot segmental panel shell elements and the soil solid elements, the relative displacements between the shell elements and the soil at a point in the middle of the wall are presented in Figures 7.8-7.12 for each earthquake loading case. These graphs show the x displacement of a node on the wall minus the x displacement of the closest node on the soil mesh. Because these numbers are mostly positive, they show that there are no penetrations and therefore the contact sets are working correctly in that they allow the wall to move away from

the soil elements but do not allow penetration. Slight error is observed because a maximum penetration is allowed based on the stiffness calculation for the contacts [70].

In Figures 7.8-7.12, it is seen that the Illinois earthquake plot (Figure 7.11) shows more relative movement than the stochastic earthquakes between the wall and the soil because, while these earthquakes have approximately the same peak acceleration, the peak acceleration of the Illinois earthquake occurs around the natural frequency of the wall structure as seen from Figure 4.16 and Table 7-2. The El Centro earthquake has a peak acceleration that is twice as large as these other four earthquakes and therefore causes the largest displacements. Nevertheless, the largest calculated separation is 0.0035 inches.

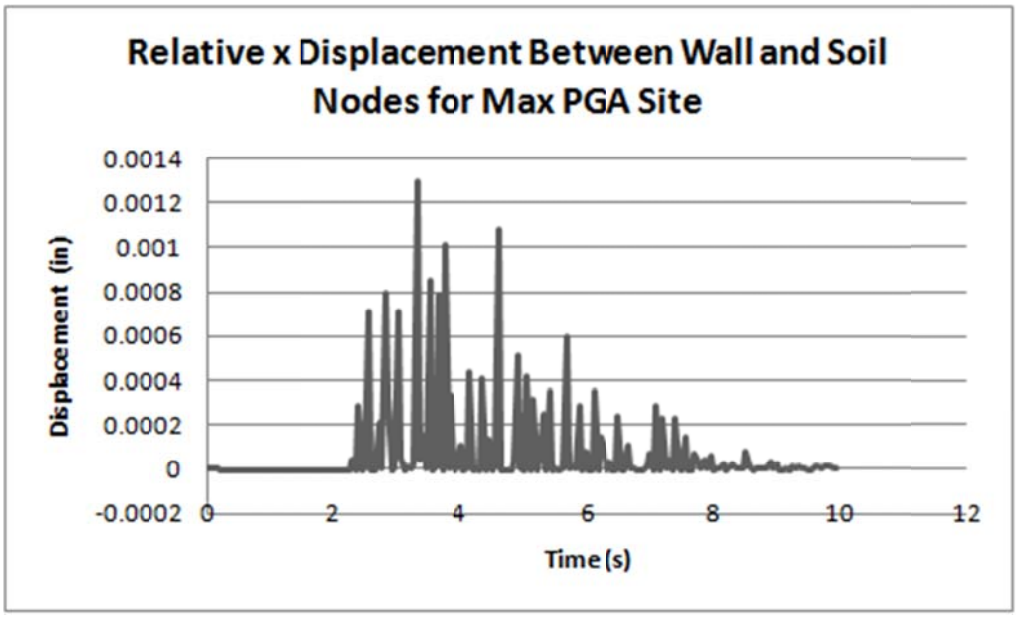

Figure 7-8: Relative x displacement between 15 foot segmental panel wall and soil nodes for max PGA site

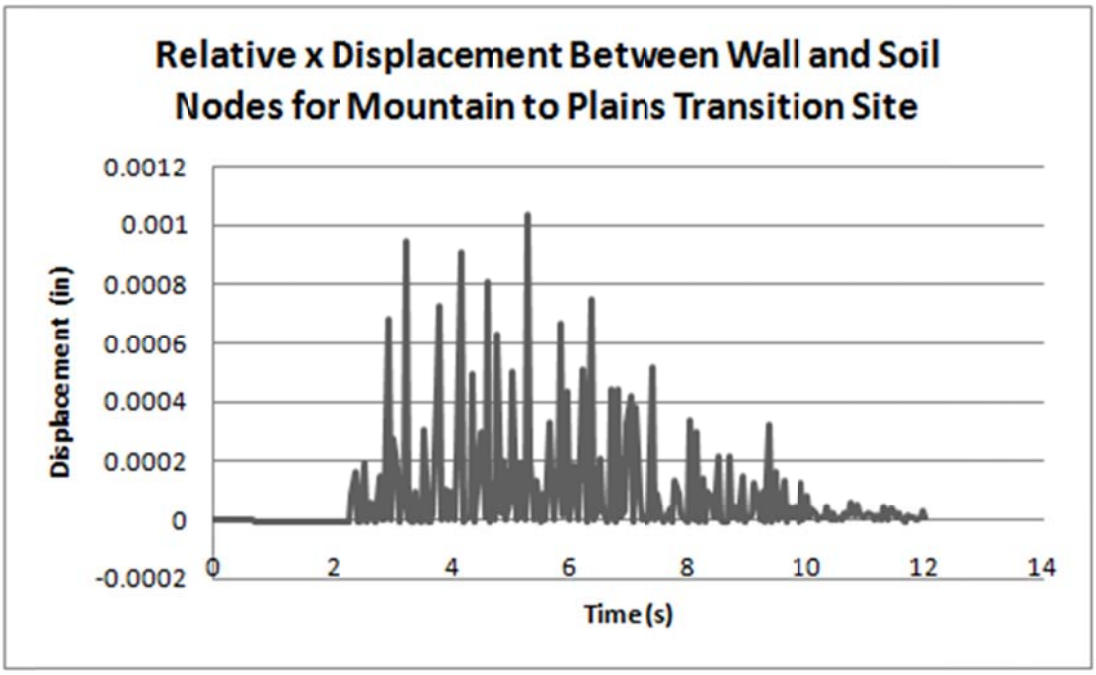

Figure 7-9: Relative x displacement between 15 foot segmental panel wall and soil nodes for mountain to plain transition site

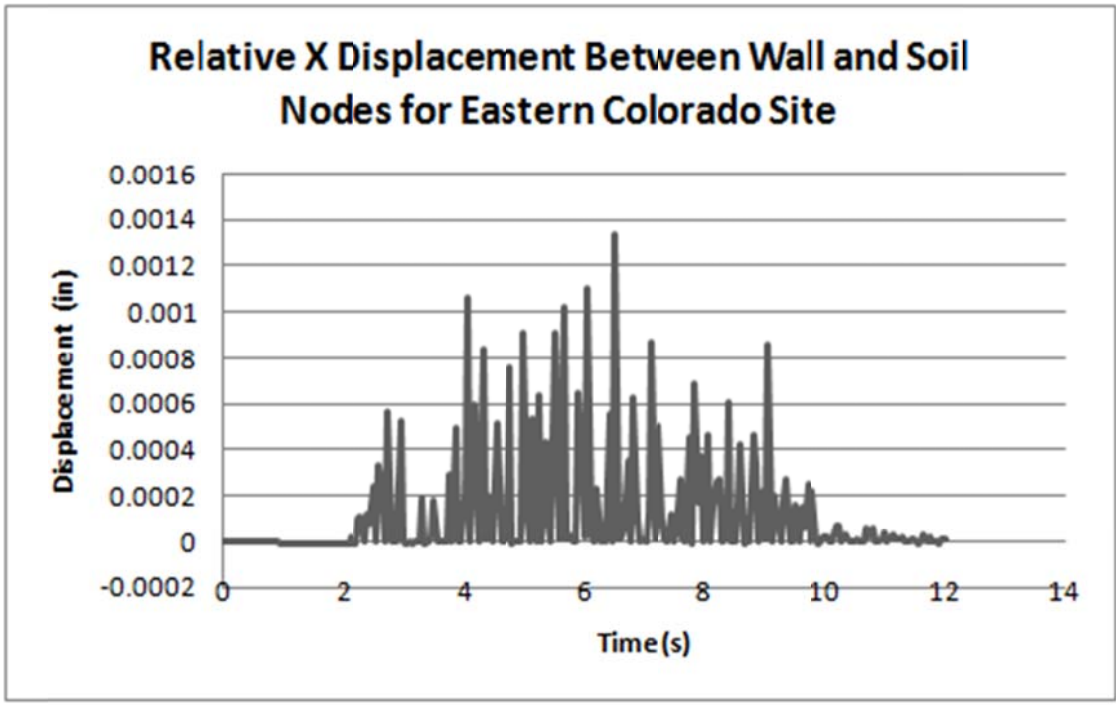

Figure 7-10: Relative x displacement between 15 foot segmental panel wall and soil nodes for Eastern Colorado site

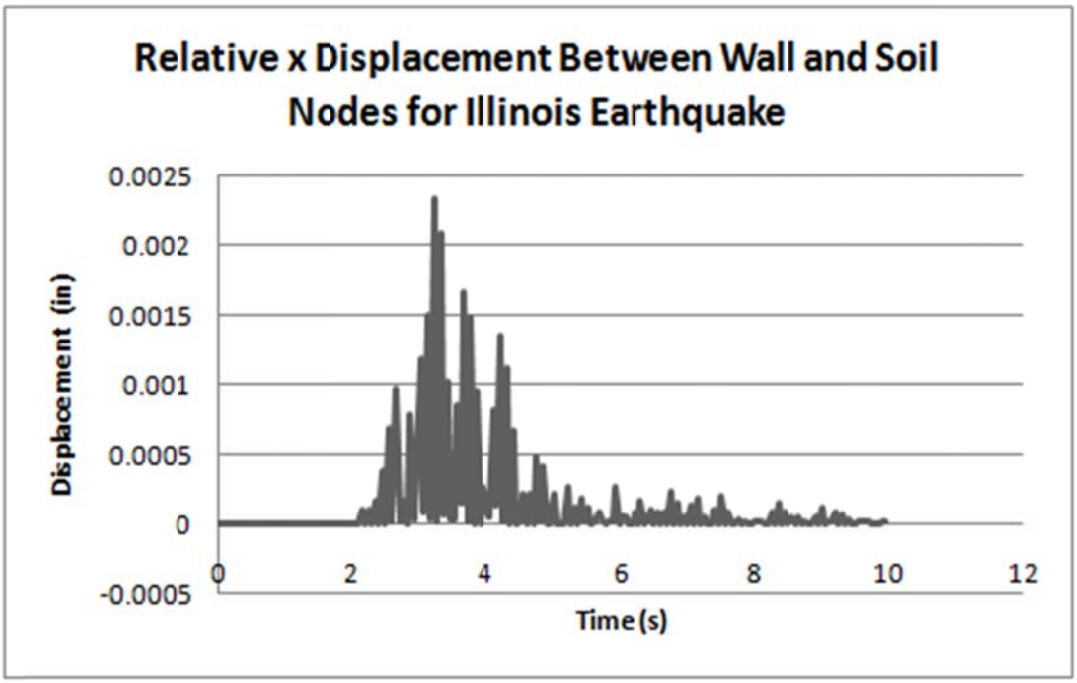

Figure 7-11: Relative x displacement between 15 foot segmental panel wall and soil nodes for Illinois earthquake

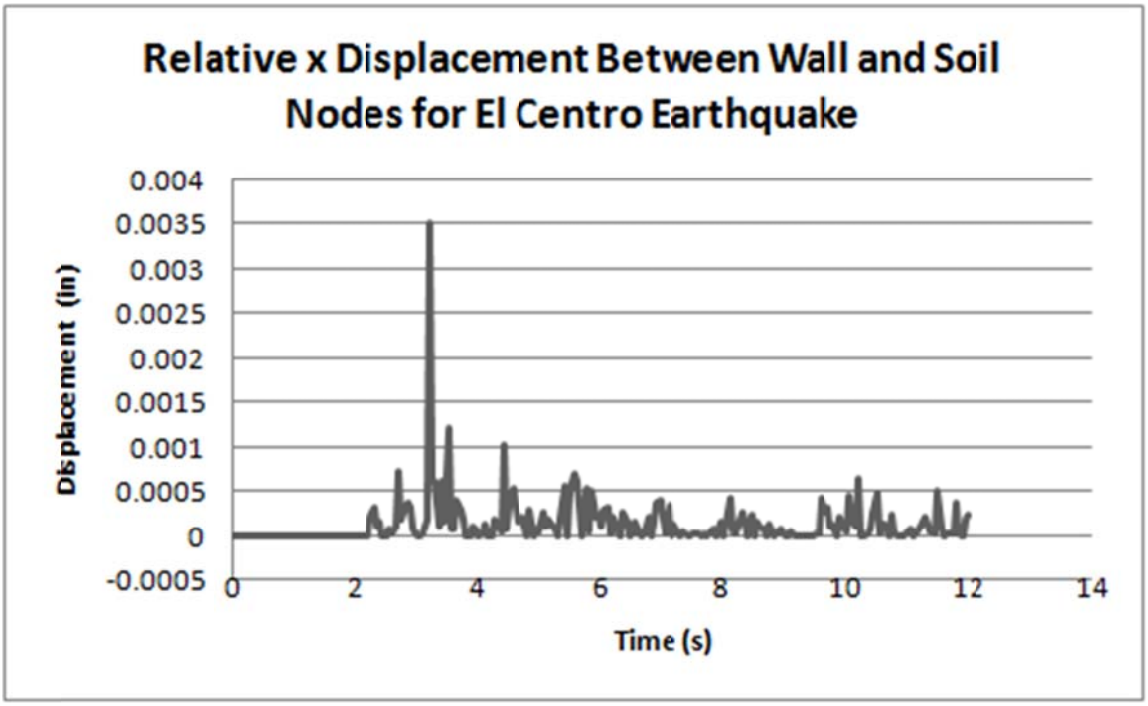

Figure 7-12: Relative x displacement between 15 foot segmental panel wall and soil nodes for El Centro earthquake

The displacements of a node at the bottom of the wall, the middle of the wall, and the top of the wall are shown in Figures 7.13-7.17. The earthquake displacements are applied to the models after the first two seconds of run time. Gravity is applied by a slow ramp up in the time interval between 0 and 1 seconds. In the time interval between 1 and 2 seconds, no further loading is applied, the gravity loading is maintained constant, and all dynamic loads are allowed to dissipate, before the earthquake motion is applied. This explains the horizontal displacements of the top and middle nodes observed in Figures 7.13-7.17. As the gravity load is applied it forces the soil to deform downwards and outwards. The earthquake motion is then observed to cause further displacements on top of the displacement caused by the gravity load. The El Centro earthquake (Figure 7.17) causes much larger displacements due the earthquake loading relative to the gravity loading and therefore the gravity loading is not as visible on the x displacement graph.

Figures 7.13-7.17 show that the middle of the wall bulges out slightly as discussed in Sabermahani et.al. [11]. The 15 foot segmental panel model wall cross-section with enhanced deformations is shown in Figure 7.18.

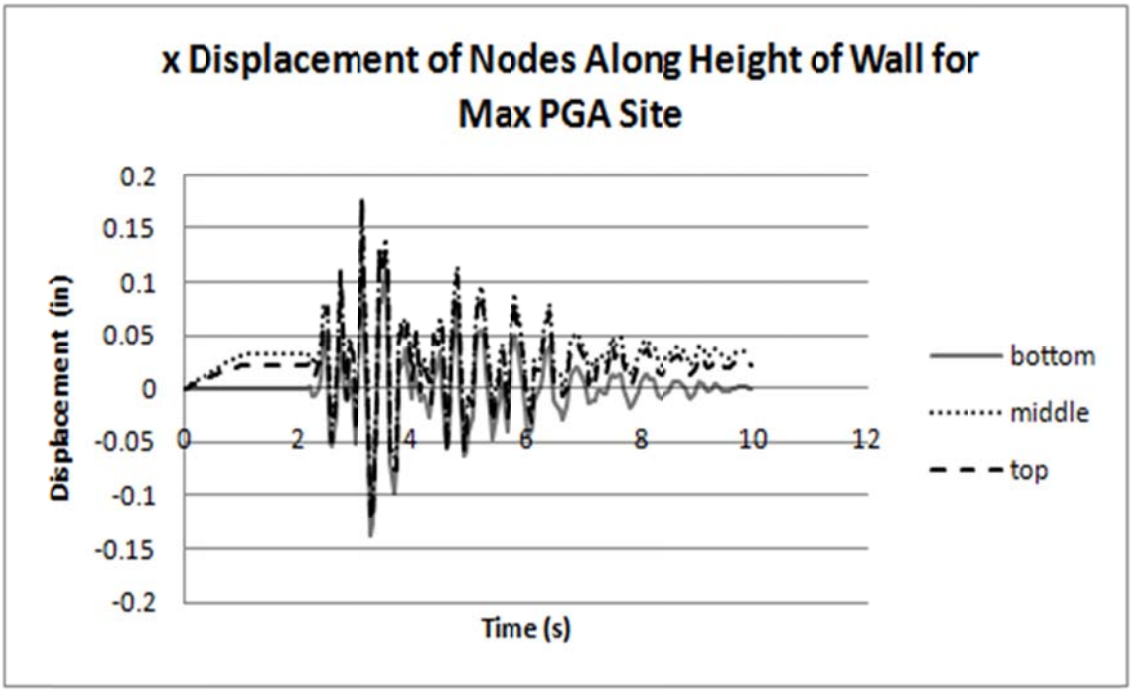

Figure 7-13: x displacement of nodes along height of 15 foot segmental panel wall for max PGA site

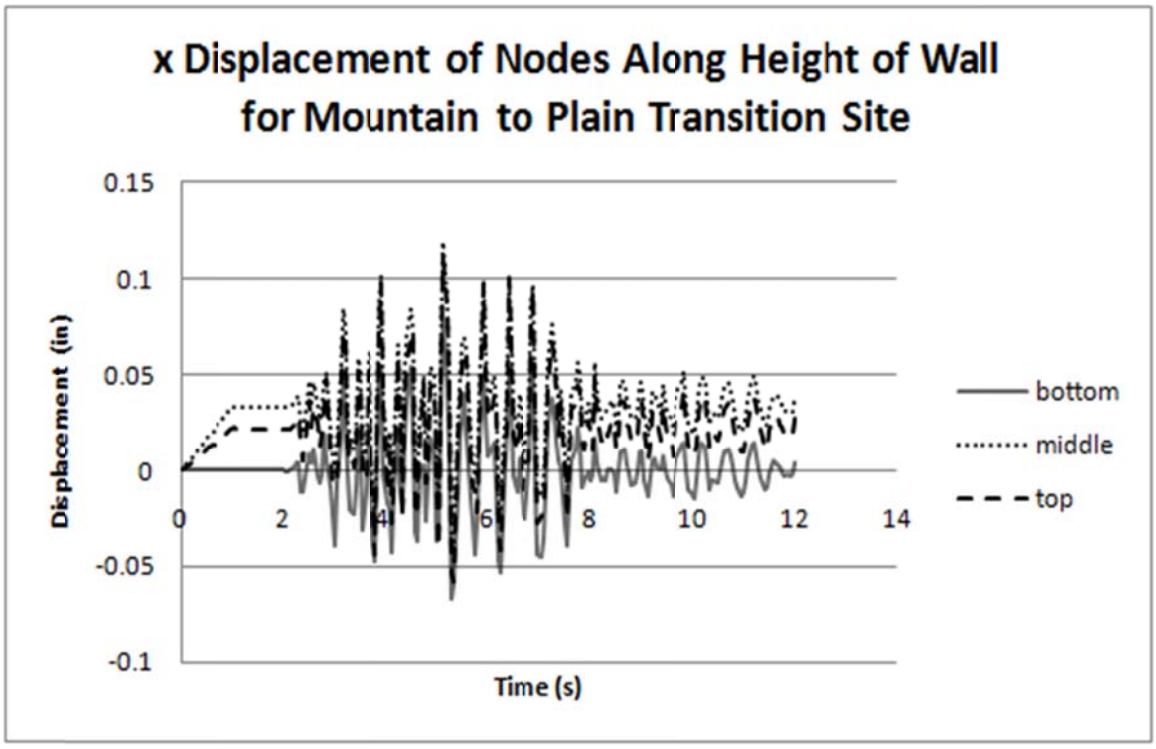

Figure 7-14: x displacement of nodes along height of 15 foot segmental panel wall for mountain to plain transition site

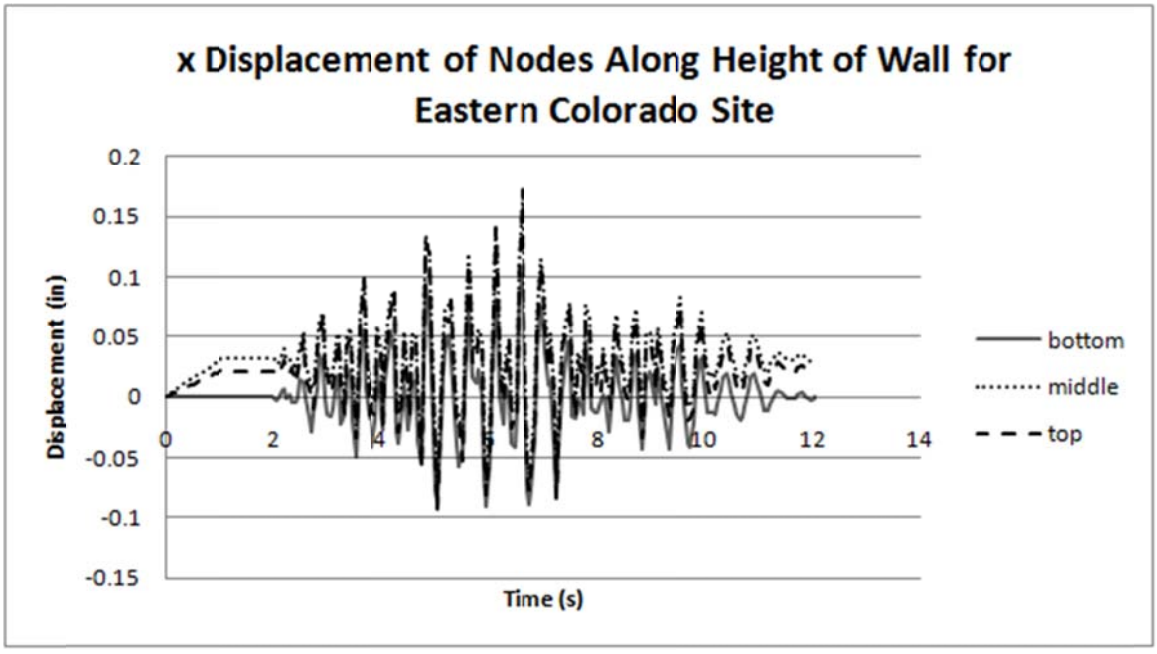

Figure 7-15: x displacement of nodes along height of 15 foot segmental panel wall for Eastern Colorado site

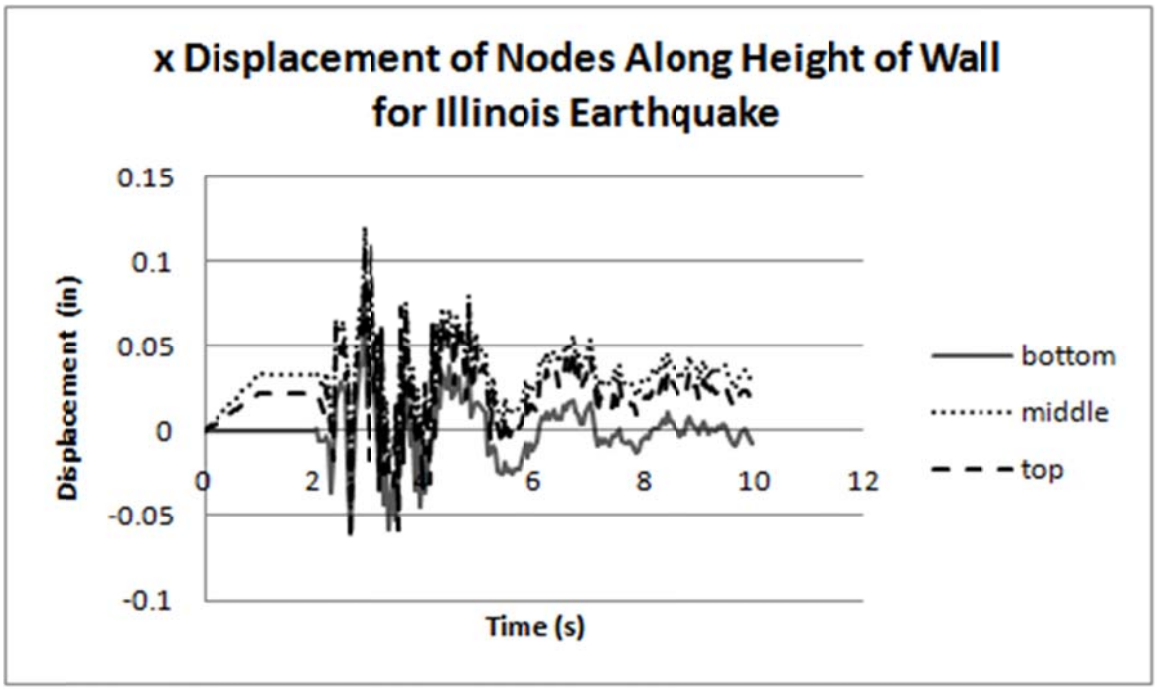

Figure 7-16: x displacement of nodes along height of 15 foot segmental panel wall for max Illinois earthquake

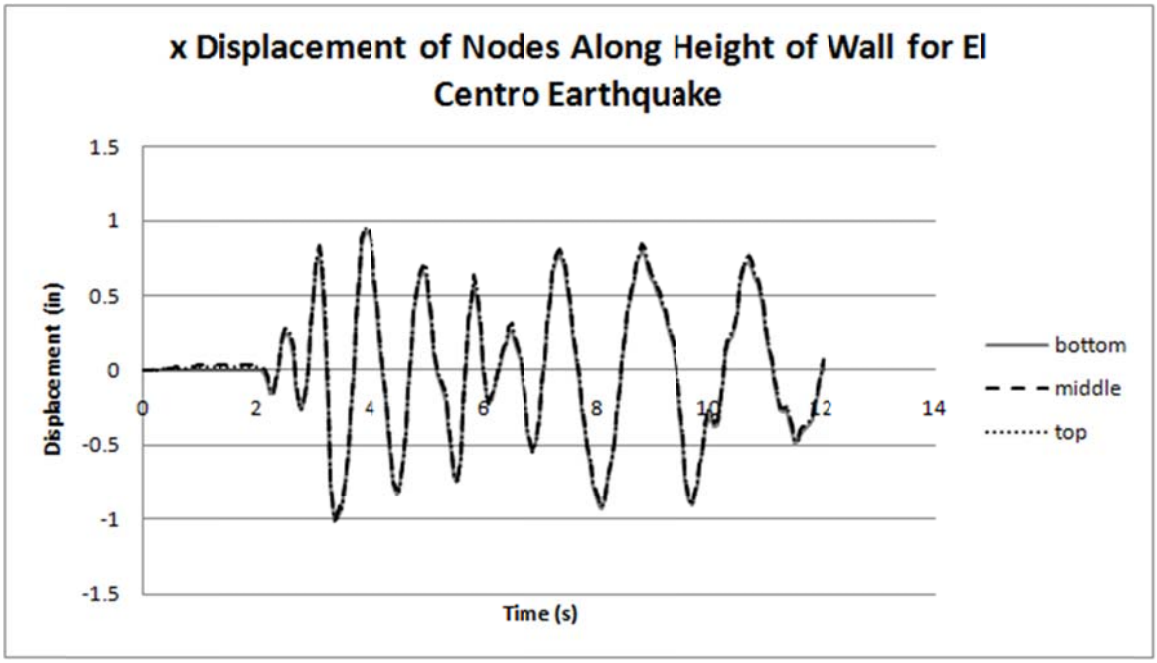

Figure 7-17: x displacement of nodes along height of 15 foot segmental panel wall for El Centro earthquake

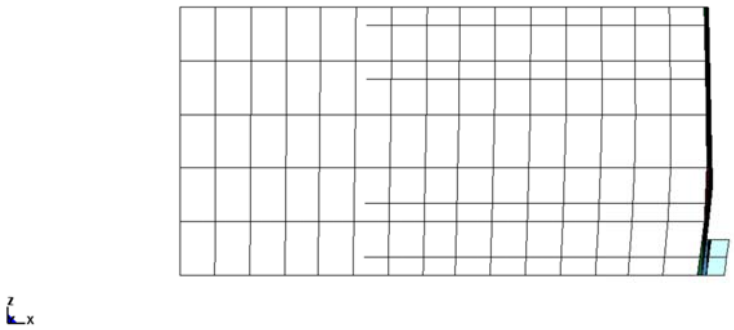

Figure 7-18: 15 foot segmental panel wall cross-section with magnified displacements to show bulging of wall

Bulging modes of failure usually occur in walls with more extensible and widely spaced reinforcement [11]. The panel wall was built to have less reinforcement than found in a modular block wall and therefore shows slight bulging where the modular block wall does not. Although the wall bulges, it still shows deformations that are consistent with the mode shapes found in the modal analysis (Figures 7.1-7.3) where the top of the wall has the most deformation from swaying in shear. Siddharthan, et al. [14] showed that MSE walls on a centrifuge will have similar deformations in that the middle will bulge out. The top residual deformation relative to the bottom was only about 4 mm or .16 in. with a maximum acceleration of 0.478g [14].

The main concerns with the segmental panel wall in this study are with stresses that develop in the reinforcement connections and stresses that develop at the interface of the main and wing walls. Figure 7.19 shows the normal stress σ_x, plot for the reinforcement in the panel wall run with the El Centro earthquake with red locations indicating highest tensile stresses and blue locations indicating largest compressive stresses. This plot represents the state where σ_x is maximum. The maximum stresses develop at the wall edges. Figure 7.20 shows the time history plot of σ_x for the element that develops the highest stress. This element develops a maximum stress of 78 psi at 5.8 seconds into the analysis. It can be seen from Figure 7.20 that 31 psi is developed due to gravity. Therefore, 47 psi is developed in the reinforcement due to actual dynamic loading.

All four of the other earthquake motions showed maximum σ_x in the middle of the main wall on the second reinforcement layer and have their maximum stress results reported in Table 7-4. If the maximum σ_x found from the El Centro motion analysis is multiplied by the cross sectional area per unit foot width of wall, it gives a force of 234 lbs/ft or 3.412 kN/m. Ling et.

al. [10], found tensile forces to be around 1.0 $\frac{kN}{m}$ for a modular block wall with half the height and 4 reinforcement layers rather than 6 for the present study. Since the wall height to reinforcement ratio is less in the analysis of Ling el al. [10], it is expected that the force would be considerably less.

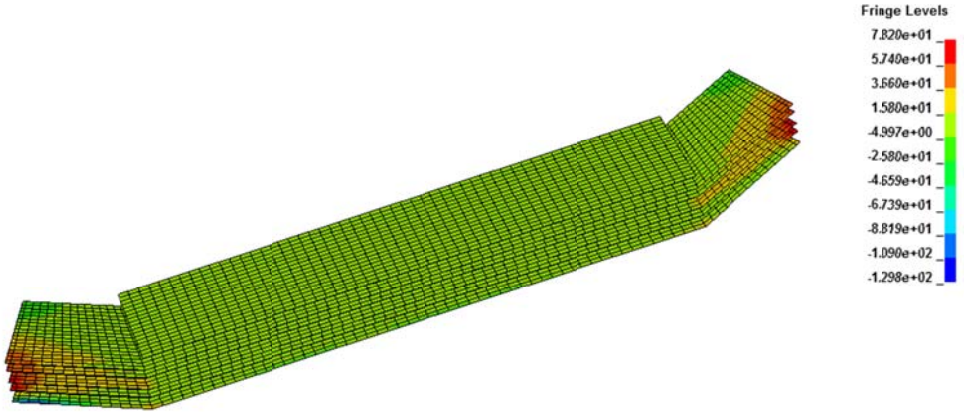

Figure 7-19: 15 foot segmental panel wall reinforcement normal x stress, σ_x, in psi for El Centro earthquake

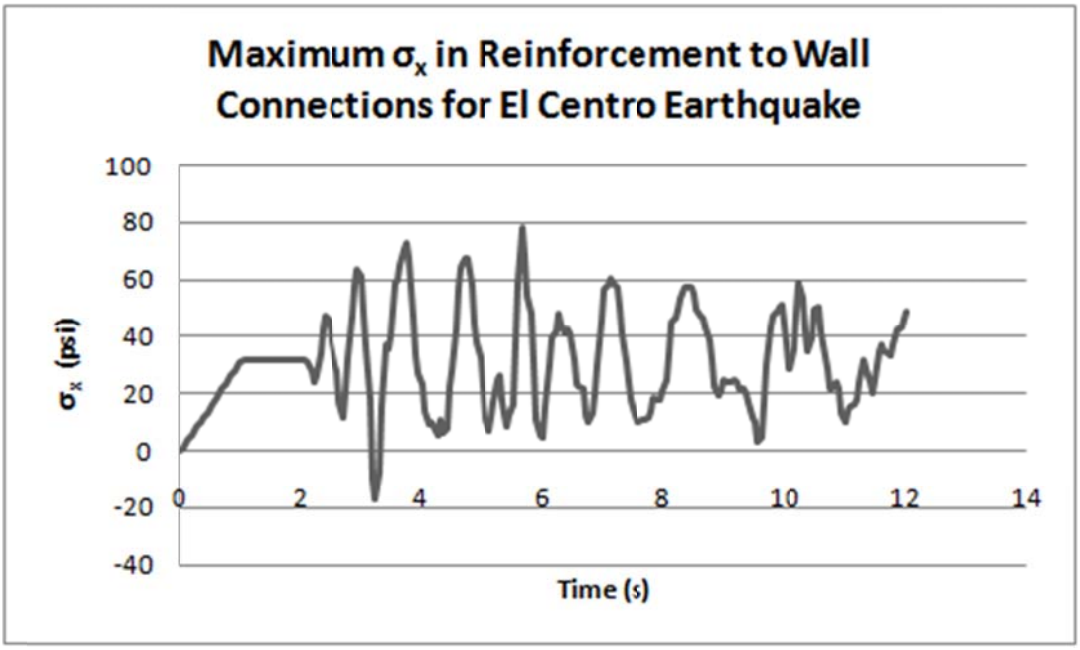

Figure 7-20: Time history plot of maximum σ_x for El Centro earthquake

Figure 7.21 shows the elements at the interface of the left wing wall and the main wall. The plot shown is at the point where the maximum shear stress $\boldsymbol{\tau_{yz}}$ develops. This stress is 188 psi at a time of 3.3 seconds for the El Centro earthquake. Figure 7.22 shows the time history plot of the element with the maximum $\boldsymbol{\tau_{yz}}$ that develops.

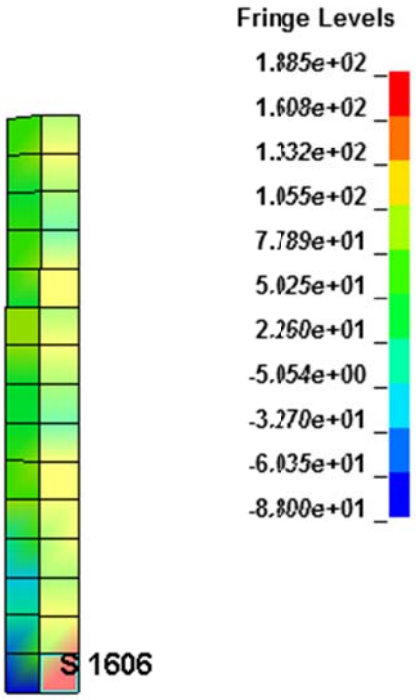

Figure 7-21: 15 foot segmental panel wall main wall to wing wall joint for El Centro earthquake $\boldsymbol{\tau_{yz}}$ in psi

It has been observed that during seismic events large stresses tend to develop at the corners of walls [54]. For the segmental panel walls, τ_{yz} was seen to be maximum in the joint between the main wall and the wing wall. Assuming the corner panel can be approximated as a beam, the American Concrete Institute (ACI) Equation 11-3 [71] can be used to estimate the shear strength of concrete:

$$v_c = 2\sqrt{f_c'} \qquad \textbf{(7-3)}$$

where f_c' is the specified compressive strength of concrete. This results in a shear strength of 126 psi, which is larger than the developed stresses calculated in the analyses of the segmental panel walls, with the exception of the El Centro loading. However, even in that case, higher stresses were developed locally, while Equation (7.3) is meant to represent an average cross-sectional

strength. It is seen from physical examples of MSE walls that failures usually occur at slip joints added to the wall (eg. [7] and [54]) this is beyond the scope of this study.

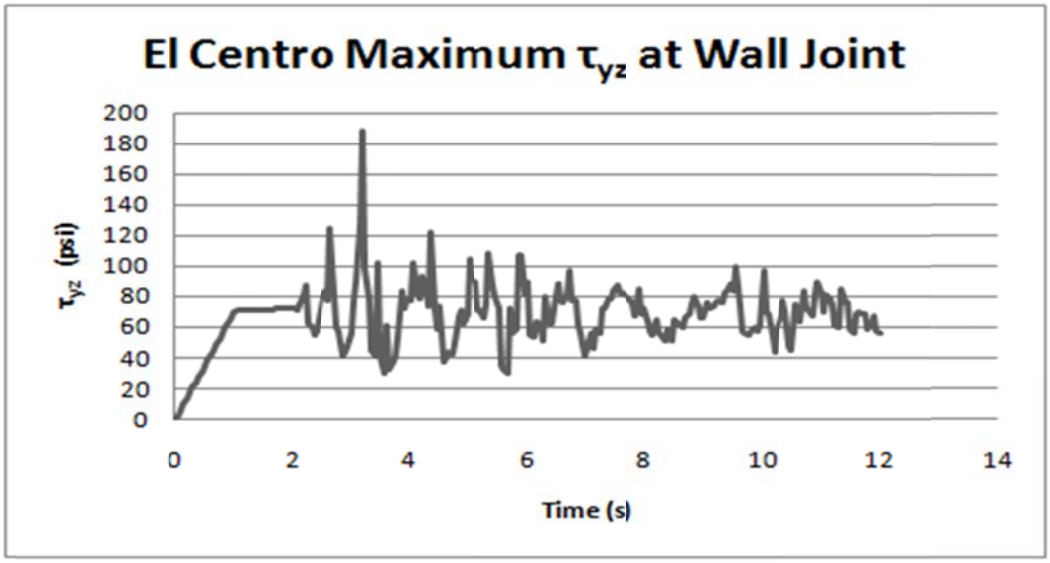

Figure 7-22: Time history plot for 15 foot segmental panel wall main wall to wing wall joint for El Centro τ_{yz} in psi

The summary of the maximum stress results found for all segmental panel wall earthquake analyses are shown in Table 7-4.

Table 7-4: Summary of 15 foot segmental panel wall earthquake analyses results

	PGA site	Mount. Plain transition site	Eastern Site	Illinois	El Centro
σ_x at Reinforcement to Wall Connections	62 psi	51 psi	58 psi	60 psi	78 psi
Max τ_{yz} Between Joint of Main Wall and Wing Walls	83 psi	72 psi	111 psi	96 psi	188i

7.1.3 Earthquake Analysis Results of 15 Foot Modular Block Wall

To demonstrate that the no-penetration contacts are appropriately implemented between the 15 foot modular block wall and the soil elements, the relative displacements between the bricks and the soil at a point in the middle of the wall are shown in Figures 7.23-7.27 for each earthquake loading case. These graphs show the x displacement of a node on the inside of the wall minus the x displacement of the closest node on the soil mesh. Because these numbers are mostly positive, they show that there are no penetrations and therefore the contact sets are working correctly in that they allow the wall to move away from the soil elements but do not allow penetration. Slight error is observed because a maximum penetration is allowed based on the stiffness calculation for the contacts [70]. It is seen that the wall nodes move out from the soil during the gravity loading because these nodes do not line up exactly for the modular block wall. The soil nodes are located slightly below the wall nodes and therefore do not bulge out as much.

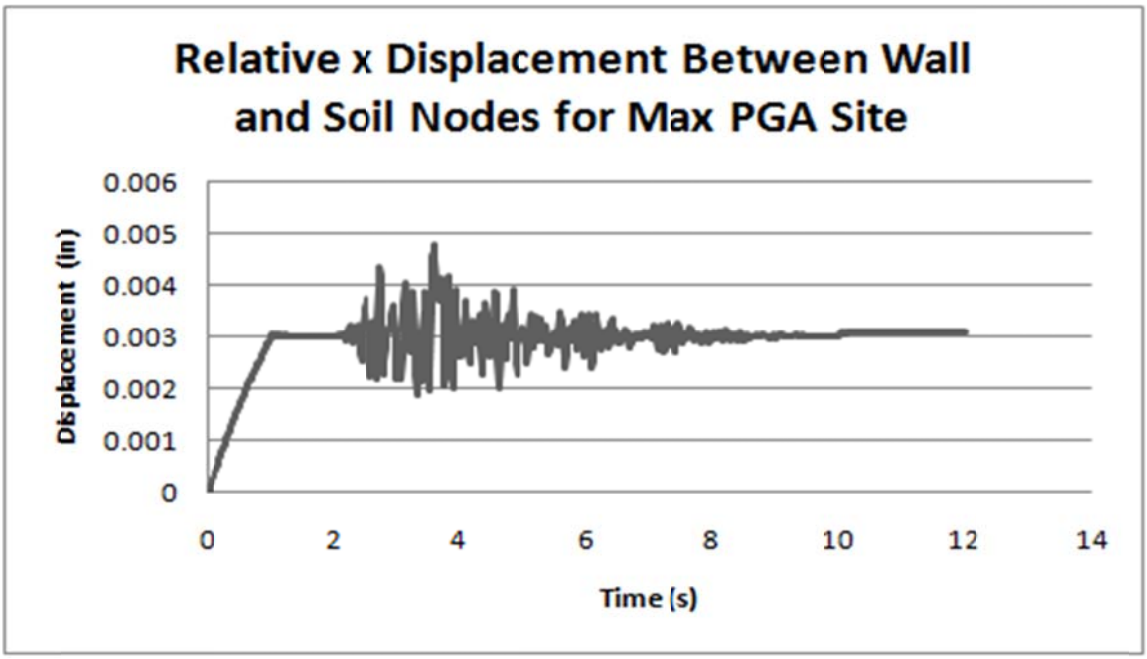

Figure 7-23: Relative x displacement between wall and soil nodes for max PGA site

In Figures 7.22-7.26, it is seen that the Illinois earthquake plot (Figure 7.26) shows more relative movement between the wall and the soil because the peak acceleration of this earthquake occurs around the natural frequency of the wall structure as seen from Figure 4.16 and Table 7-2. The other four earthquake motions have similar accelerations for the natural frequency of the wall and therefore give similar relative displacements.

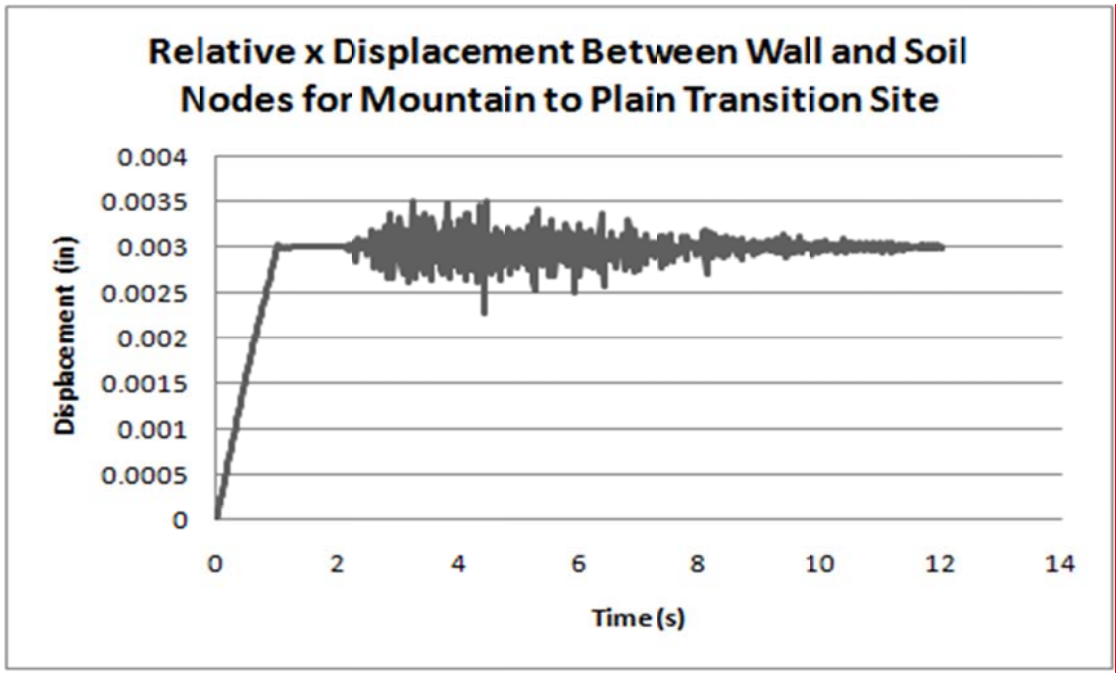

Figure 7-24: Relative x displacement between wall and soil nodes for mountain to plain transition site

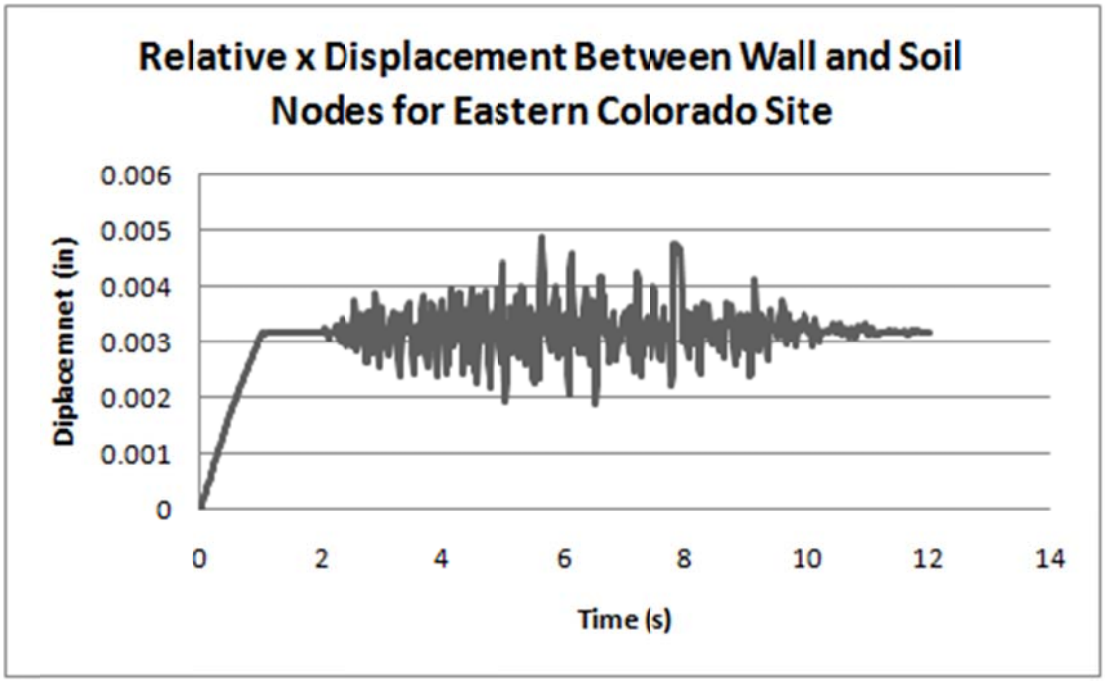

Figure 7-25: Relative x displacement between wall and soil nodes for Eastern Colorado site

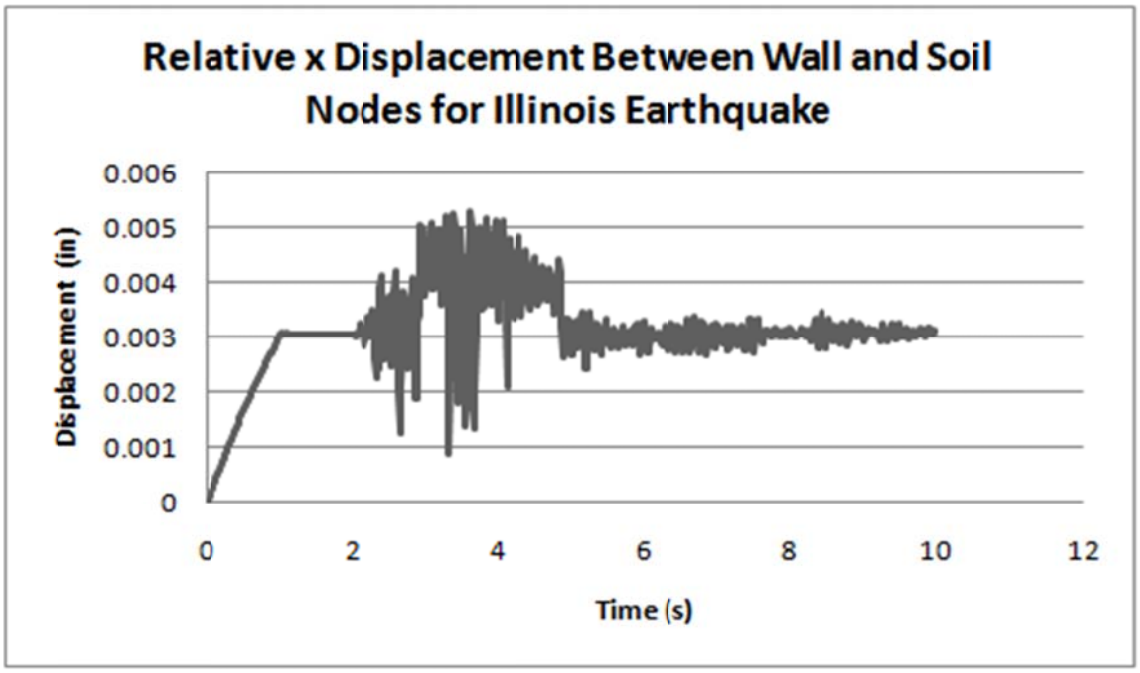

Figure 7-26: Relative x displacement between wall and soil nodes for Illinois earthquake

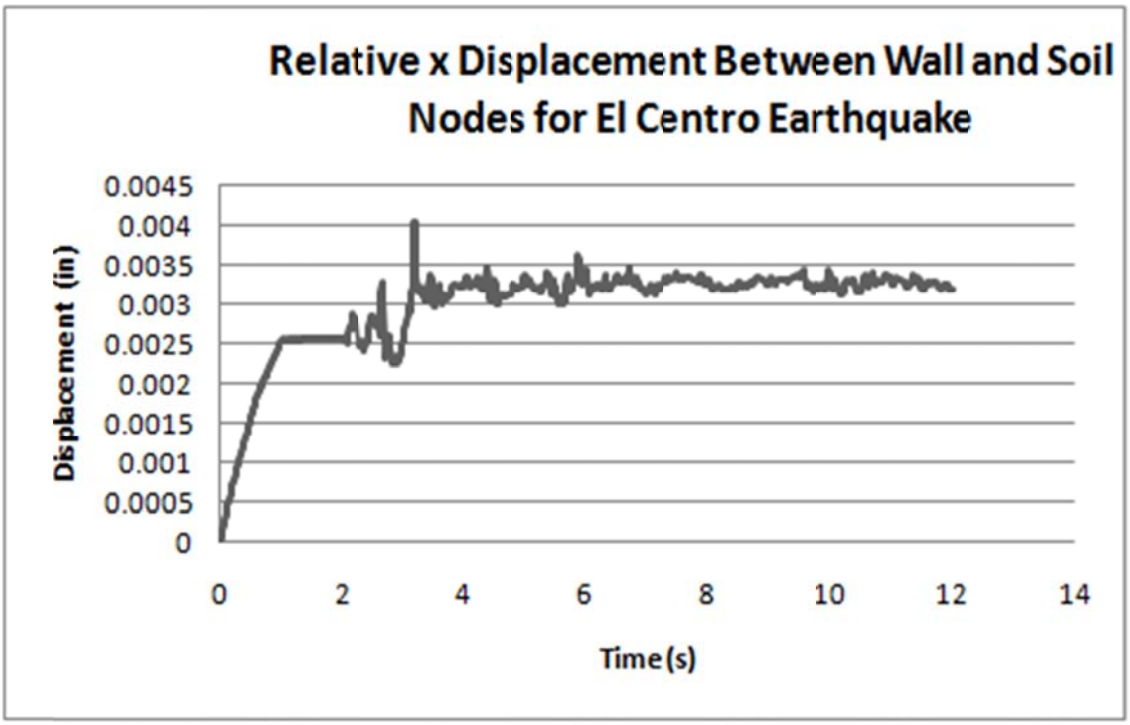

Figure 7-27: Relative x displacement between wall and soil nodes for El Centro earthquake

The displacements of a node at the bottom of the wall, the middle of the wall, and the top of the wall are shown in Figures 7.28-7.32.

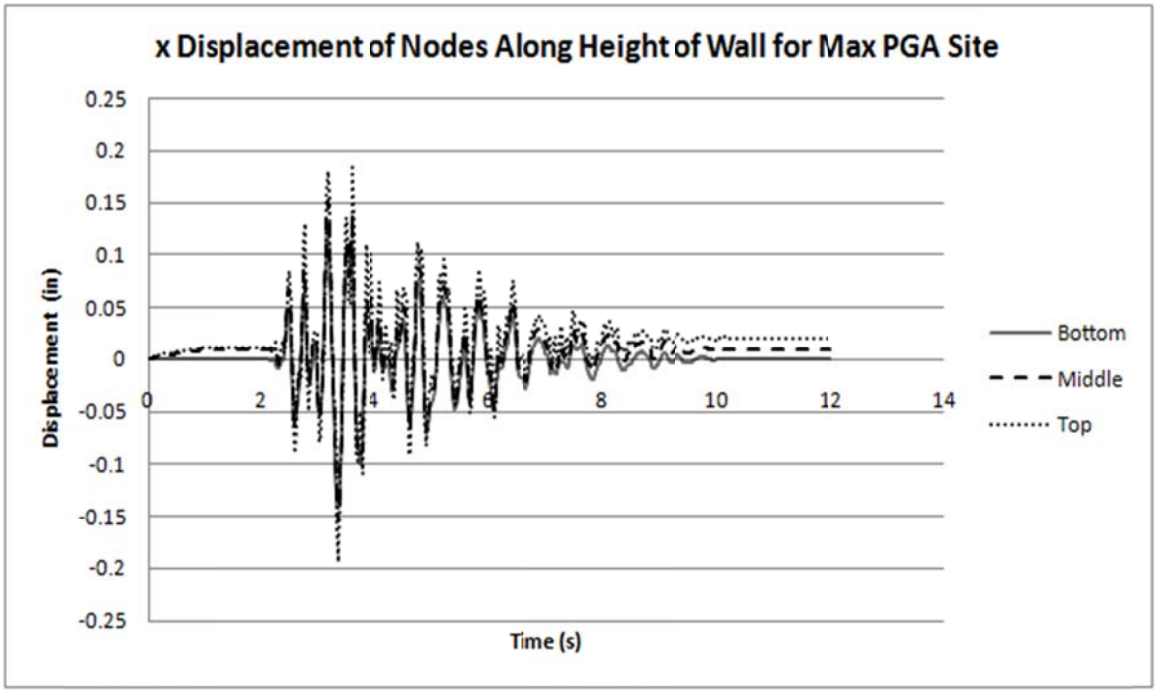

Figure 7-28: X displacement of nodes along height of wall for max PGA site

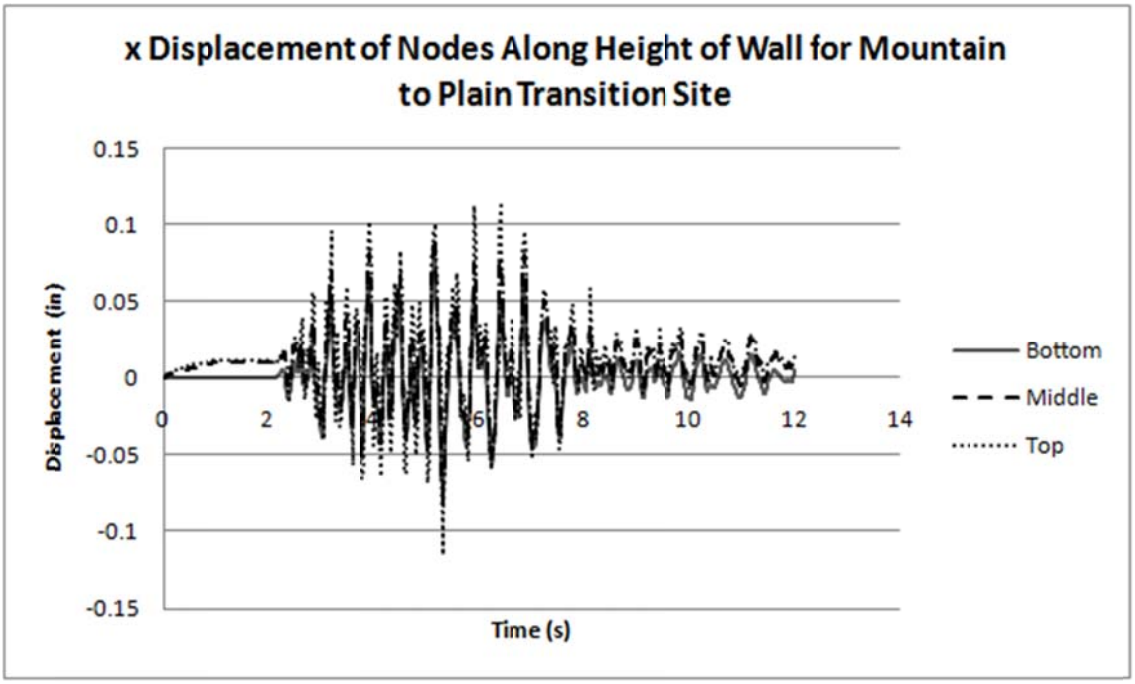

Figure 7-29: x displacement of nodes along height of wall for mountain to plain transition site

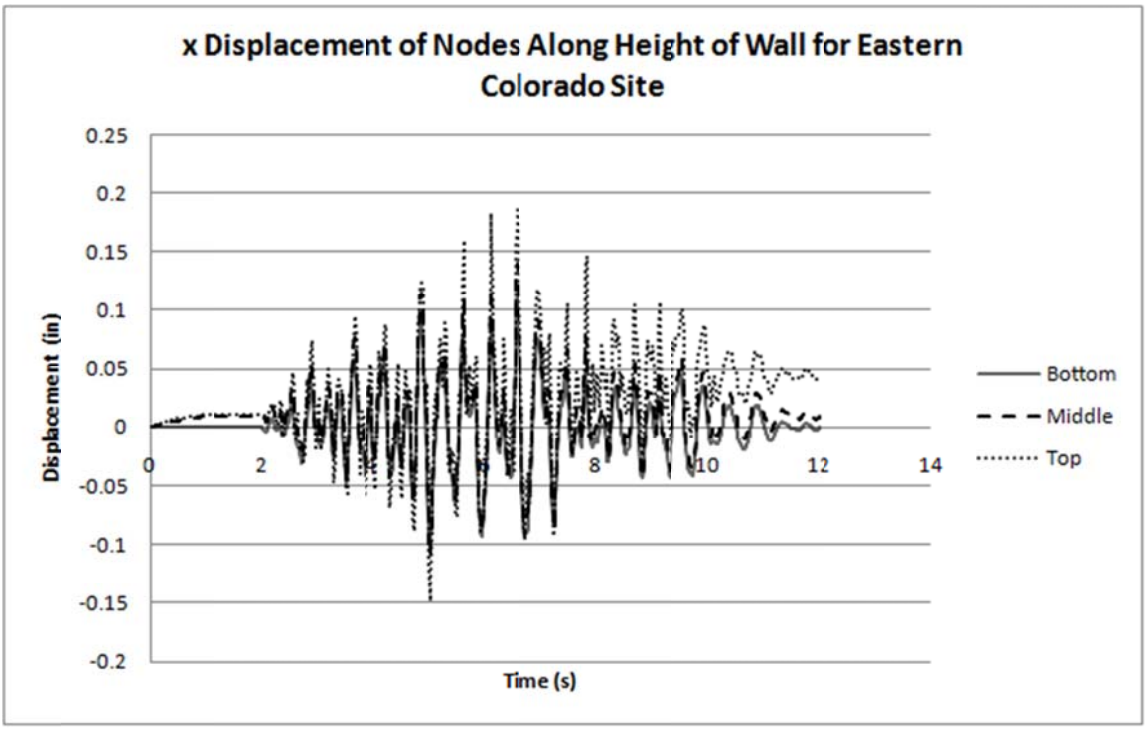

Figure 7-30: x displacement of nodes along height of wall for Eastern Colorado site

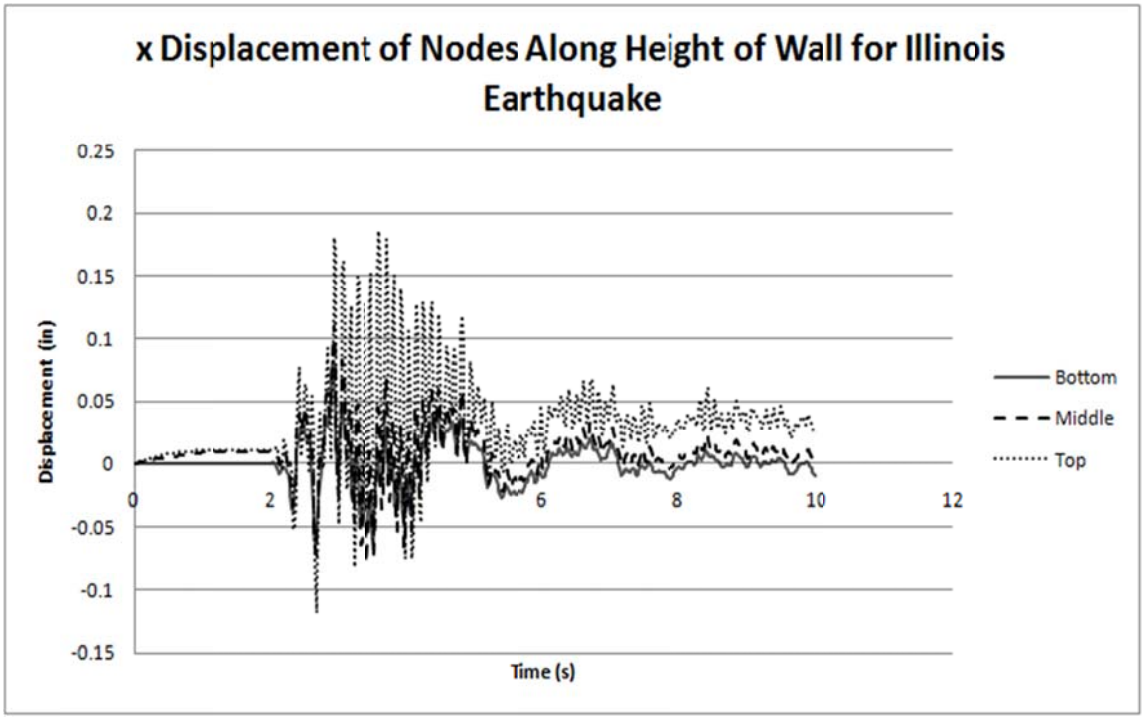

Figure 7-31: x displacement of nodes along height of wall for Illinois Earthquake

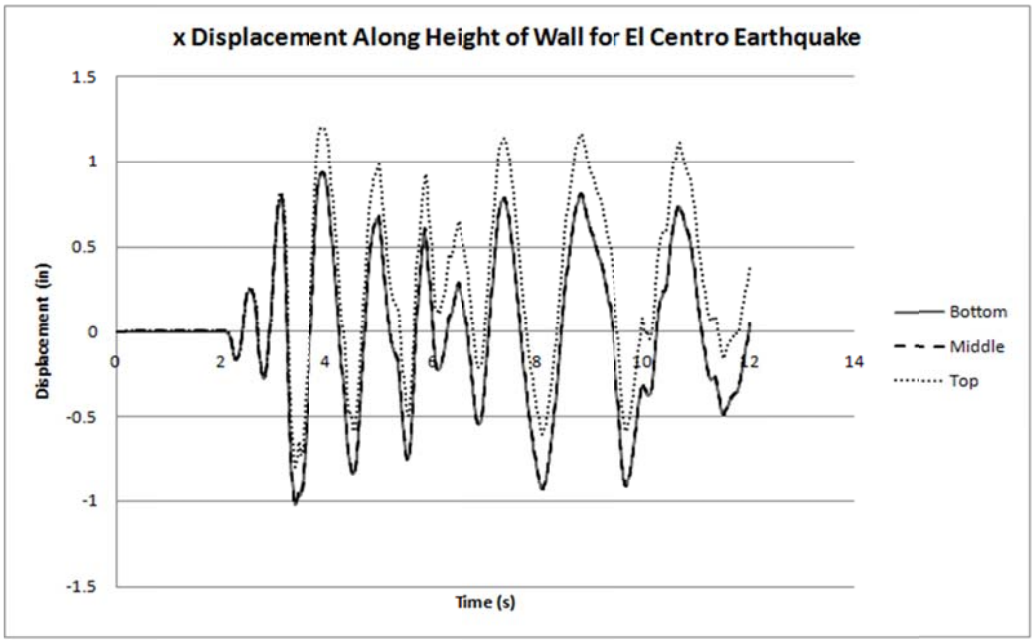

Figure 7-32: x displacement of nodes along height of wall for El Centro Earthquake

It is seen from Figures 7.28-7.32 that the walls sway in and out as demonstrated in the mode shapes found where the top of the wall has the largest displacement. The top blocks have small residual displacements toward the end of the motion. In the two dimensional analysis of a modular block MSE wall performed by Cai and Bathurst [46], residual displacements of 5-20 mm (.2-.7 in) were found for wall subjected to a 5 Hz frequency at amplitudes of .1 to .4gs. Cai and Bathurst used elements that allow for slip between each block in the wall, where the present model only allows for slip between the 4^{th} and 3^{rd} layer and 1^{st} and 2^{nd} layer. For a .25g earthquake the displacement calculated for the top two layers of blocks is only 1 mm or 0.04 in. For this study, the residual displacement of the top blocks is 0.021 in for the max PGA site loading, 0.017 in for the mountain to plain transition site loading, 0.043 in for the Eastern Colorado site loading, 0.024 in for the Illinois earthquake, and 0.39 in for the El Centro earthquake loading. The El Centro earthquake has a larger residual displacement because it has a peak amplitude of 0.4g rather than 0.22g. These results are consistent with Cai and Bathurst's findings [46].

For the 15 foot modular block wall, CDOT requested that the vertical displacements of the top layer of bricks be observed. The top bricks located closest to the wing wall joints are observed to have the maximum relative displacement, shown in Figure 7.33.

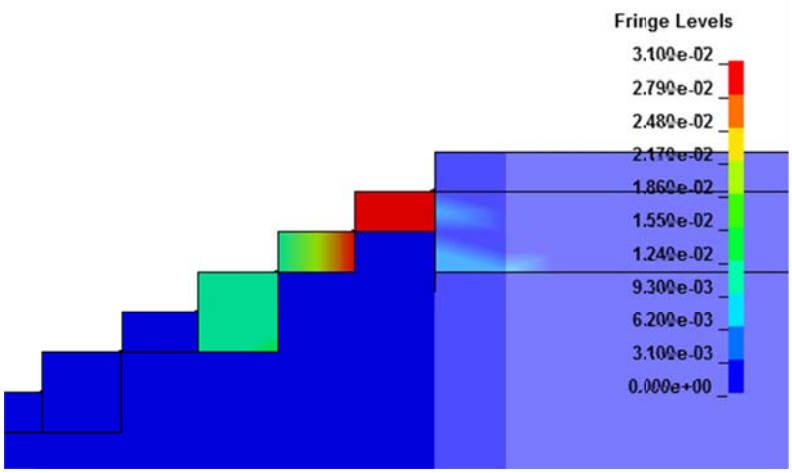

Figure 7-33: El Centro maximum vertical, relative z, displacement in inches

The maximum displacement from all earthquake loadings occurred with the El Centro earthquake at a time of 3.8 seconds. The relative z displacement of the node time history plot is shown in Figure 7.34. This shows the relative displacement between the top block and the one below it. The block with the maximum displacement for all earthquake situations occurred at the highest block of the wing wall nearest to the wing wall to main wall joint.

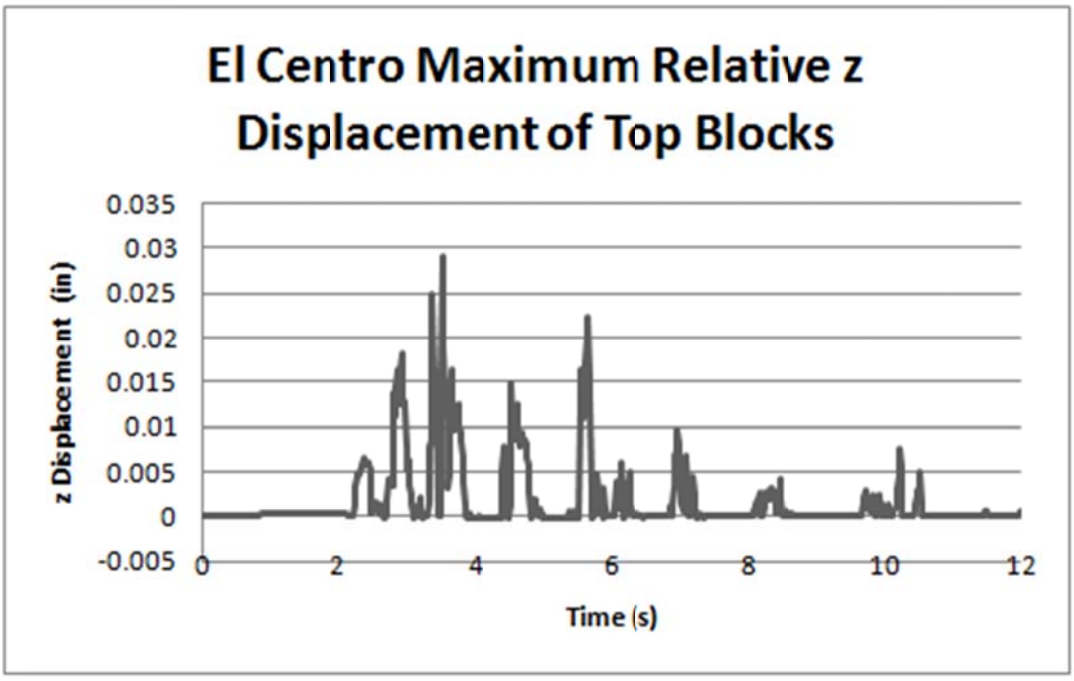

Figure 7-34: Time history plot of El Centro maximum vertical, relative z, displacement in inches

The vertical displacements shown here are very small and can be eliminated if grouting is used. In this model, the top blocks rely entirely on gravity to stay in place. Yen et al. [54] showed top blocks of a modular block MSE wall toppling because they were not supported by backfill. Most cases of modular block wall failure occur at the corners due to shear [54].

The maximum reinforcement to wall connection stress occurred in the top most layer of reinforcement that was also connected to the wing wall as shown in Figure 7.35. The maximum normal x stress, σ_x, for this case occurred for the Illinois Earthquake.

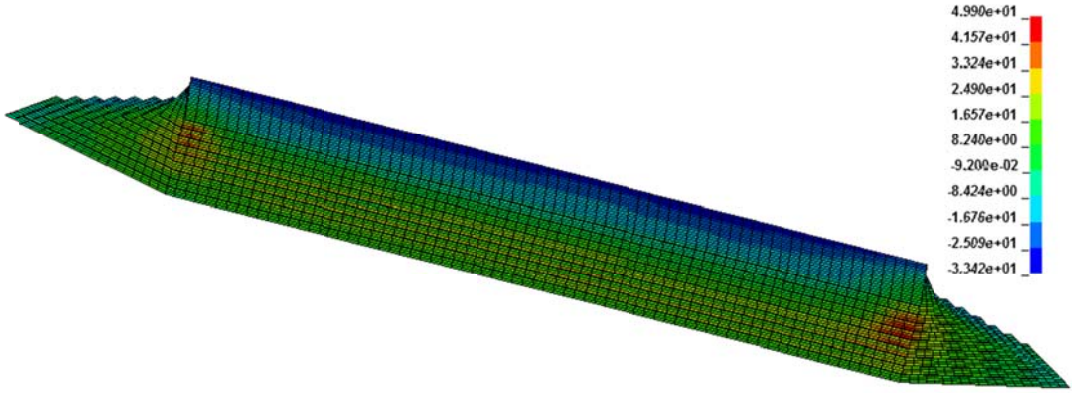

Figure 7-35: Modular block wall reinforcement normal x stress, σ_x, in psi for the Illinois earthquake

The σ_x vs. time plot for the element with the maximum stress is shown in Figure 7.36. All five of the earthquake motions showed maximum σ_x at the corners of the main wall to joint wall and have their maximum stress results reported in Table 7-5. If the maximum σ_x found from the Illinois motion analysis is multiplied by the cross sectional area per unit foot width of wall, it gives a force of 150 lbs/ft or 2.2 kN/m. Ling et. al. [10], found tensile forces to be around 1.0 kN/m for a modular block wall with half the height and 4 reinforcement layers. The model used by Ling et. al. however does not consider what might happen at the joints of two walls. It is seen that corners develop excess stresses in seismic events [54].

The main-wall to wing-wall joints have the maximum shear stress located in the middle of the wall on the back side where the wall touches the soil for all earthquake cases. The maximum shear stress found was a τ_{xy} stress which occurred on then El Centro earthquake as shown in Figure 7.37.

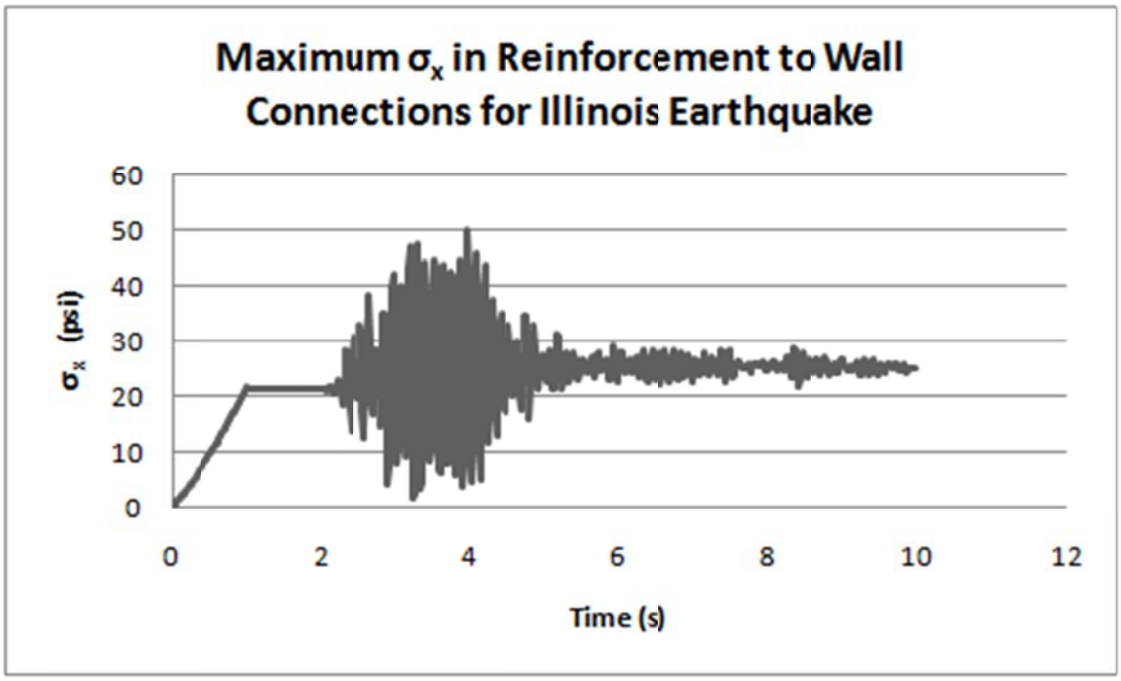

Figure 7-36: σ_x vs. time plot for element with maximum stress in Illinois earthquake

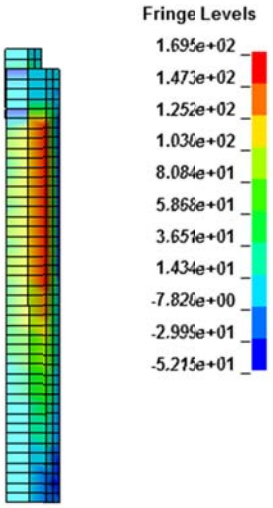

Figure 7-37: Joint of right wing wall to main wall τ_{xy} plot for El Centro earthquake. Units of stress are in psi.

The time history plot of the element with the maximum τ_{xy} is shown in Figure 7.38. For the modular block walls, the τ_{xy} was seen to be maximum in the joint between the main wall and the wing wall. This is consistent in the shear developed in Figure 3.1 [54].

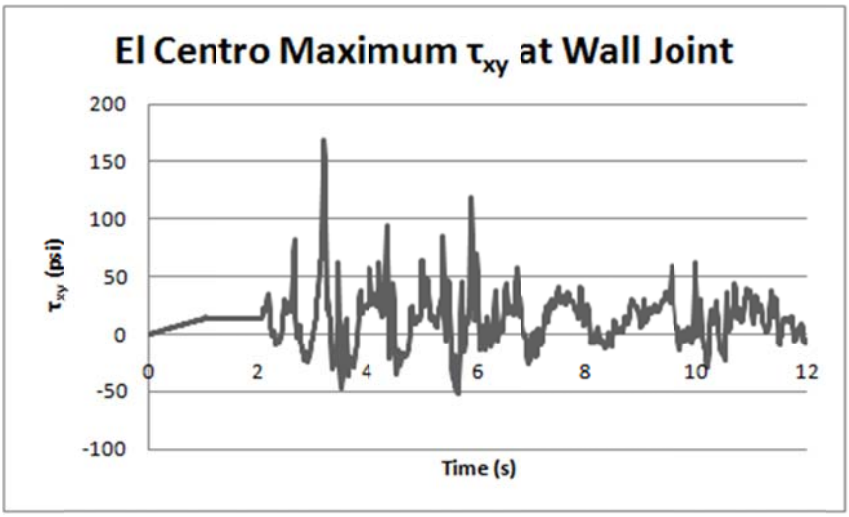

Figure 7-38: τ_{xy} vs. time for El Centro earthquake at wall joint

The ends of walls do not appear to have a "whipping" effect which has been a concern. The relative displacements of a node at the end of the wall to a node at the wall joint are plotted for the Illinois earthquake in Figure 7.39.

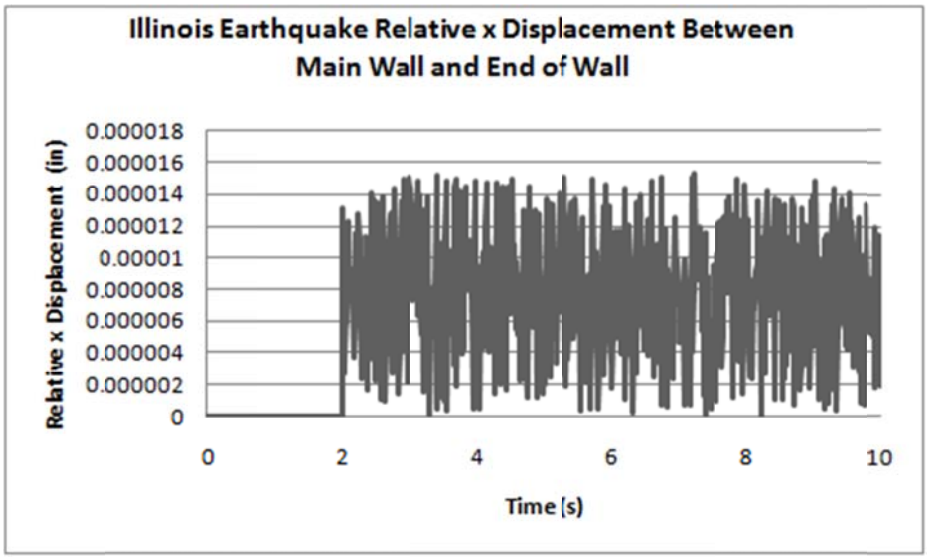

Figure 7-39: Relative x displacement of end node to node at wall joint for Illinois earthquake

There have been no reported cases of ends of walls causing a whipping effect and therefore is not a main concern (eg. [5],[6],[7],[54]). A summary of all results found is listed in Table 7-5.

Table 7-5: Summary of 15 foot modular block wall results

	Max PGA site	Mount. Plain transition site	Eastern site	Illinois EQ	El Centro
Max z Displacement of Top Blocks	0.0098 in	0.0075 in	0.018 in	0.021 in	0.030 in
Max σ_x at Reinforcement to Wall Connections	43 psi	43 psi	43 psi	50 psi	42 psi
Max τ_{xy} In Joint of Main Wall to Wing Wall	86 psi	72 psi	97 psi	127 psi	169 psi
Max Relative x Displacement of Ends of Walls	15×10^{-6}	15×10^{-6}	15×10^{-6}	15×10^{-6}	15×10^{-6}

7.2 Results for 30 Foot High Walls

7.2.1 Modal Analysis Results

Only one modal analysis was performed for the 30 foot walls, since the modal analyses for the 15 foot modular block and segmental panel walls showed to be practically identical. The first three mode shapes are similar to those of the 15 foot panel wall, but have a lower frequency. More specifically, the frequency for the first mode is calculated to be 3.45 Hz, which results in a natural period of 0.28 s and a circular natural frequency of 21.7 rad/sec. The natural period and circular natural frequency of the 30 foot wall for all three mode shapes are listed in Table 7-6.

Table 7-6: Modal analysis results for 30 foot walls		
	Natural Period (s)	Natural Frequency (rad/s)
mode 1	0.28	21.7
mode 2	0.27	23.1
mode 3	0.25	25.3

It can be seen that the natural periods for the first three mode shapes are very similar to one another. This clustering of natural frequencies is due to the fact that the corresponding mode shapes, even though they are different, are dominated by the shear mode of deformation perpendicular to the main wall facing. Assuming a plane strain cantilever shear deformation mode for the walls, the first natural period, *T*, may be analytically defined as:

$$T = 2\pi H\sqrt{\frac{\rho}{2G}} \qquad \textbf{(7-4)}$$

where *H* is the wall height, ρ is the mass density, and *G* is the shear modulus. Since the plane strain cross-section of the MSE wall is predominantly comprised of the compacted soil material, ρ and *G* of the wall may be approximated using the mass density, elastic modulus, and Poisson's ratio values for the compacted soil as previously defined. Using Eq. (7-4) for a wall height of 30.0 ft yields a first natural periods of 0.30 seconds, which is quite close to the LS-Dyna models predictions tabulated in Table 7-6, and emphasizes the dominance of the shear mode of deformation in the first three modal shapes. These values are additionally confirmed by Eq. (7-2) from Richardson and Lee [69], which predicts a natural period of 0.24 seconds for the 30 ft tall wall.

7.2.2 Earthquake Analysis Results of the 30 Foot Segmental Panel Wall

The displacements of a node at the bottom of the wall, the middle of the wall, and the top of the wall are presented in Figures 7.40-7.45. The earthquake displacements and gravity are applied as in the case of the 15 foot high walls.

Figures 7.40-7.45 show that the top nodes of the wall are pulled back towards the soil. This is an effect of the gravity loading on the model. As the gravity compresses the soil, it puts the reinforcement in tension which then pulls the top of the wall down and towards the soil.

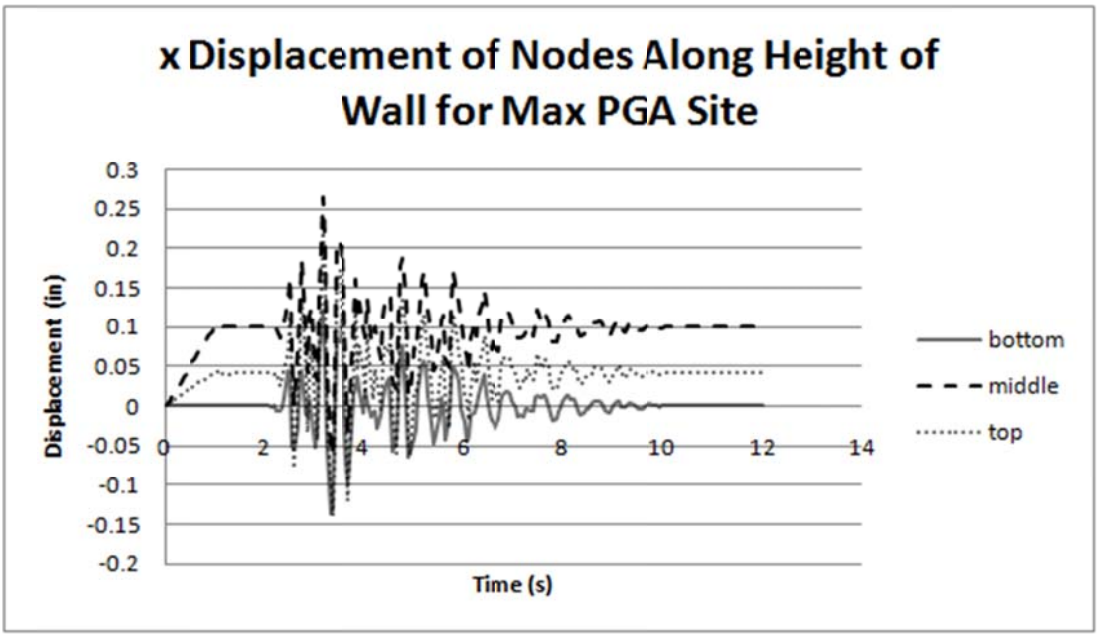

Figure 7-40: x displacement of nodes along height of 30 foot segmental panel wall for max PGA site

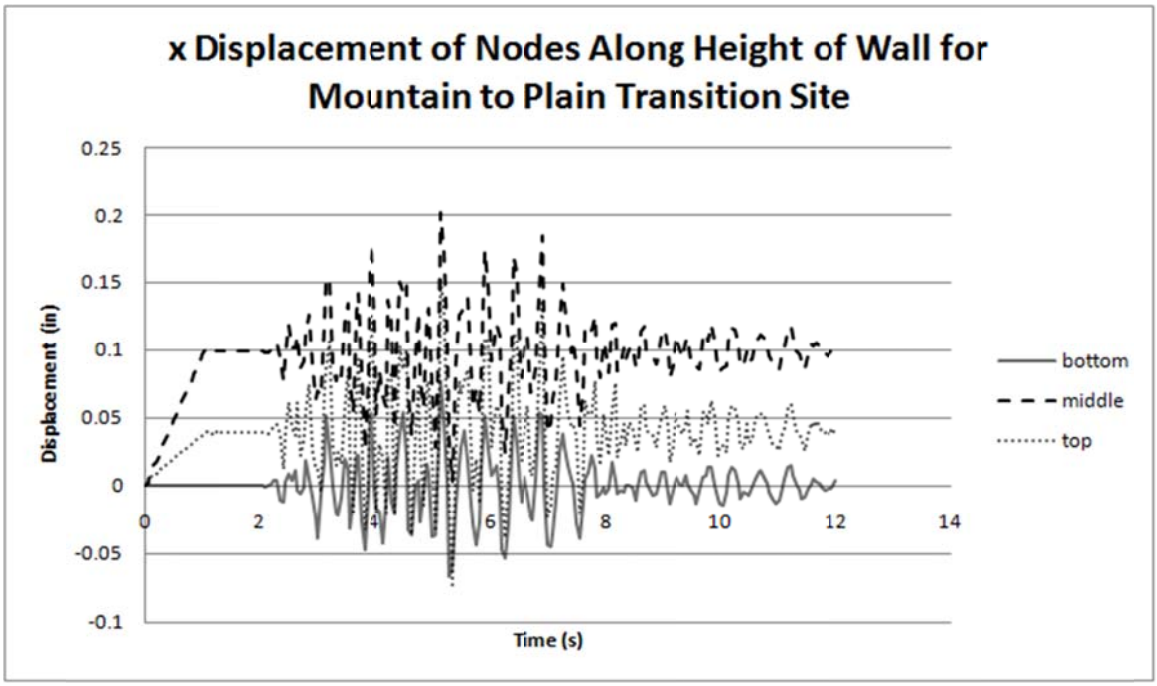

Figure 7-41: x displacement of nodes along height of 30 foot segmental panel wall for mountain to plain transition site

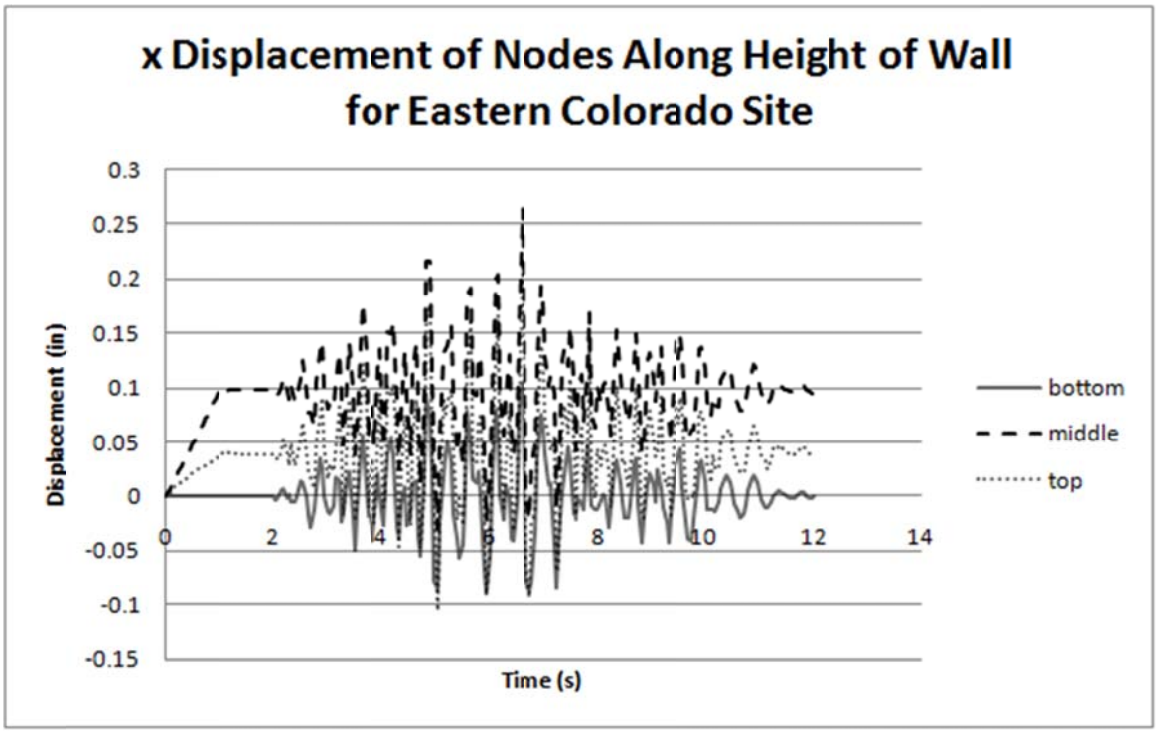

Figure 7-42: x displacement of nodes along height of 30 foot segmental panel wall for Eastern Colorado site

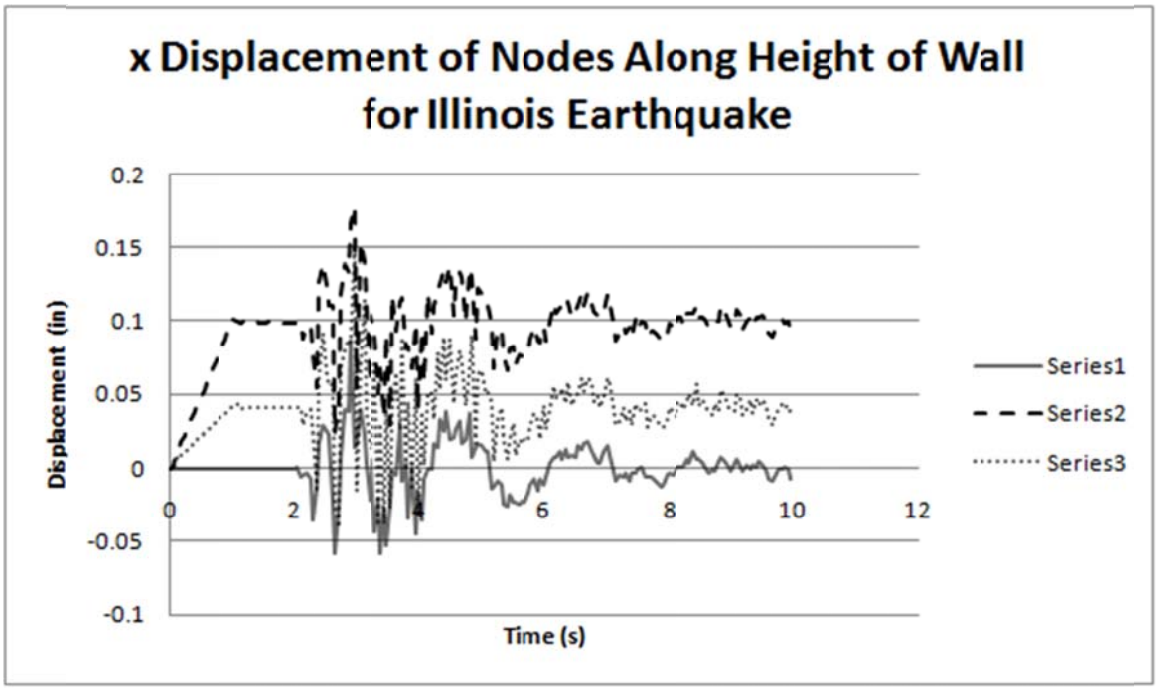

Figure 7-43: x displacement of nodes along height of 30 foot segmental panel wall for max Illinois earthquake

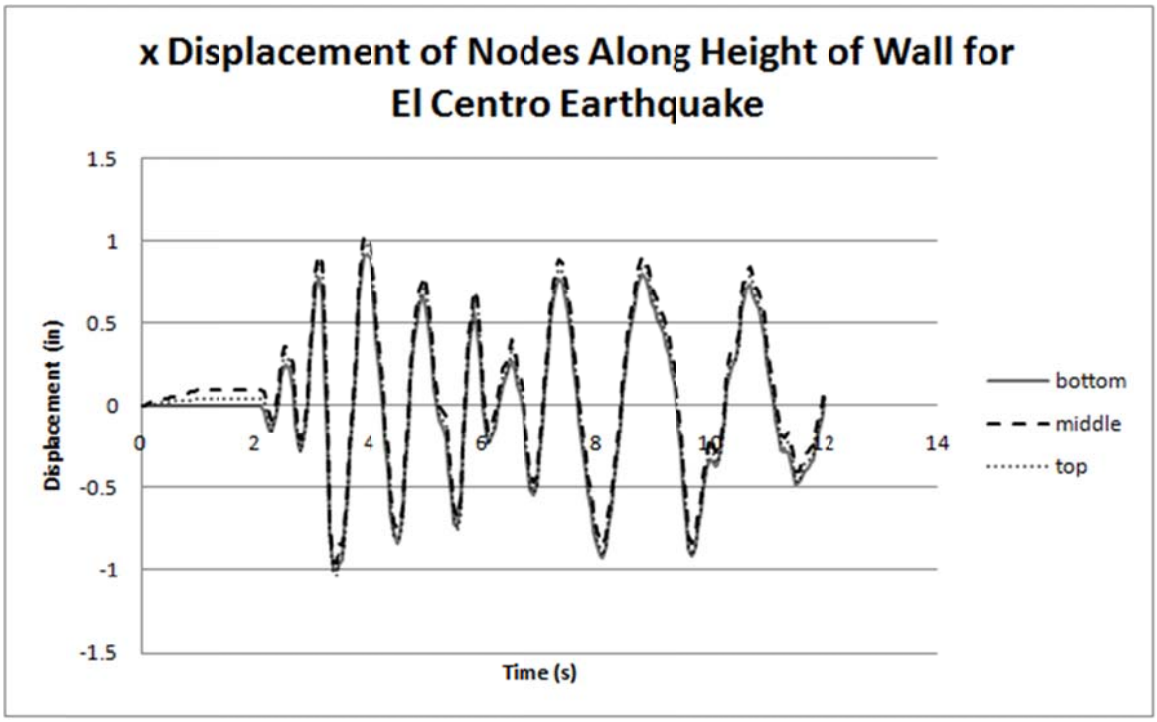

Figure 7-44: x displacement of nodes along height of 30 foot segmental panel wall for El Centro earthquake

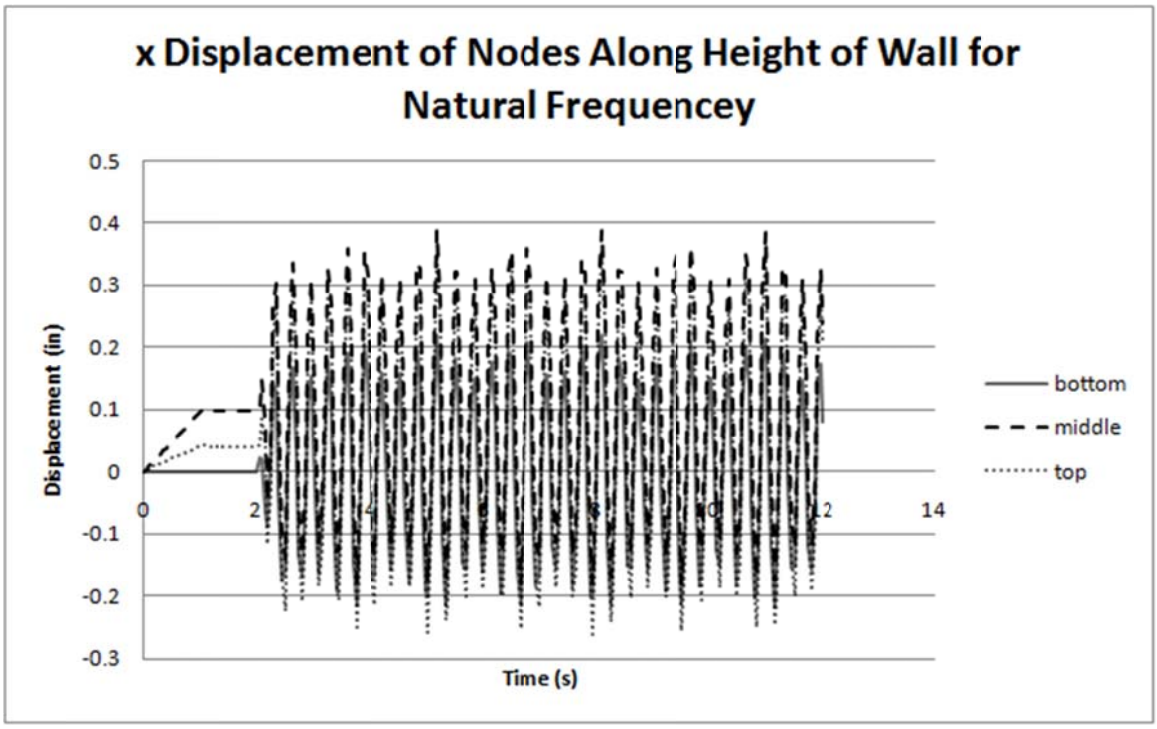

Figure 7-45: x displacement of nodes along height of wall for 30 foot segmental panel wall for natural frequency

Although the wall bulges, it still exhibits deformations that are consistent with the mode shapes found in the modal analysis (Figures 7.1-7.3) where the top of the wall has the most deformation from swaying in shear.

Figure 7.46 shows plot of the normal stress σ_x for the reinforcement in the panel wall subjected to the El Centro earthquake. The red colored areas indicate the highest tensile stresses, while the blue colored areas indicate the largest compressive stresses. This plot captures the instance where σ_x is at a maximum. The maximum stresses develop in the front and center of the reinforcement. Figure 7.47 shows the time history plot of σ_x versus time for the element that develops the highest stress. This element develops a maximum stress of 151 psi at 2.5 seconds into the analysis. It can be seen from Figure 7.47 that the stresses due to gravity are 109 psi. Therefore, 42 psi is developed in the reinforcement due to actual dynamic loading.

All four of the other earthquake motions showed the maximum σ_x in the middle of the main wall on the second reinforcement layer and have their maximum stress results reported in Table 7-7.

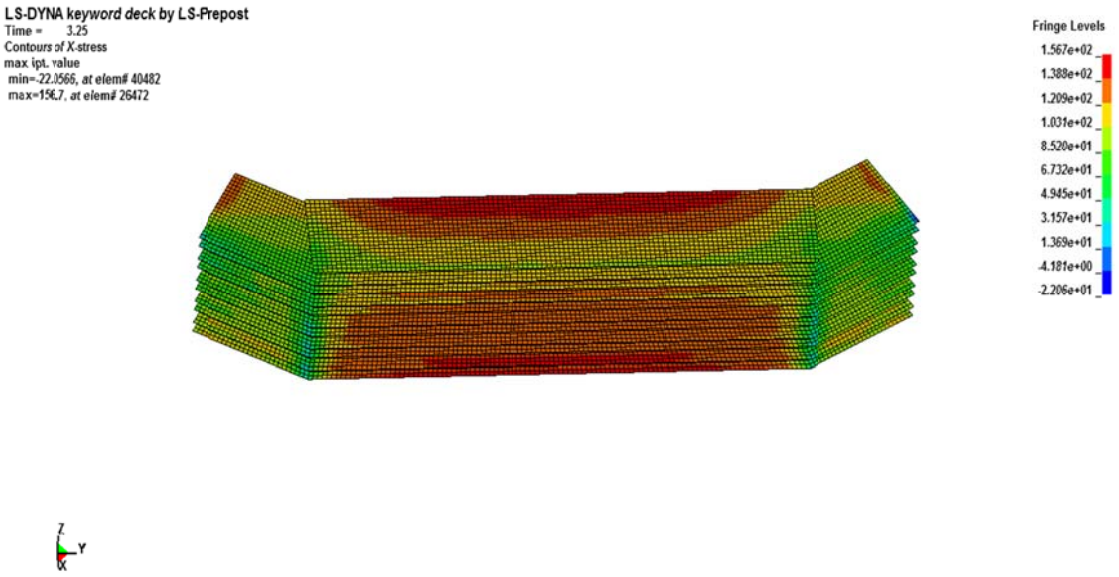

Figure 7-46: 30 foot segmental panel wall reinforcement normal x stress, σ_x, in psi for El Centro earthquake

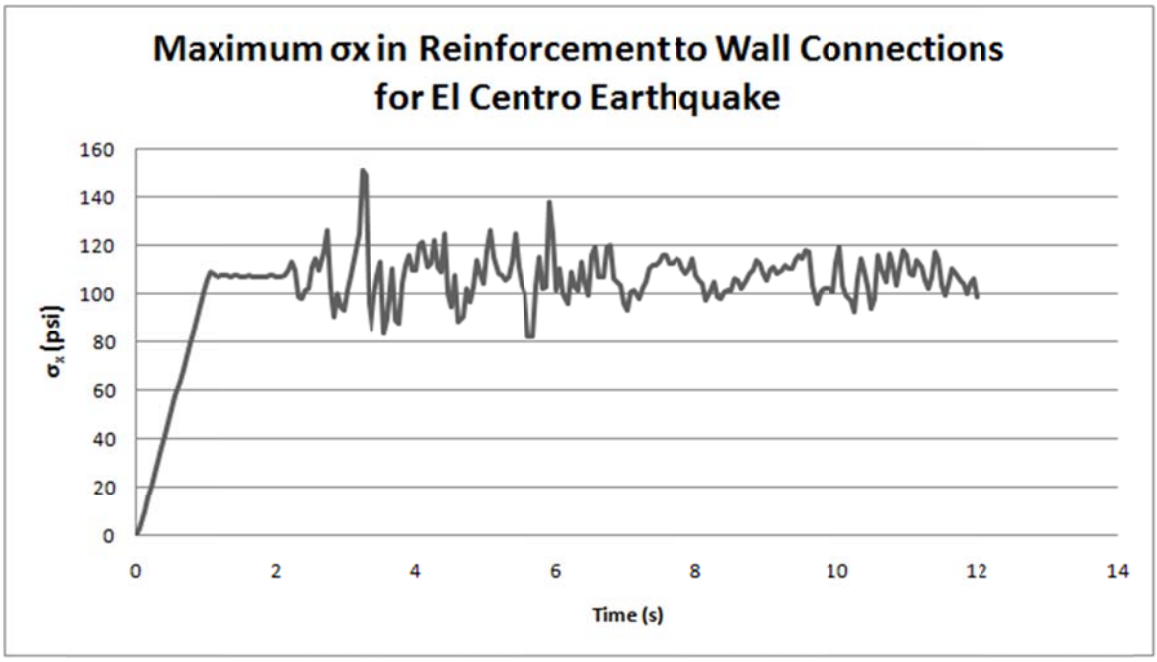

Figure 7-47: Time history plot of maximum σ_x for 30 foot segmental panel wall with El Centro earthquake

Figure 7.48 shows the shear stress τ_{yz} of the elements that form the joint of the left wing wall and the main wall. This stress is 307 psi at a time of 3.3 seconds for the El Centro earthquake. Figure 7.49 shows the time history plot of the element with the maximum τ_{yz} that develops.

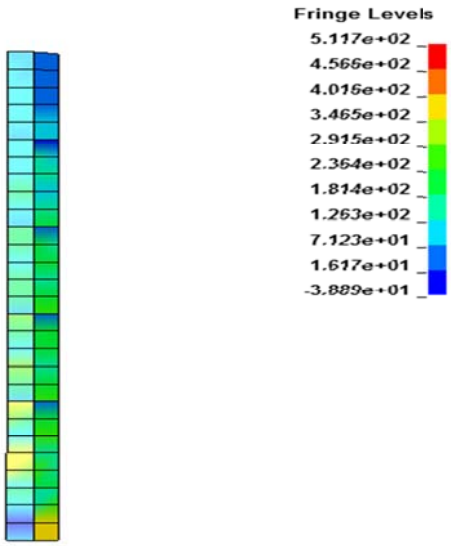

Figure 7-48: 30 foot segmental panel wall main wall to wing wall joint for El Centro earthquake τ_{yz} in psi

It has been observed that during seismic events large stresses tend to develop at the corners of walls [54]. For the segmental panel walls, τ_{yz} was found to be maximum at the joint between the main wall and the wing wall.

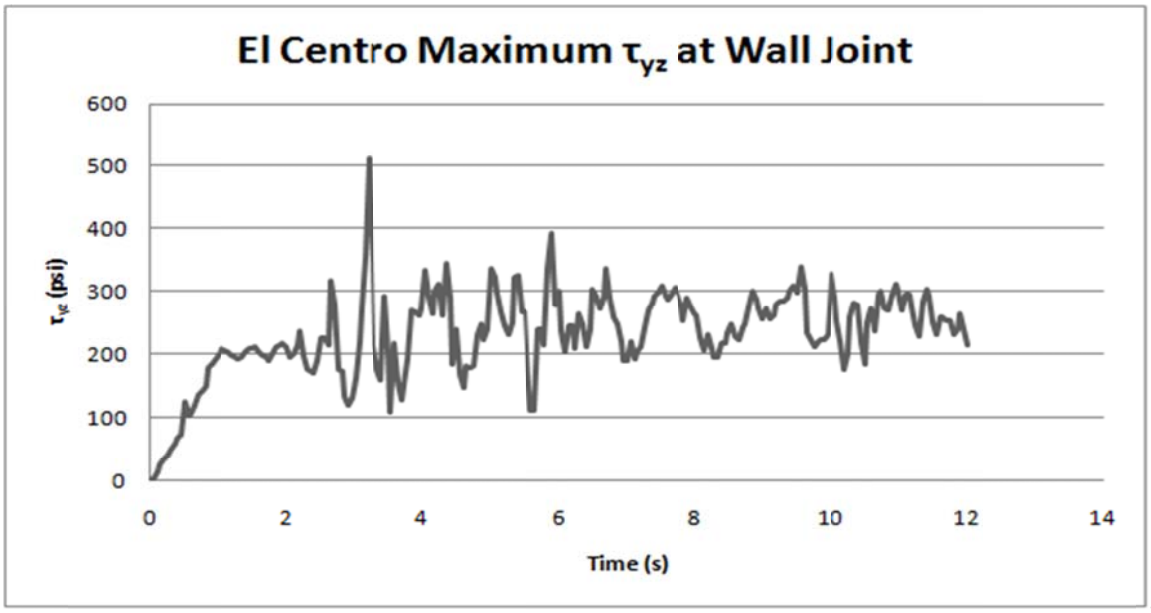

Figure 7-49: Time history plot for 30 foot segmental panel wall main wall to wing wall joint for El Centro τ_{yz} in psi

The summary of the maximum stress results found for all segmental panel wall earthquake analyses is presented in Table 7-7.

Table 7-7: Summary of 30 foot segmental panel wall earthquake analyses results

	PGA site (psi)	Mount. Plain transition site (psi)	Eastern Site (psi)	Illinois (psi)	El Centro (psi)	Natural Frequency (psi)
σ_x at Reinforcement to Wall Connections	126.8	120.1	128.6	123.1	151.3	131.2
Max τ_{yz} Between Joint of Main Wall and Wing Walls	243.7	234.5	256.2	307.1	511.7	349.3

7.2.3 Earthquake Analysis Results of 30 Foot Modular Block Wall

The displacements of a node at the bottom of the wall, the middle of the wall, and the top of the wall are presented in Figures 7.50-7.55. As in the case of the 30 foot segmental panel walls, the application of gravity puts the reinforcement in tension, which results in the top nodes of the modular block walls to be pulled back towards the soil. This is an artifact of the way that gravity is applied in the finite elements model. Whereas the actual structure applied gravity with the gradual built of the wall, gravity in the model is applied after the entire wall is build, resulting in unrealistic amounts of bulging. As the gravity compresses the soil, it puts the reinforcement in tension which then pulls the top of the wall down and towards the soil.

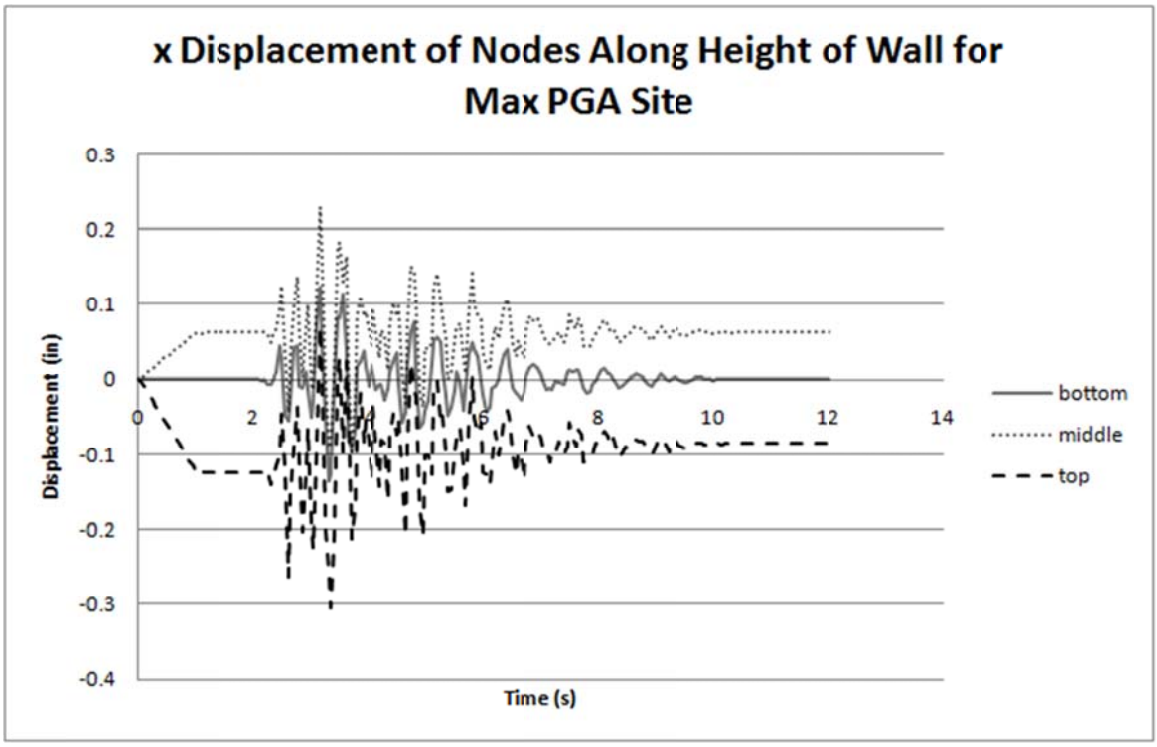

Figure 7-50: 30 foot modular block x displacement of nodes along height of wall for max PGA site

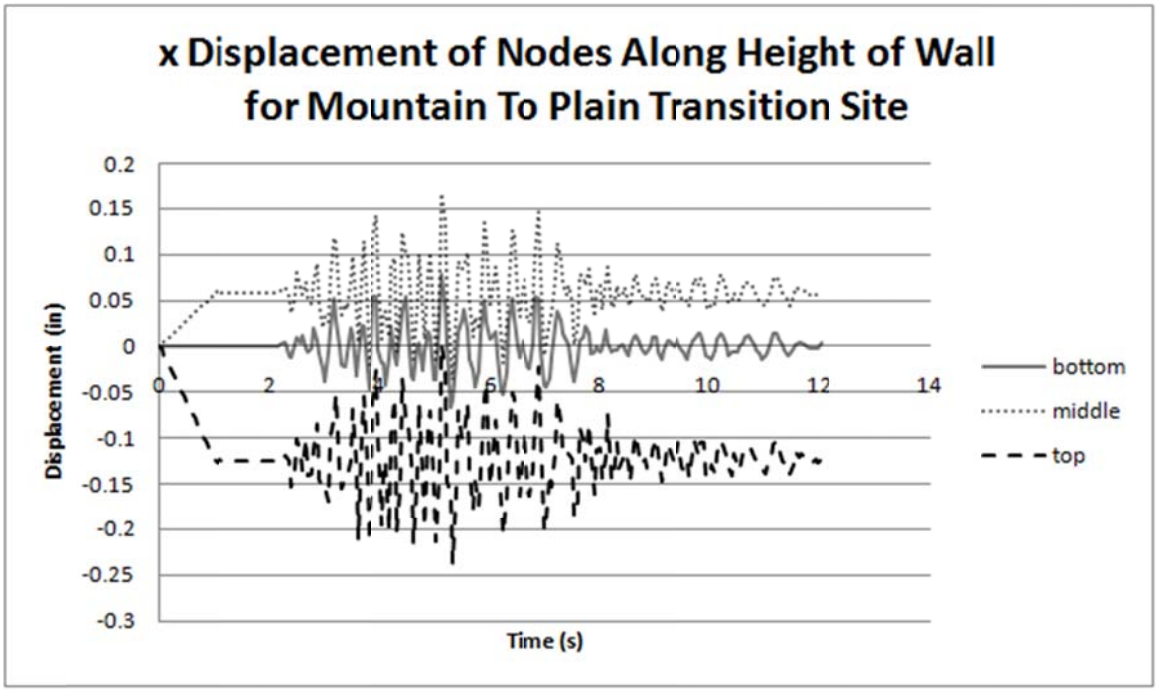

Figure 7-51: 30 foot modular block x displacement of nodes along height of wall for mountain to plain transition site

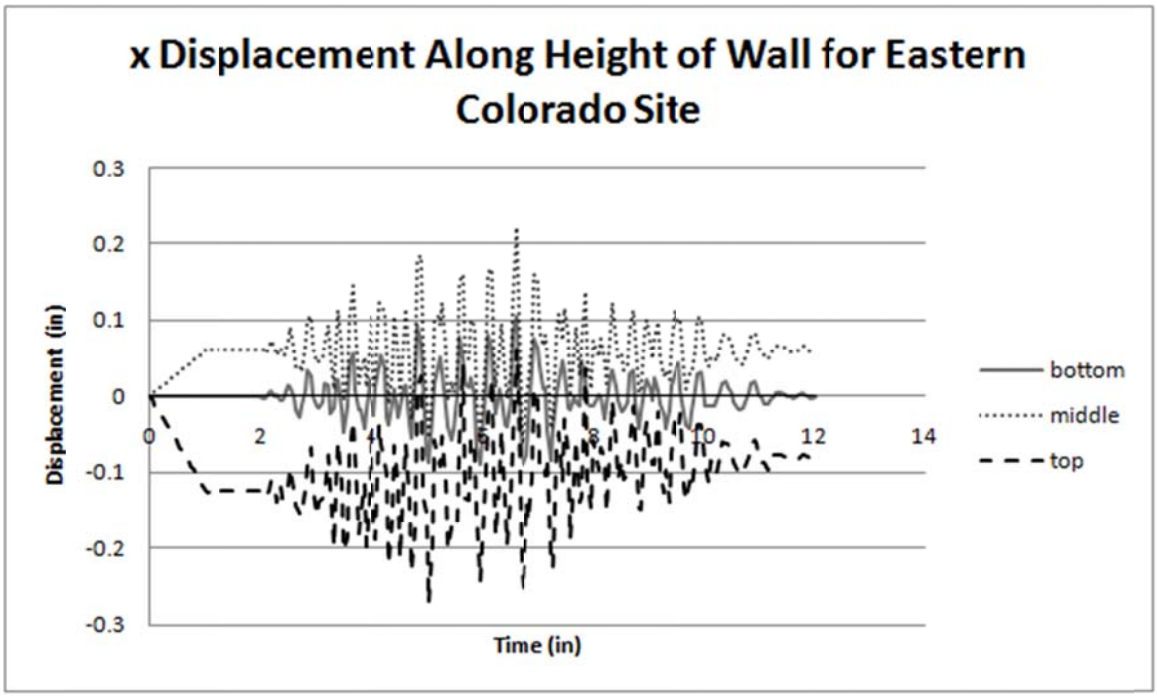

Figure 7-52: 30 foot modular block x displacement of nodes along height of wall for Eastern Colorado site

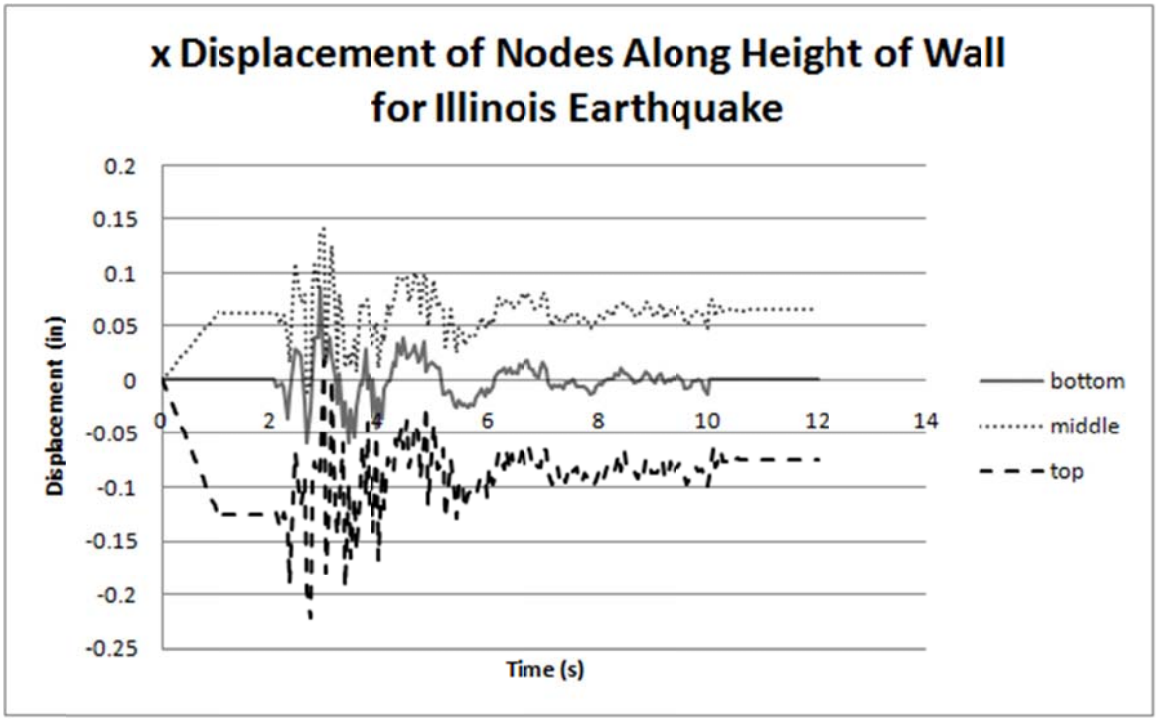

Figure 7-53: 30 foot modular bock x displacement of nodes along height of wall for Illinois Earthquake

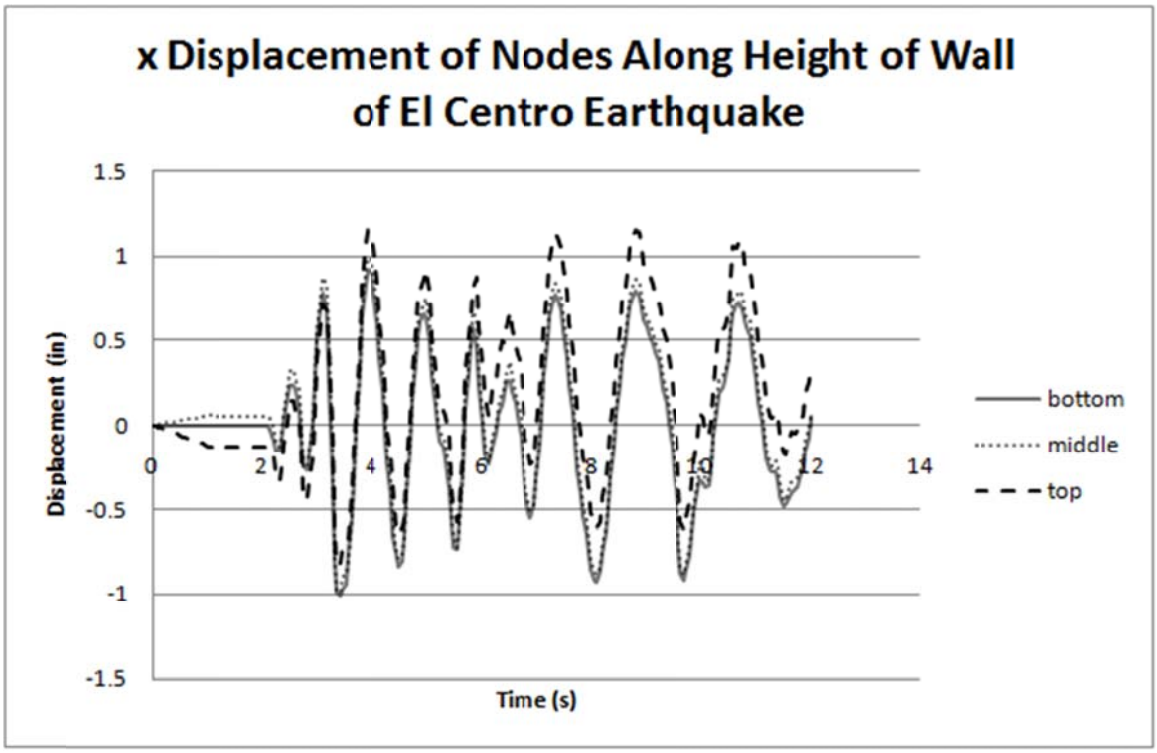

Figure 7-54: 30 foot modular block x displacement of nodes along height of wall for El Centro Earthquake

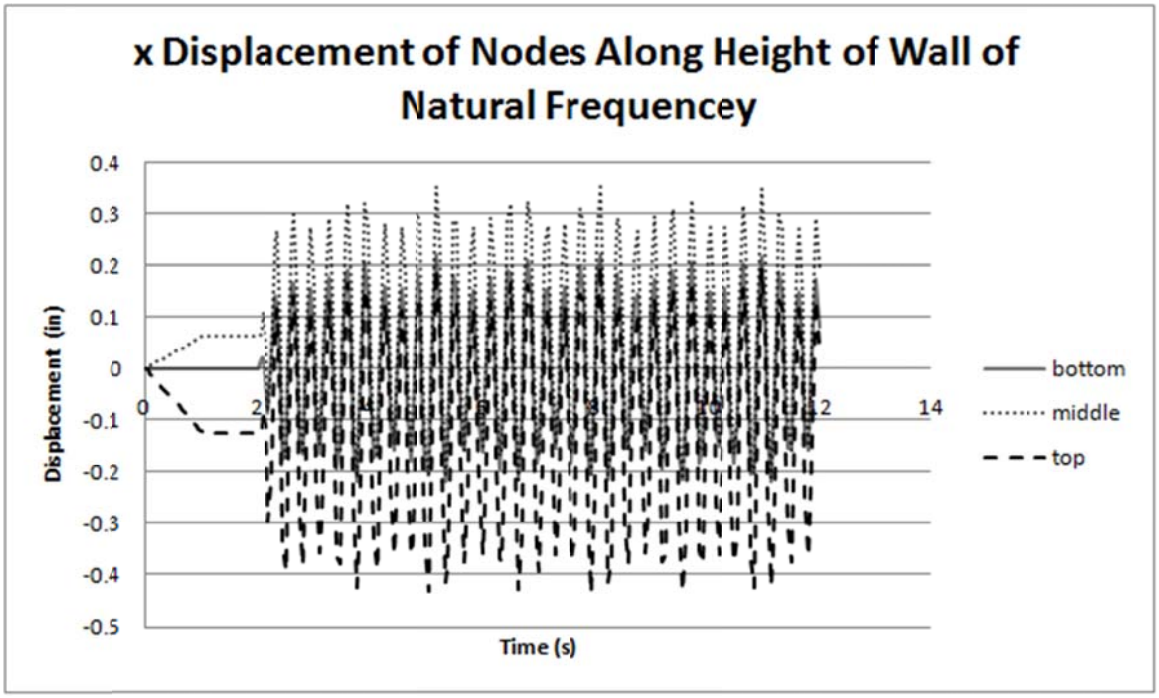

Figure 7-55: 30 foot modular block x displacement of nodes along height of wall for wall natural frequency

It is shown in Figures 7.50-7.55 that the walls sway in and out such that the top of the wall has the largest displacement. The top blocks have small residual displacements from the no-penetration contact model toward the end of the motion which are still consistent with Cai and Bathurst [46]. The same tensile effect in the reinforcement due to the applied gravity also pulls the top blocks back and causes them to rock. This unrealistic uplift of the top blocks is shown as the maximum location of the z displacement in the 30 foot modular block model. This is another effect of the model and was discarded. The maximum chatter of the top blocks was therefore observed at the same position as the maximum chatter of the 15 foot walls. The maximum displacement chatter from all earthquake loadings occurred with the Natural Frequency motion with a displacement of .0023 in. The relative z displacement of the node time history plot is shown in Figure 7.34. This displacement occurred at the highest block of the wing wall nearest to the wing wall to main wall joint.

The vertical displacements shown here are very small and can be eliminated if grouting of the top two or three layers is used. In this model, the top blocks rely entirely on gravity to stay in place. Yen et al. [54] showed top blocks of a modular block MSE wall toppling because they were not supported by backfill. Most cases of modular block wall failure occur at the corners due to shear [54]. The maximum reinforcement-to-wall-connection stress occurred in the top most layer of reinforcement that was also connected to the wing wall as shown in Figure 7.56. The maximum normal stress σ_x for this case occurred for the Illinois Earthquake.

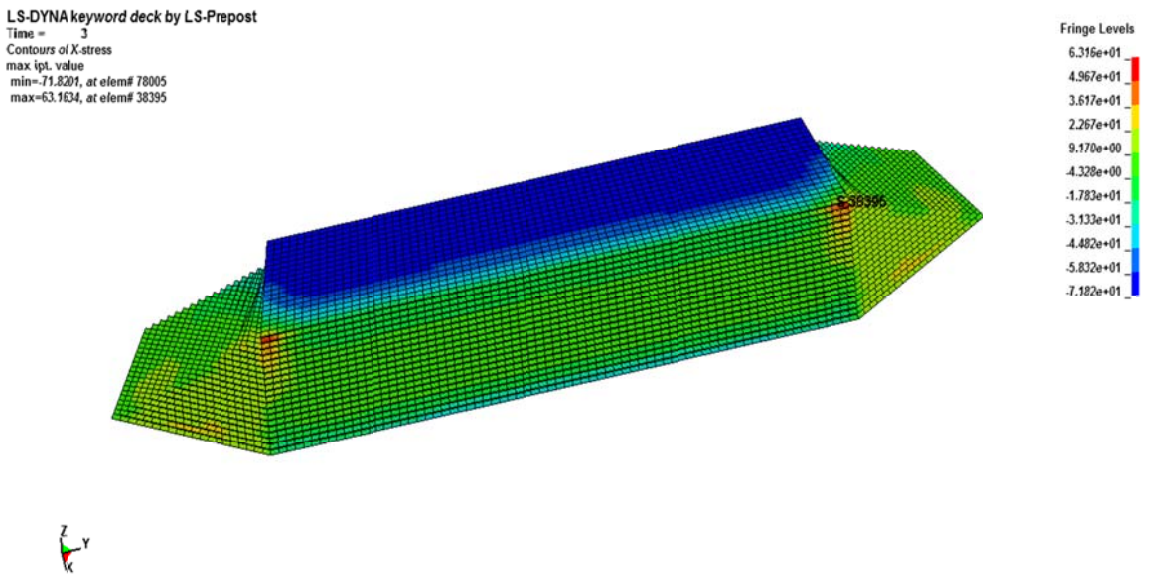

Figure 7-56: 30 foot modular block wall reinforcement normal x stress, σ_x, in psi for the Illinois earthquake

The σ_x vs. time plot for the element with the maximum stress is presented in Figure 7.57. All five of the earthquake motions developed a maximum σ_x at the intersection between the main wall and the wing wall facing components and have their maximum stress results reported in Table 7-8. If the maximum σ_x due to the Illinois motion is multiplied by the cross sectional area per unit foot width of wall, it gives a force of 189 lbs/ft or 2.5 kN/m. Ling et. al. [10], found tensile forces to be around 1.0 kN/m for a modular block wall with half the height and 4 reinforcement layers. The model used by Ling et. al. however does not consider what stress concentrations at the joints of two walls. It is seen that corners develop excess stresses in seismic events.[54].

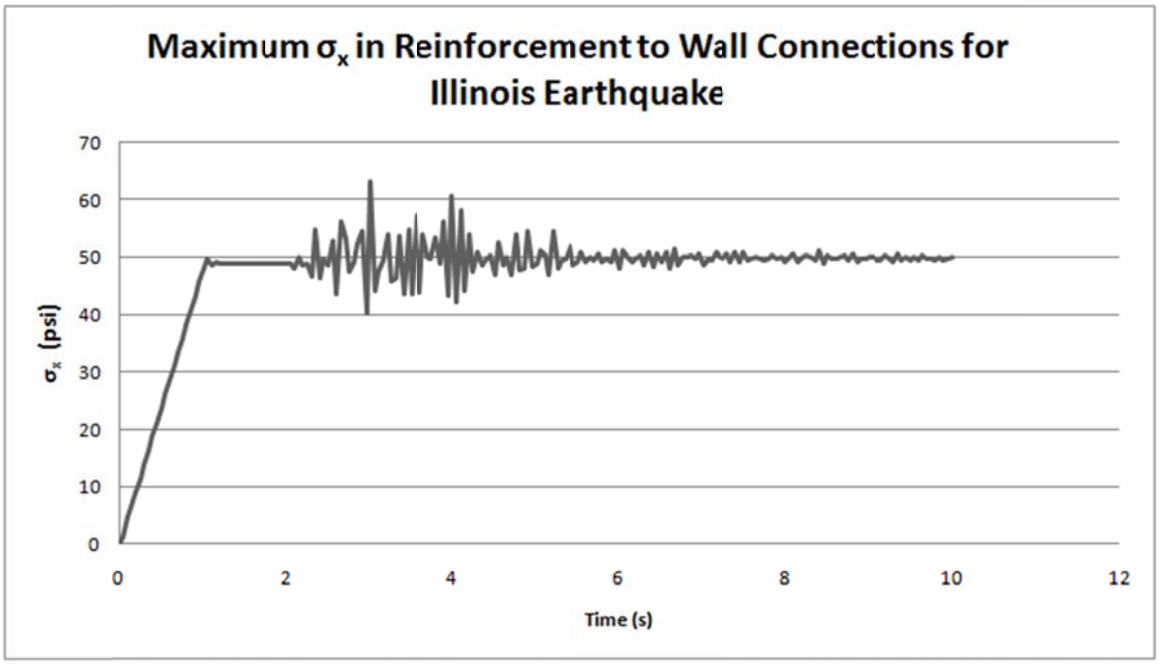

Figure 7-57: σ_x vs. time plot for element with maximum stress in Illinois earthquake

The maximum shear stresses for all walls occurred at the intersection between the main wall and the wing wall facing components at mid-height. This is consistent with the shear developed in Figure 3.1 [54]. The maximum shear stress found was induced by the El Centro earthquake at this location as shown in Figure 7.58. The time history plot of the element with the maximum τ_{xy} is shown in Figure 7.59.

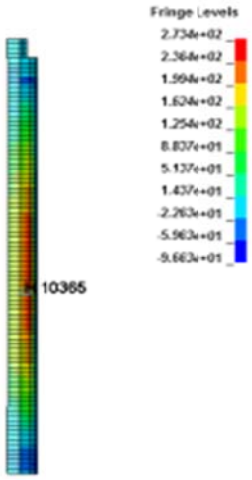

Figure 7-58: 30 foot modular block joint of right wing wall to main wall τ_{xy} plot for El Centro earthquake. Units of stress are in psi.

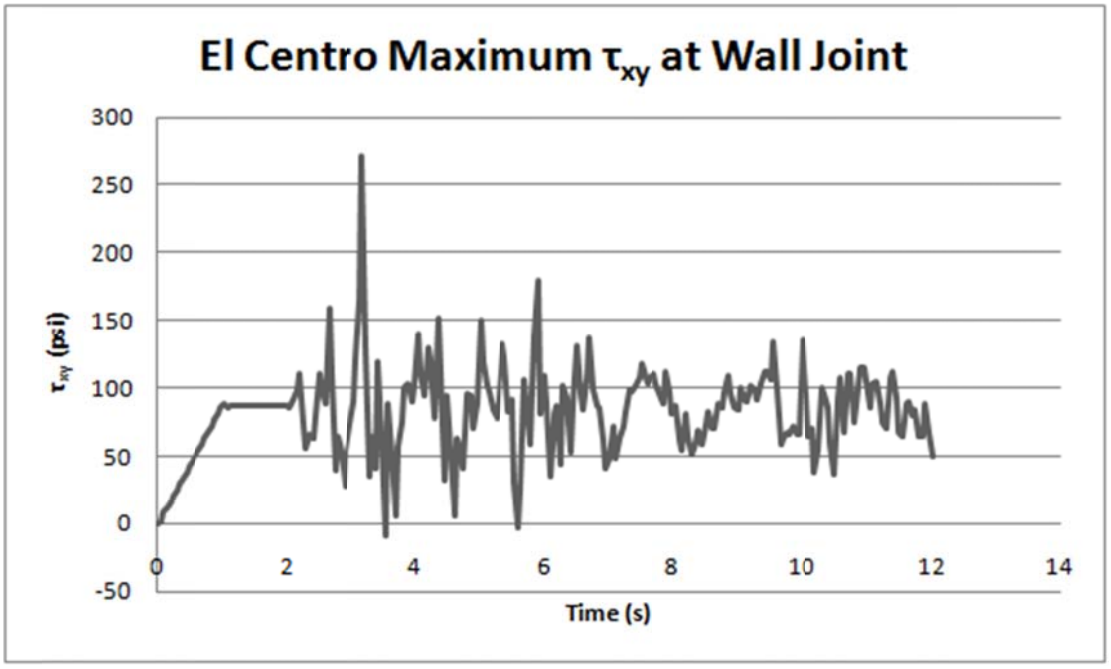

Figure 7-59: τ_{xy} vs. time for El Centro earthquake at wall joint

The ends of walls do not appear to have a "whipping". The maximum calculated relative displacement of a node at the end of the wall to a node at the wall joint for all cases is 0.0000015 in.

There have been no reported cases of ends of walls causing a whipping effect and therefore is not a main concern (eg. [5],[6],[7],[54]). A summary of all results found is listed in Table 7-8.

Table 7-8: Summary of 30 foot modular block wall results

	Max PGA site	Mount. Plain transition site	Eastern site	Illinois EQ	El Centro	Natural Frequency
Max z Displacement of Top Blocks (in)	0.0011	0.0013	0.0015	0.0009	0.0016	0.0023
Max σ_x at Reinforcement to Wall Connections (psi)	52.6	56.1	58.2	63.16	61.24	58.7
Max τ_{xy} In Joint of Main Wall to Wing Wall	167.7	130	152.014	134.9	272.03	150.4
Max Relative x Displacement of Ends of Walls (in)	15×10^{-6}	15×10^{-6}	15×10^{-6}	15×10^{-6}	15×10^{-6}	15×10^{-6}

8.0 CONCLUSIONS AND RECOMMENDATIONS

The goal of this study was to use advanced finite element models of MSE walls subjected to seismic loads in order to observe: (1) the vertical displacements of the top row of blocks on modular block MSE walls; (2) the horizontal deformations of tapered down ends of walls on modular block MSE walls; (3) the stresses at the interface of the wing wall to the main wall for both modular block and segmental panel MSE walls and (4) the reinforcement connection stresses for both modular block and segmental panel MSE walls. This was achieved by constructing two modular block wall models, one with 15 ft and one 30 ft height; and two segmental panel walls, with heights of 15 ft and 30 ft. The reinforcement lengths and spacing were obtained from the shop drawings provided by CDOT of physical MSE walls built in Colorado. From the analyses of these MSE wall models the following conclusions were drawn:

- The first three mode shapes were found for both the 15 ft segmental panel wall and the 15 ft modular block wall and were all found to have a period of approximately 0.13 seconds. This is consistent with the empirical equation for calculating an MSE wall natural period by Richardson and Lee [69], and an analytical simple shear model developed in this study. A similar analysis was performed using RISA-3D with very similar results. Because the natural periods of these two walls were so close together only one modal analysis was performed on the 30 ft segmental panel wall, where a natural period of 0.28 seconds was calculated for the first mode shape. This is also consistent with Richardson and Lee [69] and the analytical simple shear model that was developed in this study.
- For the 15 ft and 30 ft segmental panel walls there was slight bulging that occurred in the middle of the wall that is consistent with the failure mode described by Sabermahani et.al. [11] and the experimental results found by Siddharthan, et al. [14]. Walls generally deform in a fashion that is consistent with the mode shapes described in section 7.1. The displacements of the modular block walls were found to be consistent with the two dimensional finite element analyses performed by Cai and Bathurst [46].
- The maximum forces in the geogrid reinforcement (including both gravitational and seismic loadings) per unit length of wall for the 15 ft segmental panel wall, the 15 ft modular block wall, the 30 ft segmental panel wall, and the 30 ft modular block wall were calculated as 234

lbs, 150 lbs, 454 lbs, and 189 lbs, respectively. These maximum forces resulted from the El Centro earthquake for the segmental panel walls and from the Illinois earthquake for the modular block walls (Table 8.1). However, it can be noted from Tables 7-4, 7-5, 7-7, and 7-8 that the maximum values of the tensile forces in the geogrid from the Colorado earthquakes have maximum values that are very similar in magnitude to the reported maximum values from the "extreme" El Centro and Illinois motions examined in this study.

Table 8-1: Summary of maximum reinforcement forces per unit length

Facing Type and Reinforcement Spacing:	Wall Height: 15 feet	Wall Height: 30 feet	Reinforcement Tensile Strength	Peak Connector Strength
Modular Block with 18" Typical Spacing	150 lb/ft (Please see Figure 7-35 for the location of the maximum stress)	189 lb/ft (Please see Figure 7-56 for the location of the maximum stress)	19,500 lb/ft (UX1000)	14,133 lb/ft (Two Standard Connectors to a Mesa block)
Segmental Panel with 3' Maximum Spacing or 30" average)	234 lb/ft (Please see Figure 7-19 for the location of the maximum stress for the El Centro motion; the stress maximizes in the middle of the main wall for the other earthquake loadings (See Table 7-4)).	454 lb/ft (Please see Figure 7-46 for the location of the maximum stress)	19,500 lb/ft (UX1000)	9,600 lb/ft (HDPE Connector Tabs)

- The maximum force that the uniaxial geogrid 1000 MSE (UX1000MSE) can carry before breaking is 19,550 lbs per unit length of wall for reinforcement that extends 17 ft into the soil. Segmental panel walls are often built with connector tabs made of HDPE on the back of the panels. A typical tensile strength of HDPE is 3200 psi or 9,600 lbs per unit length of wall.

For a UX1100MSE geogrid connected to one Mesa standard block using two standard connectors the peak connection strength is 14,133 lbs per unit length of wall for 17 ft of reinforcement [2]. The seismic motions do not develop breakage stresses for the lower strength reinforcements.

- The maximum shear forces that developed at the joints between the main wall and the wing walls occurred vertically for the segmental panel walls and horizontally for the modular block walls. For the 15' and 30' segmental panel walls, the maximum shear stresses were 188 psi and 511.7 psi, respectively. For the 15' and 30' modular block walls, the maximum shear stresses were 169 psi and 272.03 psi, respectively. These shear stresses (all caused from the "extreme" El Centro earthquake motion with a larger magnitude than that expected for CDOT designs) were not significant enough to be expected to result in failure of the concrete joint connections.
- In the 15 ft modular block wall, the maximum vertical displacement of the top blocks was observed at the topmost block of the wing wall. This block is not crucial to the structural integrity of the wall. This block only displaced a maximum of 0.003 in for the 15 ft wall and .0023 in for the 30 ft wall. Bricks displace less for the 30 foot wall due to a lower natural frequency. The top blocks in the MSE wall models used were only held together by friction and gravity. Typical MSE wall construction requires grouting through the top block layers, which would eliminate the small block movement that was observed in the model when no grouting was used. If it desired to remove this very small vertical motion entirely, at least the top three rows of blocks should be grouted to the underlying blocks, as the top row of blocks and the next two rows of blocks were allowed to vertically chatter in this model. More severe earthquake motions such as the Chilean Earthquake could potentially cause larger magnitudes of block chattering [54], but these motions were too large to be considered for this study.
- The "whipping" effect by the ends of the wing walls in the modular block models were found to be small. The max relative displacement in the x direction was .000015 in for all earthquake loadings. This is not a factor for MSE wall design.
- The results of this study show that segmental and modular block walls representative of typical current CDOT design practices performed well with respect to both serviceability and strength requirements, even under AASHTO's newly stringent requirement for the

consideration of a 1,000-year return period earthquake. The CDOT wall systems have also been shown to perform well even under extreme loading conditions centered about the natural frequencies of the walls and historic significant earthquakes such as the El Centro earthquake.

- Three separate example Colorado sites (the max PGA site, the mountain to plain transition site, and the Eastern Colorado site) were examined to assess if varying underlying geographical conditions affected the seismic response of the MSE wall structures subjected to the 1,000-year return period earthquake. From Tables 7-4, 7-5, 7-7 and 7-8, it can be seen that the magnitudes of the relevant stresses and displacements amongst the corresponding MSE walls at the three different sites are all on the same order of magnitude; it does not appear that the differences are significant enough to merit individualized design procedures in CDOT MSE wall design for each geographic region.
- The results of these linear elastic finite element studies indicate that seismic design for MSE walls in Colorado does not need to be routinely performed, even considering the recent more stringent AASHTO requirements. Looking at Tables 7-4, 7-5, 7-7, and 7-8, it can be seen that the MSE walls, which were modeled based upon walls designed using typical current CDOT MSE wall design procedures, performed very well under all of the seismic loads examined. The CDOT MSE walls performed very well under elevated seismic loadings without having to explicitly consider seismic-specific concerns in their design. Additionally, as noted in Anderson et. al [75], at the 2011 meeting of the AASHTO Subcommittee on Bridges and Structures, state and federal bridge engineers agreed that seismic analysis is not required for MSE walls which are <=9.1 m and subject to a design acceleration <=0.4 g. This means that the MSE walls examined herein do not need to be designed for seismic loads as per the AASHTO recommendation.

9.0 FUTURE WORK

The next most relevant step to this research is to study the effects of inelastic material properties. For this study, it was assumed that a simple analysis using linear elastic material is sufficient given the relatively small earthquake magnitudes. A more material complex model can result in larger wall deformations, especially for taller walls and larger earthquake magnitudes. A future study on walls with metallic reinforcing strips should also be performed in the future.

REFERENCES

1. AASHTO LRFD Bridge Design Specifications, Customary U.S. Units, 4th Edition, including 2009 Interim Revisions. Section 11-10.

2. "Tensar International Corporation, Retaining Walls/Reinforced Slopes, Mesa Systems Unit Faces." *Tensar International Corporation*. Web. 27 Mar. 2011. <http://www.tensarcorp.com>.

3. Mechanically Stabilized Earth Wall: Inspector's Handbook, 2000, Paul D. Passe, Florida Department of Transportation, http://www.dot.state.fl.us/structures/Manuals/mse.pdf

4. Colorado Department of Transportation Bridge Design Manual, 2009, Section 5

5. Tatsuoka, F., Tateyama, M., Mohri, Y., Matsushima, K. 2007 "Remedial Treatment of Soil Structures Using Geosynthetic-Reinforcing Technology" *Geotextiles and Geomembranes* ScienceDirect Vol. 25 pp. 204-220

6. Fang, Y., Yang, Y., Chen, T. 2003 "Retaining Walls Damaged in the Chi-Chi Earthquake", *Canadian Geotechnical Journal* Vol. 40-6 pp. 1142-1153

7. Pamuk, A., Ling, H., Leshchinsky, D., Kalkan, E., Adalier, K. 2004 "The 1999 Kocaeli (Izmit), Turkey, Earthquake" Fifth International Conference on Case Histories in Geotechnical Engineering, New York

8. Bathurst, R.J., Zarnani, S., Gaskin, A., 2007. "Shaking table testing of geofoam seismic buffers.", *Soil Dynamics and Earthquake Engineering* Vol. 27-4, pp. 324–332.

9. Zarnani, S., Bathurst, R.J. 2009. "Influence of constitutive model on numerical simulation of EPS seismic buffer shaking table tests", *Geotextiles and Geomembranes*, Vol. 27-4, pp. 308–312

10. Ling, H., Mohri, Y., Leshchinsky, D., Burke, C., Matsushima, K., Liu H. 2005 "Large-Scale Shaking Table Tests on Modular-Block Reinforced Soil Retaining Walls" *ASCE Journal of Geotechnical and Geoenvironmental Engineering* Vol.131-4 pp. 465-476

11. Sabermahani, M., Ghalandarzadeh, A., Fakher, A. 2009 "Experimental study on seismic deformation modes of reinforced–soil walls" *Geotextiles and Geomembranes* Vol. 27-2 pp. 121-136

12. El-Emam, M. and Bathurst, R.J. 2005. "Facing contribution to seismic response of reduced-scale reinforced soil walls", *Geosynthetics International*, Vol. 12- 5, pp. 215-238.

13. El-Emam, M., Bathurst, R.J. 2007. "Influence of reinforcement parameters on the seismic response of reduced-scale reinforced soil retaining walls" *Geotextiles and Geomembranes*, Vol 25. pp. 33-49.

14. Siddharthan, R. V., Ganeshwara, V., Kutter, B. L., El-Desouky, M., Whitman, R. V. 2004 "Seismic Deformation of Bar Mat Mechanically Stabilized Earth Walls. II: A Multiblock Model" *Journal of Geotechnical and Geoenvironmental Engineering*, ASCE, Vol. 130, No.1, pp.14-25

15. Dewoolkar, M., Chan, A., Ko, H., Pak, R. 2009 "Finite Element Simulations of Seismic Effects on Retaining Walls with Liquefiable Backfills" *International Journal for Numerical and Analytical Methods in Geomechnaics* Vo. 33-6 pp. 791-816

16. Abdel-Rahman, A. H., Ibrahim, M. A. 2010 "Soil/Geogrid Behavior Subjected to Cyclic Loading" National Research Center, Egypt.

17. Bathurst, R. J. 1993 "Laboratory Testing of Modular Masonry Concrete Block-Geogrid Facing Connections," *Geosynthetic Soil Reinforcement Testing Procedures*, ASTM STP 1190, S.C. Jonathan Cheng, ED., American Society for Testing and Materials, Philadelphia

18. Mononobe N, Matsuo H 1929, On the determination of earth pressure during earthquakes. In Proc. Of the World Engineering Conf., Vol. 9, str. 176

19. Seismic Analysis and Design of Retaining Walls, Buried Structures, Slopes, and Embankments, 2008, NCHRP 611, Transportation Research Board.

20. Prakash S., and Saran, S. 1966. "Static and Dynamic Earth Pressure Behind Retaining Walls." Proceedings, 3rd Symposium on Earthquake Engineering, Roorkee, India, Vol. 1, pp 273–288.

21. Richards R. and Shi, X. 1994. "Seismic Lateral Pressures in Soils with Cohesion." *Journal of Geotechnical Engineering*, ASCE, Vol. 120, No. 7, pp 1230–1251.

22. Chen, W. F. and Liu, X. L. 1990. *Limit Analysis in Soil Mechanics.* Elsevier.

23. Shukla, S. K., Gupta, S. K., and Sivakugan, N. 2003 "Active Earth Pressure on Retaining Wall for c-Φ Soil Backfill under Seismic Loading Condition" *Journal of Geotechnical and Geoenvironmental Engineering*, ASCE, 135(5), 690-696.

24. Cai, Z. and Bathurst, R.J. 1996. "Deterministic Sliding Block Methods for Estimating Seismic Displacements of Earth Structures", *Soil Dynamics and Earthquake Engineering*, Vol. 15, No, 4, pp. 255-268

25. Choudhury, D., Sitharam, T. G., Subba Rao, K.S. 2004 "Seismic Design of earth-retaining structures and foundations", *Current Science: Special Section: Geotechnics and Earthquake Hazards*, Vol. 87, No. 10.

26. Newmark, N. M. 1965. "Effects of Earthquakes on Dams and Embankments." *Geotechnique*, Vol. 15, No. 2, pp. 139–193.

27. Callisto, L., Soccodato, F. M. 2010 "Seismic Design of Flexible Cantilevered Retaining Wall" *Journal of Geotechnical and Geoenvironmental Engineering*, ASCE, Vol. 136, No. 2, pp 344-354

28. Siddharthan, R., Ganeshwara, V., Kutter, B., El-Desouky, M., Whitman, R. 2004 “Seismic Deformation of Bar Mat Mechanically Stabilized Earth Walls. I: Centrifuge Tests” *ASCE Journal of Geotechnical and Geoenvironmental Engineering* Vol. 130-1 pp. 26-35

29. Cai, Z. and Bathurst, R. J. 1996. “Seismic induced permanent displacement of geosynthetic reinforced segmental retaining walls” *Canadian Geotechnical Journal* , Vol. 31, pp 937-955

30. Franklin, A. G. & Chang, F. K. Permanent displacement of earth embankments by Newmark sliding block analysis. *Misc. Paper S-71-17, Soil and Pavements Lab.,* US Army Eng. Waterways Expt. Stn., Vicksburg, Miss., 1977.

31. Richards, R. & Elms, D. G. Seismic behavior of gravity retaining walls. *J. Geotech. Engng Div., ASCE,* 1979, 105(GT4), 449-464.

32. Whitman, R. V. & Liao, S. Seismic design of gravity retaining walls. *Proc. 8th WCEE,* San Francisco, Vol. 3, pp. 533-540.

33. Sarma, S. K. Stability analysis of embankment and slopes. *J. Geotech. Engng Div., ASCE,* 1979, 105(GT12), 1511-1523.

34. Makdisi, F. I. & Seed, H. B. Simplified procedure for estimating earth dam and embankment earthquakeinduced deformations. J. *Geotech. Engng Div., ASCE,*1978, 104(GT7), 849-867.

35. Yegian, M. K., Marciano, E. A. & Ghahraman, V. G. Earthquake-induced permanent deformations: probabilistic approach. *J. Geotech. Engng, ASCE,* 1991, 117(1), 1158-1167.

36. Ambraseys, N. N. & Menu, J. M. Earthquake-induced ground displacements. *Earthq. Engng Struct. Dyn.,* 1988, 16(7), 985-1006

37. Bathurst, R. J., Allen, T. M., Nowak, A. S. 2008 “Calibration concepts for load and resistance factor design (LRFD) of reinforced soil walls” *Canadian Geotechnical Journal* Vo. 45, pp 1377-1392

38. Budge, A. S., Bay, J. A., and Anderson, L. R. 2006 “Calibrating Vertical Deformations in a Finite Element Model of an MSE Wall” ASCE, GeoCongress 2006 Proc. 187, 243

39. Yoo, C., Kim, S., 2008 “Performance of a Two-tier Geosynthetic Reinforced Segmental Retaining Wall Under a Surcharge Load: Full-scale Load Test and 3D Finite Element Analysis”, Sungkyunkwan University, 300 Chun-Chun Dong, Jan-An Gu, Suwon, Kyong-Gi Do 440-746, Republic of Korea

40. Karpurapu, R.G. and Bathurst, R.J. 1995., “Behaviour of Geosynthetic Reinforced Soil Retaining Walls using the Finite Element Method”, *Computers and Geotechnics*, Vol. 17, No. 3, pp. 279-299

41. Yogendrakumar, M., Bathurst, R. J., Finn, W. D. L. 1992 “Dynamic Response Analysis of Reinforced-Soil Retaining Wall” *ASCE Journal of Geotechnical Engineering* Vol. 118 pp 1158-1167

42. Rowe, K.R., Ho, S.K., 1997. “Continuous panel reinforced soil walls on rigid foundations”, *ASCE Journal of Geotechnical and Geoenvironmental Engineering* vol. 123 (10), pp 912–920.

43. Green, R. A., Olgun, C. G., Ebeling, R. M., Cameron, W. I. 2003 “Seismically Induced Lateral Earth Pressures on a Cantilever Retaining Wall” Sixth US Conference and Workshop on Lifeline Earthquake Engineering, Long Beach, California, ASCE, TCLEE Monograph No. 25: 946-955

44. Trandafir, A. C., Ertugrul, O.L., 2010 “Earthquake Response of a Gravity Retaining Wall with Geofoam Inclusion” Department of Geology and Geophysics, University of Utah and Department of Civil Engineering Middle East Technical University.

45. Davies, P. R. E., Dodds, A., McIlquham, J. D. 2010 “Seismic Design Approach for Large Counterfort Wall Retaining Structures” Golder Associates and Arup, Australia.

46. Cai, Z. and Bathurst, R.J. 1995. “Seismic Response Analysis of Geosynthetic Reinforced Soil Segmental Retaining Walls by Finite Element Method”, *Computers and Geotechnics*, Vol. 17 No. 4, pp. 523-546

47. Arizona MSE Spec ASD latest 2010, Section 929: Mechanically Stabilized Earth (MSE) Walls

48. Caltrans LRFD Bridge Design Aids, 2009 section 3-8 Mechanically Stabilized Embankment

49. Idaho Mechanically Stabilized Earth (MSE) Retaining Wall Specs, 2010

50. SCDOT Geotechnical Design Manual chapter 14, Geotechnical Seismic Design, 2010

51. Allen, T. M., and Bathurst, R. J., 2001, *Prediction of Soil Reinforcement Loads in Mechanically Stabilized Earth (MSE) Walls at Working Stresses*, Washington State Department of Transportation, Report WA-RD 522.1, 353

52. WSDOT Geotechnical Design Manual, chapter 15, Abutments, Retaining walls, and Reinforced Slopes, 2010

53. Oregon Department of Transportation Geotechnical Design Manual Volume 1, Section 6.2.3 Bridge Abutments and Retaining Walls, 2010

54. Yen, W. P., Alzamora, D. Buckle, I., Ger, J., Chen, G., Allen, T., Arias, J., 2011, *Post-Earthquake Reconnaissance Report on Transportation Infrastructure: Impact of the February 27, 2010, Offshore Maule Earthquake in Chile*, U.S. Department of Transportation, Federal Highway Administration, Report FHWA-HRT-11-030

55. Seible, F.1996 “Structural Response Assessment of Soil Nail Wall Facings” University of California, San Diego, Department of Structural Engineering, SSRP-96/01

56. “LRFD Procedures for Geotechnical Seismic Design - Phase I” 2009 http://www.wsdot.wa.gov/Research/Results/ProjectDelivery.htm#Materials Accessed

57. D.M. Boore, 2005, *SMSIM-Fortran Programs for Simulating Ground Motions from Earthquakes: Version 2.3-A Revision of OFR 96-80-A* United States Department of the Interior, U.S. Geological Survey

58. *Minimum Design Loads for Buildings and Other Structures,* American Society of Civil Engineers, ASCE-7

59. "Global Vs30 Map Server." *U.S. Geological Survey Earthquake Hazards Program*. Web. 25 May 2011. <http://earthquake.usgs.gov/hazards/apps/vs30/>.

60. Núñez A. G. L. "Investigation of Resetting Stiffness Application to Multistory Buildings" Colorado School of Mines, Colorado, April 2009.

61. Chopra A. K., 2007 *Dynamics of Structures, Theory and Applications to Earthquake Engineering* New Jersey

62. "COEFFICIENT OF FRICTION." *Cost Effective Solutions in Civil, Structural, Architectural, Electrical & HVAC Engineering*. Web. 08 May 2011. <http://www.supercivilcd.com/FRICTION.htm>.http://www.engineeringtoolbox.com/concrete-properties-d_1223.html

63. *The Engineering Toolbox*. 08 May 2011. <http://www.engineeringtoolbox.com/concrete-properties-d_1223.html>

64. "Polyethylene." *Wikipedia, the Free Encyclopedia*. Web. 08 May 2011. <http://en.wikipedia.org/wiki/Polyethylene>.

65. Engineering Properties of Marlex Resins. Chevron Phillips Chemical Company LP. PE TSM-1, 2002

66. "Young's Modulus for Soil on the Geotechnical Information Website." *Geotechnical Information Website*. Web. 08 May 2011. <http://www.geotechnicalinfo.com/youngs_modulus.html>.

67. Hatami, K., Bathurst, R.J., 2000. Effect of structural design on fundamental frequency of reinforced-soil retaining walls. Soil Dynamics and Earthquake Engineering 19, 137–157.

68. Wu, G., 1994, *"Dynamic Soil-Structure Interaction: Pile Foundations and Retaining Structures"*, Ph.D. Thesis, Department of Civil Engineering, University of British Columbia, Vancouver, British Columbia, Canada, p.213

69. Richardson, G.N. and Lee, K.L., 1975, "Seismic Design of Reinforced Earth Walls", Journal of the Geotechnical Engineering Division, Vol. 101, GT2, pp. 167-188.

70. Livermore Software Technology Corporation. Web. 27 Mar. 2011. <http://www.lstc.com/lspp/content/overview.shtml>.

71. Building Code Requirements for Structural Concrete (ACI 318-08) and Commentary, 2008, American Concrete Institute

72. Mechanically-Stabilized Earth (MSE) Retaining Wall Panels, 2005, Iowa Department of Transportation, IM 445.03

73. *Ls-Dyna Keyword User's Manual*, Livermore Software Technology Corporation (LSTC) May 2007.

74. *LS-PrePost BlockM User Guide*, Livermore Software Technology Corporation (LSTC) September 2008.

75. Anderson, P.L., Gladstone, R.A., Sankey, J.E., 2012. "State of the Practice of MSE Wall Design for Highway Structures," *GeoConrgress 2012: State of the Art and Practice in Geotechnical Engineering*. Ed. Hryciw, R., Athanasopoulos-Zekkos, A. , and Yesiller, N. GSP 225.

APPENDIX A

PEAK GROUND ACCELERATION FOR 1000 YEAR RETURN PERIOD IN THE CONTERMINOUS UNITED STATES MAP

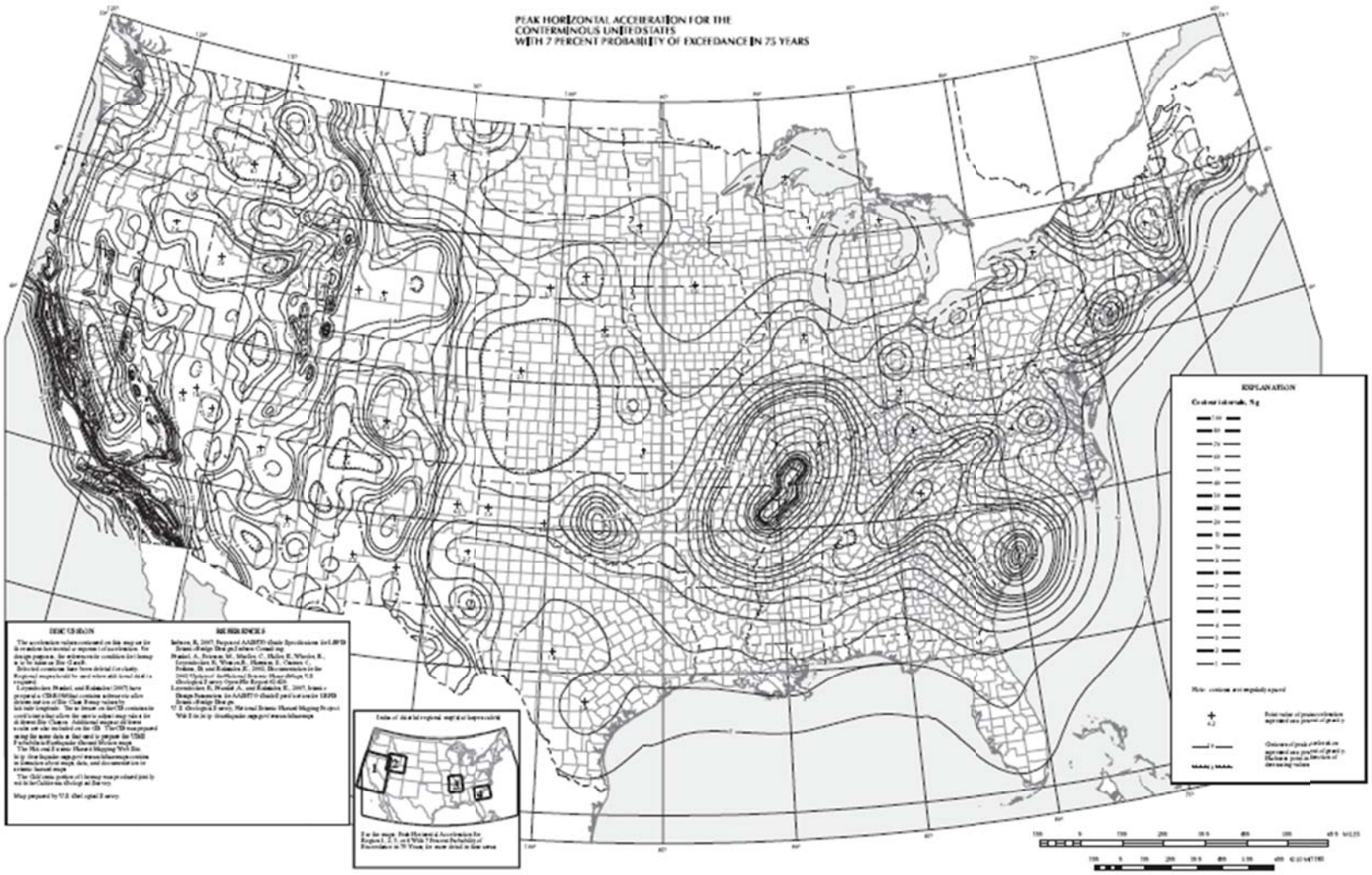

Figure A - 1: Peak Ground Acceleration for 1000 Year Return Period: Conterminous United States [1]

APPENDIX B

NATIONAL DEPARTMENT OF TRANSPORTATION SURVEY QUESTIONS AND LIST OF CONTACTS

State DOT Contacts:

DOT MSE wall contacts	Email	Name	Phone	Responded (y/n)
Alabama	dixonk@dot.state.al.us	Kidada C. Dixon	334-206-2277	y
Alaska	clint.adler@alaska.gov	Clint Adler	907-451-5321	n
Arizona	nwetz@azdot.gov	Norman Wetz	602-712-8093	y
Arkansas	jon.annable@arkansashighways.com	Jonathan Annable	501-569-2369	y
California	kathryn_griswell@dot.ca.gov	Kathryn Griswell	916-227-7330	y
Connecticut	leo.fontaine@ct.gov	Leo Fontaine	8605943180	y
Delaware	jsoneji@mail.dot.state.de.us	Jiten K. Soneji	302-760-2322	y
Florida	Darryll.Dockstader@dot.state.fl.us	J. Darryll Dockstader	(850) 414-4617	y
Georgia		Paul Liles	404-631-1985	y
Hawaii	herbert.chu@hawaii.gov	Herbert Chu	808-832-3405 ext. 232/483-2575	n
Idaho	tri.buu@itd.idaho.gov	Tri Buu	208 334 8448	y
Illinois	william.kramer@illinois.gov	Bill Kramer	217-782-7773	y
Indiana	msmadi@indot.in.gov	Malek Smadi	317-610-7251 ext. 226	y
Iowa	Robert.Stanley@dot.iowa.gov	Bob Stanley	(515)239-1026	y
Kansas	brennan@ksdot.org	James Brennan	785-296-3008	y
Kentucky	bart.asher@ky.gov	Bart Ascher	502-564-2374	n
Louisiana	gavin.gautreau@la.gov	Gavin Gautreau	225-767-9110	n
Maine	kitty.breskin@maine.gov	Kitty Breskin	207-592-7605	y
Maryland	jrobert@sha.state.md.us	Jeff Robert	410-545-8327	y
Massachusetts	peter.connors@mhd.state.ma.us	Peter Connors	617-973-7304	y
Michigan	endresr@michigan.gov	Robert Endres	517-322-1207	y
Minnesota	blake.nelson@dot.state.mn.us	Blake Nelson	651-366-5599	y
Mississippi	jwilliams@mdot.state.ms.us	James Williams	601-359-1798	n
Missouri	thomas.fennessey@modot.mo.gov	Thomas W.	573-526-4340	y

		Fennessey		
Montana	kechristensen@mt.gov	Kevin Christensen	406-444-6008	n
Nebraska	omar.qudus@nebraska.gov	Omar Qudus	402-479-4394	y
Nevada	msalazar@dot.state.nv.us	J. Mark Salazar	775.888.7875	y
New Hampshire	tcleary@dot.state.nh.us	Thomas Cleary	603-434-4721	y
New Jersey	kuangyu.yang@dot.state.nj.us	Kuang-Yu Yang	609-530-5302	y
New Mexico	robert.meyers@state.nm.us	Bob Meyers	505 827-5466	y
New York	jdigregorio@dot.state.ny.us	Joe DiGregorio	518-457-4769	y
North Carolina	biswas@dot.state.nc.us,	Dr. Mrinmay Biswas	919-508-1865	y
North Dakota	jketterl@nd.gov	Jon Ketterl	701.328.6908	y
Ohio	Jawdat.Siddiqi@dot.state.oh.us	Jawdat Siddiqi	614-728-2057	n
Oklahoma	rcurb@odot.org,	Ron Curb	405-522-3795	n
Oregon	jonathan.n.guido@odot.state.or.us	Jonathan N. Guido, PE, GE	503-986-3993	y
Pennsylvania	dazzato@state.pa.us	Patricia Kiehl	717-772-0568	y
Road Island	rsnyder@dot.ri.gov	Robert Snyder	401 222-2524 X 4553	n
South Carolina	sizemorejc@scdot.org	Jeff Sizemore	803-737-1571	y
South Dakota	dan.vockrodt@state.sd.us	Dan Vockrodt	605-773-4466	y
Tennessee	ed.wasserman@tn.gov	Edward P. Wasserman	615-741-3351	y
Texas		Marcos Galvan	512-416-2224	y
Utah	dsjoblom@utah.gov	Darin Sjoblom	801-964-4474	y
Vermont	chris.benda@state.vt.us	Christopher Benda	802-828-6910	y
Virginia		Ashton Lawrer	804-786-2355	y
Washington	ALLENT@wsdot.wa.gov	Tony Allen	360-709-5450	y
West Virginia	donald.l.williams@wv.gov	Donald Williams	304-677-4000	y

Wisconsin	robert.arndorfer@dot.state.wi.us	Bob Arndorfer	608-246-7940	y
Wyoming		Michael E. Menghini	307-777-4427	y

APPENDIX C
MSE WALL SCHEMATICS

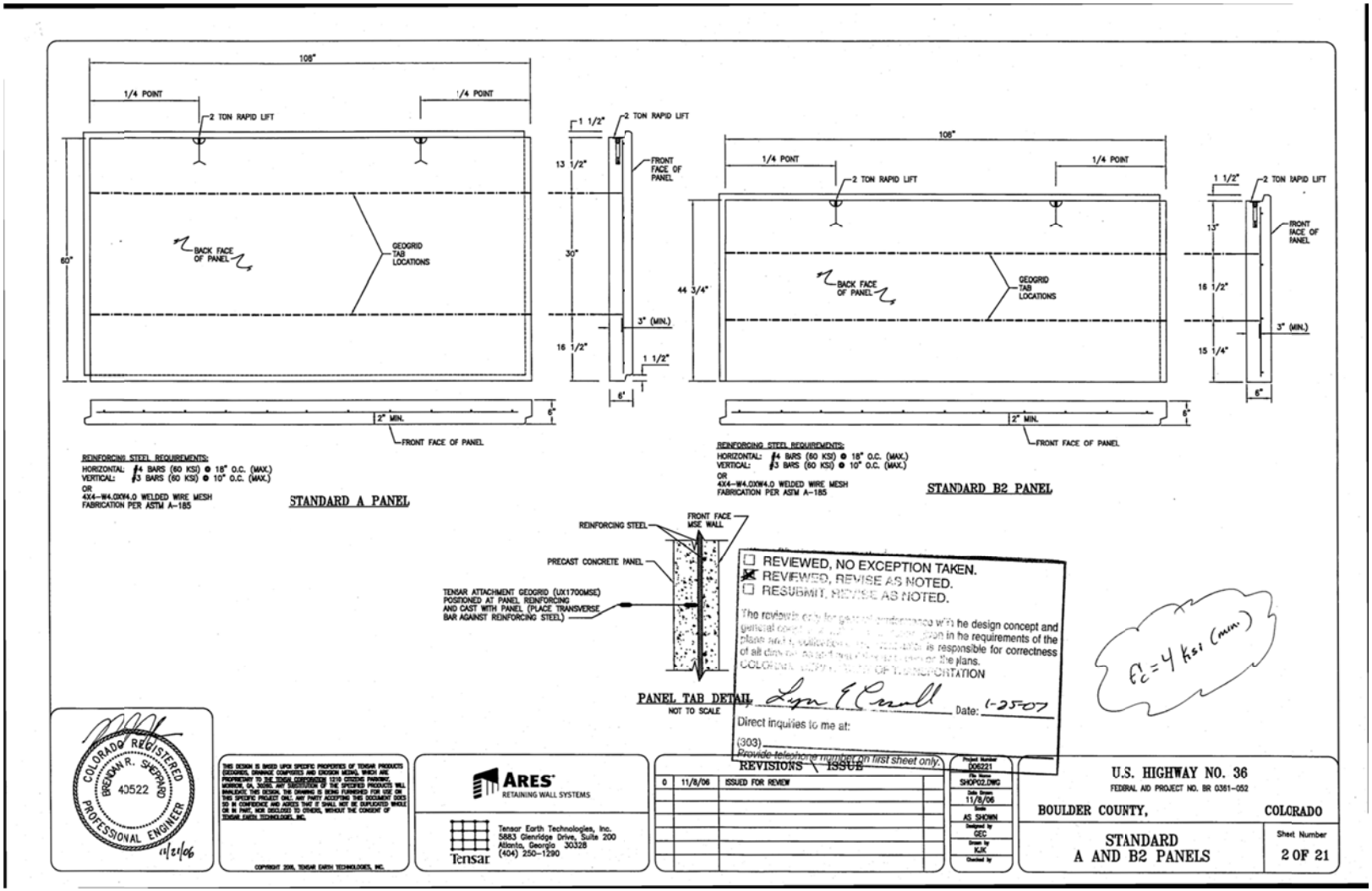

Figure C - 1: Type A panel wall dimensions

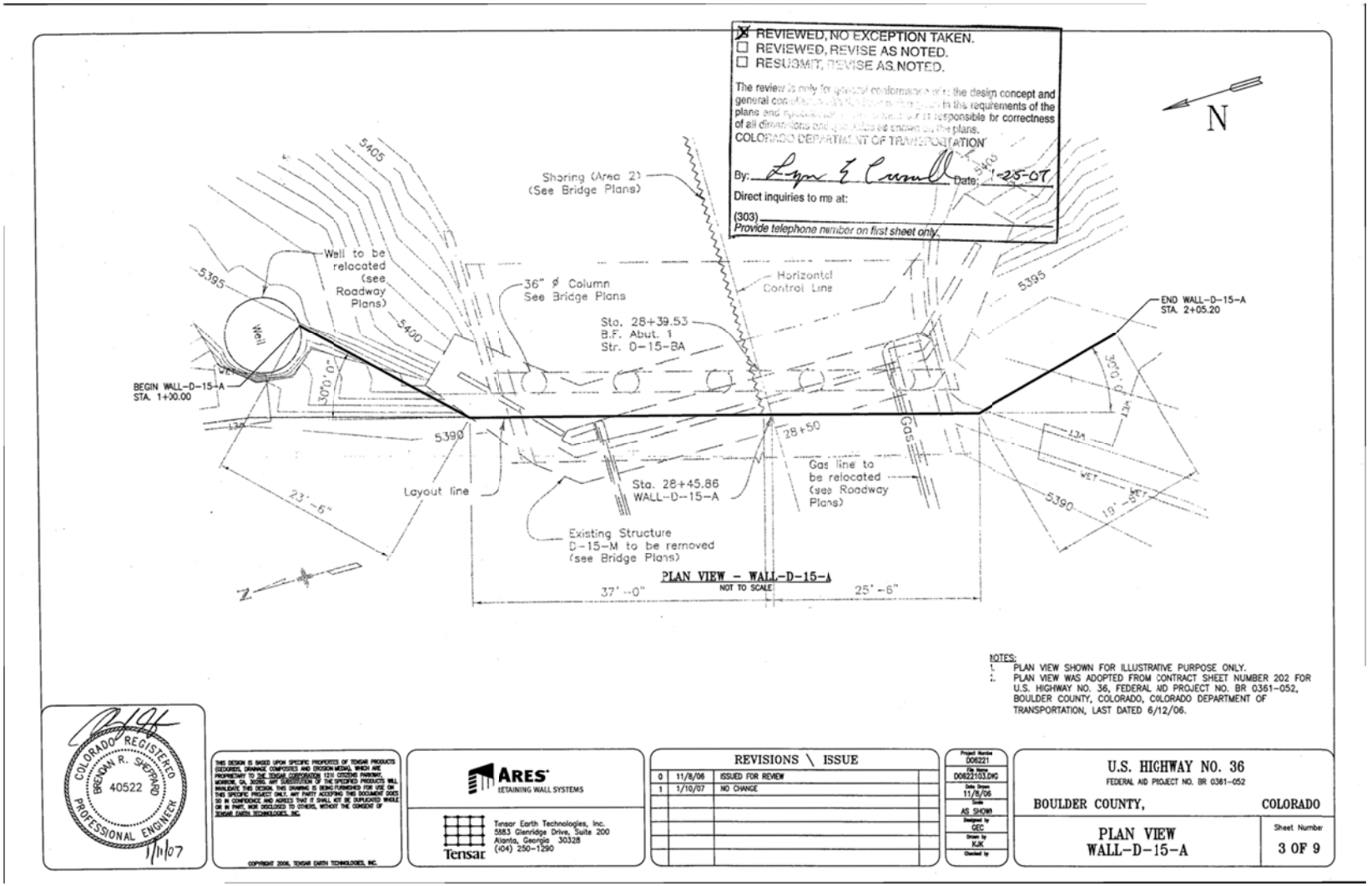

Figure C - 2: Typical panel wall plan view

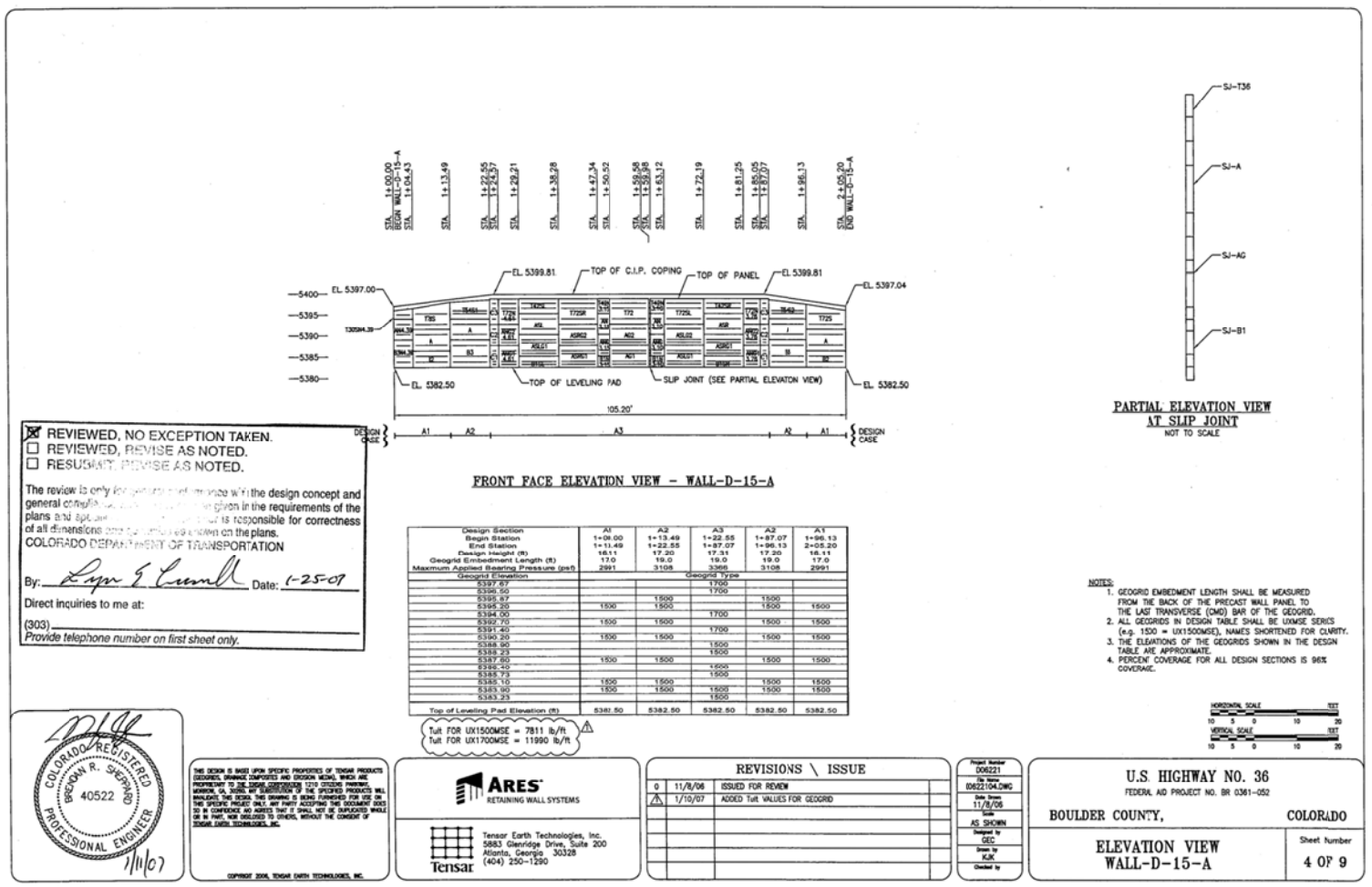

Figure C - 3: Typical panel wall layout

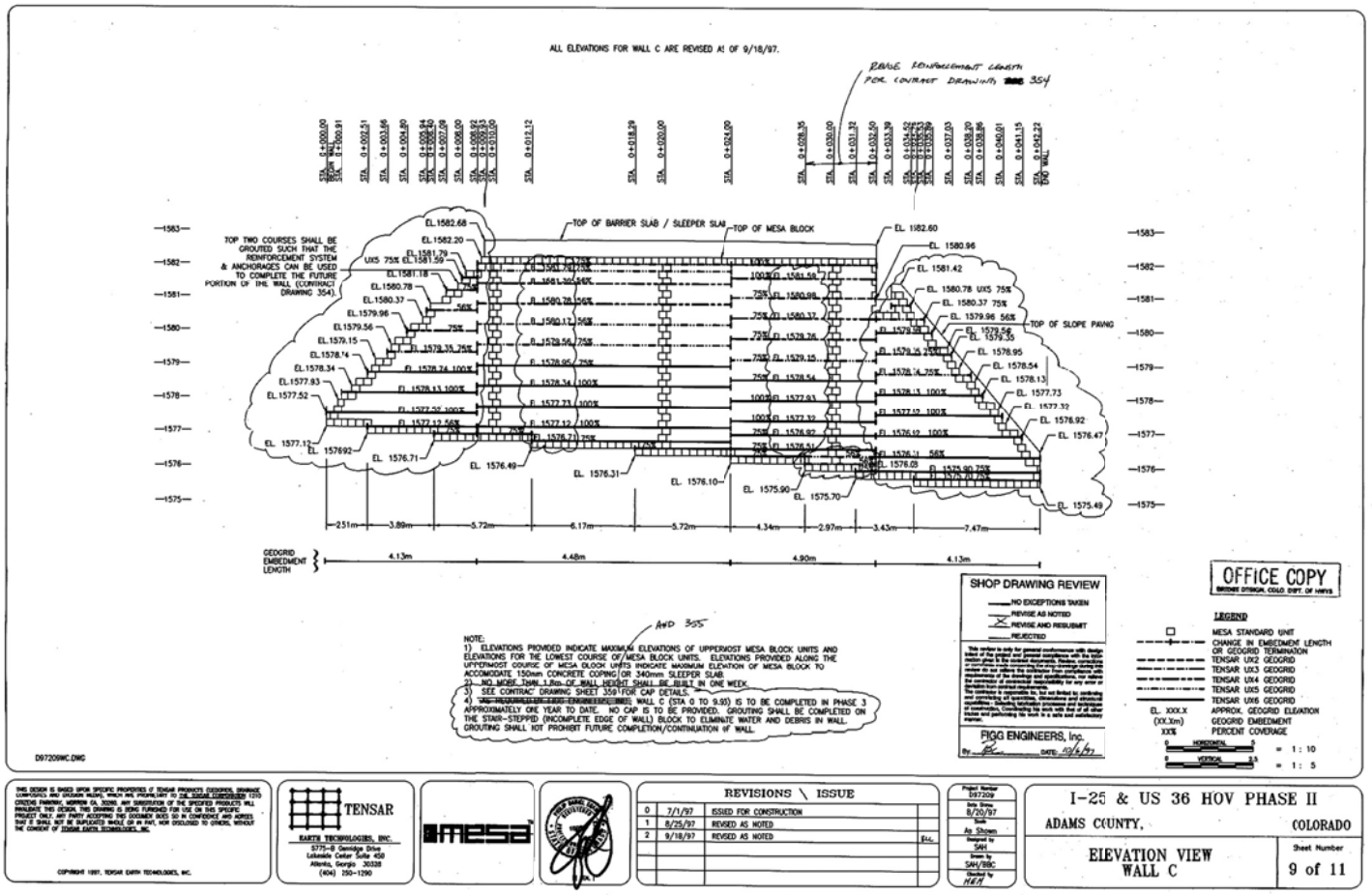

Figure C - 4: Typical modular block wall layout

APPENDIX D

LS-DYNA MODEL CONSTRUCTION

LS-Prepost version 2.4 was used for the creation of these wall models. The program groups each feature into 7 different “pages” which are made up of different keyword cards that may be edited and added to the LS-Dyna keyword file. The shell meshes were created by using the Mesh feature on page 7. The coordinates of each mesh piece can be made by typing the coordinates of the four corners into the 4N-Shell entity. The number of elements in the x and y directions can also be specified in the NxNo. and NyNo blanks. Once the pieces of the shell mesh are built, the nodes can be merged by using the DupNod feature on page 2. The pieces of mesh can also be moved to the same part using the “Movcpy” feature also located on page 2. Mesh pieces can also be translated, reflected, and rotated using the Trnsfrm, Reflect, Translt, and Rotate features on page 2. For further instructions on use of these features see the online LS-Prepost documentation [70] and LS-Dyna Keyword Manual [73].

The soil part was first drawn using the program SolidWorks and then saved as an IGES file. This file was then imported into LS-Dyna in order to create a proper mesh. The soil mesh was created using the feature BlockM on page 7. In this feature the number of lines that make up each element can be specified in each direction (i, j or k). The position of these lines can also be specified in the position list. Once a block of elements with the proper spacing is created, this block can be projected to lines, surfaces and point of the imported IGES file to create the soil mesh. The elements can also be distributed linearly, or moved or rotated. In order to draw lines recognized by LS-Dyna on the IGES file, the feature curves on page 7 can be used. To create a curve or line, select “create”, “by point” at the bottom of the screen and select two points that you would like the line to run between. Once this is done a line of the blocks generated in BlockM can be projected to the line created on the IGES file. Projections may need to be repeated several times to get a smooth surface. Further explanation of the BlockM feature can be found in the LS-Dyna documentation: BlockM User Manual [74].

For the segmental panel walls, each individual panel was made to be its own mesh by selecting the area of the mesh that is the same size as the panel and using the “detach” feature on page 2. This makes each panel have its own nodes and boundaries separated from the rest of the mesh. Once all the panels are detached, hinges were placed at all edge nodes. This was done by creating a node group through the “setD” feature on page 5. To create node groups select “create” and set the group type to “*SET_NODE” from the pull down menu. If “area” is selected

below the graphics window then several nodes can be selected at a time by clicking and dragging a box around the desired nodes. For these particular node groups only two nodes touching each other go into a group at a time. This allows the wall to translate freely separate from the rest of the nodes in the wall. Once all the node groups are created, the "*Cnstrnd" feature on page 3 is used to make sure the nodes are free to rotate but are forced to translate together, mimicking the hinged boundaries at the junctions of each panel. The direction in which the nodes are forced to translate together can be selected. For this study the nodes are forced to translate in all directions in order to create the effect of the panels being hinged together. See the LS-Dyna keyword manual [73]. One alternative way to constrain all different node groups together when there are multiple node groups is to use a spreadsheet program, such as Microsoft Excel, to write the needed keywords and numbers to a text file. If this file is saved as a formatted space deliminated file it can simply be copied and pasted into the text version of the LS-Dyna keyword file.

The panel wall and the geogrid reinforcement were connected together by using the duplicate node feature on page 2. To use this, an area was selected in the graphics window that just showed one reinforcement layer at a time and the wall it was attached to. With this done, the option can be selected "show duplicate nodes" and then "merge duplicate nodes". This way the soil and reinforcement acts as one mesh and the resultant stresses can be read at the duplicate nodes.

The next contact used is implemented between the soil front face and the panel wall face. In order to set this contact, two segment set groups need to be created. The "Selpar" feature located on page 1 can be used to view one part at a time. The same "SetD" feature on page 5 can be used with the pull down menu set to *SET_SEGMENT. If area is selected, a group of elements can be selected at once by drawing a box around them with the cursor in the graphics window. This feature highlights the face of the whole element rather than just the nodes. Once this is done, "*contact" on page 3 is used to set the no penetration contact between the wall and the soil. This contact simply ensures that the wall does not move into the soil in the dynamic situation and vice versa. From the *contact feature, select "AUTOMATIC_SURFACE_TO_SURACE" and select edit. If the SSTYP, and MSTYP inputs are set to 0, this tells the program that segment sets will be used. The ID for these are input into SSID and MSID which stand for slave segments and master segments. In this case, the wall is the slave and the soil is the master. The static and dynamic coefficients of friction can be input in the FS and FD section. If the section A card is

checked, then the soft input can be set to 1. This option is most commonly used when dissimilar materials have a contact set between them. The default soft formulation uses the size of the contact segment and its material properties to determine the contact spring stiffness. This method works best when the material properties are the same order of magnitude. When the soft formulation is set to 1, the stiffness of the near contact springs are based on the nodal masses that come into contact and the time step size. The spring stiffness is calculated as:

$$k = .01\frac{m}{\Delta t^2} \qquad \textbf{(D-1)}$$

The reinforcement is constrained in the soil by the *CONSTRAINED_LAGRANGE_IN_SOLID keyword. This can be created through the "Cnstrnd" feature on page 3. If the SSTYP and MSTYP are both set to 1, then the part ID can be selected for the slave (reinforcement) and master (soil) parameters. The CTYPE parameter for this contact is set to 2 so that the shell mesh is constrained with respect to acceleration and velocity. This contact keeps the reinforcement from simply falling out of the soil when outside forces are applied.

The last contact is made between the soil and the orthotropic elastic elements. These nodes are tied together by the contact TIED_SURFACE_TO_SURAFACE. This keyword can be edited through the "*contact" feature on page 3. Segment sets were again made for the faces of the elements at the back of the soil mesh and the faces of the elements at the front of the orthotropic elastic element mesh. This keyword is implemented the same way the *CONTACT_AUTOMATIC_SURFACE_TO_SURACE contact is implemented. This contact ties the two surfaces together so that they move as one solid part.

Different material cards can be created by using the "*Mat" feature on page 3. The material type can be selected from the list by pulling down the arrow next to "Groupby" and selecting "All". This list can then be sorted by setting the "Sort" pull-down menu to "Type". The material type 001 (Elastic) and 002 (orthotropic elastic) are used in this study. The input parameters needed for each card are the material ID number (MID), mass density (RO), Young's modulus of elasticity (E), and Poisson's ratio (PR).

In order to implement the orthotropic elastic elements, a vector is defined that specifies which direction the material properties apply to. To do this, use the feature “*Define” on page 3. Next select “COORDINATE_VECTOR” and edit. For this study the direction C is said to be the Z direction in the global model. Therefore the local coordinate system needs to be the same as the global coordinate system defined using the *DEFINE_COORDINATE_VECTOR keyword. This is done by saying the x coordinate on the x axis (XX) is equal to 1.0 and the y coordinate of the local x-y vector is equal to 1.0 with all other coordinates 0.

The section keyword needs to be defined for each part to tell the program what kind of element it is using. For the panel wall, a *SECTION_SHELL keyword is defined for both the concrete and reinforcement parts. In this keyword the element formulation (ELFORM) is set to option 16 which is a fully integrated shell element. This formulation gives the element the option to bend as well as stretch and compress. The thickness of the shell element is also specified here which is 6 in for the concrete and 0.25 in for the reinforcement. The solid elements share the same section solid keyword. The solid elements have an element formation of 2 which is the fully integrated solid option. This has been seen to produce more accurate results from previous models. For the modular block wall the *SECTION_SOLID keyword is defined for the brick elements.

Once the sections and material properties are defined they need to be assigned to each part by using the “PartD” feature on page 5. Here the part can be selected in the bottom right hand window and the option “assi” can be selected. Next the section ID and Material ID can be selected for that part. Once the “Apply” button is pressed, this material will have the properties assigned to it.

The boundary conditions for this model can be applied by creating another node set group that includes all nodes that would be touching the ground. Once this group is created, the keyword *BOUNDRY_SPC_SET, located on page 3, can be created. This card needs the node set ID and then the degrees of freedom can be fixed by selecting a 1 under DOFX, DOFY, and DOFZ for translations and DOFRX, DOFRY, and DOFRZ for rotations. The next boundary condition applied is the non-reflecting boundary condition. This is applied to a segment set that includes the soil sides and the back. This option does not reflect waves back into the soil everywhere that there is an infinite boundary. This keyword is defined using the same “*boundary” feature on page 3.

To perform a modal analysis of this structure, the *CONTROL_IMPLICIT_EIGENVALUE and *CONTROL_IMPLICIT_GENERAL keywords must be used. These are created using the "*control" feature on page 3. The implicit general card changes the analysis from its default explicit analysis to an implicit analysis. An initial time step size is entered in for the DTO value. LS-Dyna iterates to find the correct time step from this value. In the implicit eigenvalue card, the number of mode shapes desired can be specified. For this study the mode shape number (NEIG) was set to 3.

To perform an earthquake analysis, the two implicit keywords are not used. For this study, the non-reflecting boundary condition was removed as well for the panel wall in order to attempt to reduce run times. When performing an earthquake analysis the time step needs to be specified in which LS-Dyna writes results out to a file. This is done though the "*Dbase" feature on page 3. If Binary_D3plot is selected, then all results are written to the a file that can be read using LS-Prepost. The time step used is .02 seconds in order to match the time steps of the earthquakes used.

The earthquake loading is applied by creating a curve using the "*Define"" feature on page 3. The earthquake can be imported into the *DEFINE_CURVE keyword by selecting "impost XY plot". The earthquake must be in a CSV, comma deliminated excel file in order for the program to read in data. Next the "*Boundary" feature can be used to apply the acceleration curve to the bottom nodes of the model through the prescribed motion set keyword. The node set ID used is the same as that used for the boundary conditions. The DOF is set to 1 which tells the program the motion is applied in the X direction. The VAD is set to 1 which says that this motion is an acceleration. The BIRTH value is set to 1.0 which is the time in which this motion will start. This motion will start at 2.0 seconds to give the program a chance to fully apply gravity, then come to equilibrium without causing too much vibration.

Gravity is applied by defining a curve that applies the acceleration linearly over 1 second of time and stays for the duration of the run time. This keeps the model from unnecessarily bouncing. This curve is then applied to the whole model using the "*LOAD_BODY_Z" keyword. In LS-Dyna, gravity is positive in the negative Z direction. Using the "*CONTROL_TERMINATION" keyword, a time that ends the run duration can be input that will stop the model from running.